

HADLEY CENTRE  
FOR CLIMATE PREDICTION AND RESEARCH

Development of the Global Mean Sea Level  
Pressure Data Set GMSLP2

by

T A Basnett and D E Parker

CRTN 79

May 1997

CLIMATE  
RESEARCH  
TECHNICAL  
NOTE

Hadley Centre  
Meteorological Office  
London Road  
Bracknell  
Berkshire RG12 2SY

rep.00089

CLIMATE RESEARCH TECHNICAL NOTE NO. 79

DEVELOPMENT OF THE GLOBAL MEAN SEA LEVEL PRESSURE

DATA SET GMSLP2

by

T A Basnett and D E Parker

Hadley Centre for Climate Prediction and Research  
Meteorological Office  
London Road  
Bracknell  
Berkshire RG12 2SY

NOTE: This paper has not been published. Permission to quote from it should be obtained from the Director of the Hadley Centre.

© Crown Copyright 1997

# Development of the Global Mean Sea Level Pressure Data Set GMSLP2

T.A. Basnett and D.E. Parker

Hadley Centre, Meteorological Office, Bracknell, U.K.

May 1997

## ABSTRACT

GMSLP2 is a fully global mean sea-level pressure data set, developed in collaboration with R.J.Allan (CSIRO, Australia) and M.J.Salinger (NIWA, New Zealand). It is an historical, gridded monthly data set covering the period 1871-1994, and the latest version, GMSLP2.1, has been developed by blending a combination of existing gridded mean sea-level pressure analyses with marine and land observations, using Laplacian interpolation techniques. A range of quality-controls was used to remove random and systematic errors from the observations. However, owing to the scarcity of reliable observed data, especially in the earlier decades, it was subsequently necessary to remove biases from the blended analyses in some areas, such as the Southern Ocean.

GMSLP2.1 has already been invaluable for atmospheric model validation purposes and in several empirical studies, such as a joint CSIRO-Meteorological Office (UKMO) Atlas of El Niño Southern Oscillation and climate variability. A key ongoing use is in connection with atmospheric model simulations of recent climate, aimed at detecting climate change and attributing it to human activities. In addition, GMSLP is being used in connection with the "Changes to the Climate of the UK" project.

### 1. Introduction

There has long been a requirement for a reliable global gridded data set of observed mean sea level (MSL) pressure, that would be suitable for both analysing climate variability and for validating climate model output. One of the earliest attempts to map global MSL pressure was made by Buchan (1868), who mapped mean monthly global MSL pressure for 1857-1866, based on observations derived from a representative sample of 360 stations worldwide. Notable work in this field was carried out by Lamb and Johnson (1966), who published contoured global charts of January and July MSL pressure for each year in 1750-1966. However, existing gridded MSL pressure data sets generally have a restricted coverage, being either hemispheric or 'near-global', and consist mostly of analysed data derived from hand-drawn analyses in the pre-computer era and more recently from routine GCM operational analyses or reanalyses. Also, owing to the change of analysis technique, these data sets are unlikely to be homogeneous. Although there are several 'observed' MSL pressure data sets available, which are either blends of analysed and observed data or statistical reconstructions based on observations, none of these has global coverage.

GMSLP is a global, observed, monthly, historical MSL pressure data set, which has been developed in collaboration with R.J.Allan (CSIRO) and M.J.Salinger (NIWA). The data set begins in 1871 and is composed of gridded values on a 5° latitude and 5° longitude resolution, centred on whole multiples of 5°, e.g. 55°N, 5°W. It has been constructed from a blend of existing gridded data sets, provided by us (UKMO-Jackson, 1986 unpublished), NCAR (Trenberth and Paolino, 1980), Scripps Institute of Oceanography (SIO)(Barnett et al., 1984), University of East Anglia (UEA)(Jones and Wigley, 1988; Jones, 1991) and CSIRO (Allan); plus observed data extracted from the UKMO Marine Data Bank (UKMOMDB), Comprehensive Ocean-Atmosphere Data Set (COADS)(Woodruff et al., 1987), UKMO monthly CLIMAT message archives and land station time series provided by Allan and Salinger.

A key use of GMSLP is in the multivariate analysis of results of atmospheric model simulations of recent climate, aimed at detecting climate change and attributing it to human activities. Thus, simulations of historical surface pressure given observed sea surface temperatures and increasing greenhouse gases, sulphate aerosols, etc., are being compared with observations and used to help interpret simulated air temperature changes. A further aim of GMSLP is to facilitate the validation of other atmospheric model results. GMSLP is also being used in the interpretation of observed global and regional climate variations (Parker et al., 1994). Particular examples are: variations in the El Niño Southern Oscillation (Allan et al., 1996), variations in south Pacific atmospheric circulation in observations and in atmospheric model simulations, and the effect of atmospheric circulation on land surface air temperature patterns. The data set will also allow an improved assessment of the effects of atmospheric circulation changes on UK climate and, therefore, a more thorough interpretation, for the UK area, of model simulations with increasing greenhouse gases.

## **2. Brief description of 'input' gridded data sets**

The input gridded data sets are summarized in Table 1. Here we provide brief details of their construction.

NCAR and UKMO are both Northern Hemisphere data sets based on 5° by 5° area and 5° latitude by 10° longitude grids respectively. The pre 1940 data in both cases were extracted from German and US Naval hand analyses, although both data sets have subsequently been affected by independent correction schemes, described by Trenberth (1980) and Jackson (1986). Since 1940 the data sets have relied on separate data sources. The UKMO historical file for recent years is based on the UKMO operational analysis.

The CSIRO data set, as yet unpublished, is a 'near global' data set, based on a 10° by 10° area grid, constructed from a blend of land observations extracted from historical station records and marine observations from COADS.

The SIO data set (Barnett et al., 1984) also has 'near global' coverage, but on a 5° latitude by 10° longitude grid. These data were derived from a variety of different sources, including MSL pressure analyses from various national weather centres and raw ships' observations.

The data sets provided by Jones and Wigley (1988) and Jones (1991) are both limited area 5° latitude by 10° longitude grids covering part of the Southern Hemisphere. They are based solely on land station observations, which were interpolated onto 'hemispheric' grids using regression techniques.

## **3. GMSLP1**

### **3.1 Creation of GMSLP1**

Initially GMSLP was constructed from a simple blend of the existing gridded data sets (each interpolated onto a 5° latitude by 5° longitude grid), by calculating the median of all available gridded values at each grid-point in each month. If only one gridded value was available, then this was included in order to maximise temporal and spatial coverage. If two values were available, their mean was taken. Observing stations' data were used to arbitrate in an area of serious disagreement between gridded inputs over north-eastern Asia.

This method was first applied using UKMO, NCAR and SIO Northern Hemisphere data dating back to 1951, yielding GMSLP1.0, and resulted in marked improvements relative to the original UKMO data set, most noticeably over Greenland and north-east Asia during the winter months of 1981-

1991. Results from GMSLP1.0 are shown by Parker et al. (1994). This same technique was then applied on a global scale using all available gridded input data sets, yielding GMSLP1.1. The new data set contained many of the major global features, for example subtropical highs and sub-polar lows, but there were discontinuities across boundaries between the merged input data sets, suspect values in the region of the Central Asian Massif and an inability to capture extremes of MSL pressure in extratropical regions.

## **3.2 Analysis of GMSLP1.1**

### **3.2.1 Discontinuities across data set boundaries**

Discontinuities, in the form of distorted isobars and extreme gradients, occurred across the boundaries of input data sets and in areas where one or more of the input data sets contained missing data. The majority of these irregularities were fairly subtle and occurred in the Northern Hemisphere, which contained many missing data areas in the input data sets, but there was also a major discontinuity at 60°S, at the confluence of three data sets, CSIRO, Jones and Wigley, and Jones. Figure 1(a) is a time series of the annual grid-point MSL pressure values for each of the input data sets at (60°S,45°W). It clearly shows that there is a serious discrepancy between the data sets, with CSIRO 10hPa higher on average than both the Jones and Wigley and Jones data sets, although it should be noted that the latter two data sets are not derived from wholly independent sources. Figure 1(b) is a Southern Hemisphere circumpolar climatology of GMSLP1.1 created using all available input data sets and it clearly shows a major discontinuity at 60°S, which is the interface between relatively high values generated by the mean of CSIRO and Jones to the north and relatively low values to the south from Jones and Wigley. This discontinuity is most strongly marked in the southern regions of the Atlantic and Indian oceans by a pressure gradient in excess of 3hPa per degree of latitude. Figure 1(c) shows that by removing CSIRO from the blend in this area it is possible to create a much more realistic gradient.

### **3.2.2 Suspect values over regions of high orography**

MSL pressure values over mountainous regions, especially those in central Asia, were found to be suspect as the input data sets all differed, both from each other and from the observed record. Figure 2(a), showing the interpolated annual differences between the input data sets and Irkutsk (52.2°N,104.2°E), clearly illustrates these discrepancies. However, in areas of high orography even the observed data must be viewed with caution, as in the absence of metadata it is impossible to know whether the station level pressure has been reduced correctly to sea-level. Therefore there will always be some degree of uncertainty in these mountainous regions.

### **3.2.3 Lack of extreme values in the extratropics**

In extratropical regions, especially in the Southern Hemisphere, the CSIRO values of MSL pressure were not as extreme as indicated by observed data, i.e. anticyclones were not strong enough and conversely depressions not deep enough. This is shown by the time series of annual differences of the input data sets from the observed record at Ponta Delgada (37.4°N,25.4°W) in the Azores (Figure 2(b)) and Grytviken (54.2°S,36.3°W) near the Southern Hemisphere polar front (Figure 2(c)). Both sets of time series show that the UKMO, NCAR and Jones data sets all lie within 1hPa of the observed values, whereas the time series extracted from CSIRO differ considerably, being on average 2.5hPa too low at Ponta Delgada and 6hPa too high at Grytviken. Comparison of the CSIRO data set with the other gridded input data sets confirmed these findings: for example, the CSIRO data set was 2-3hPa lower in the subtropical highs than the SIO analyses (Figure 3). The reason for the biases in the CSIRO data set may simply be that the 10° resolution of CSIRO is too coarse to resolve the maxima and minima in these extratropical regions. However, the differences between data sets cover vast areas (Figure 3), so there may well be other problems, perhaps with

quality control or gridding techniques.

To limit these problems, GMSLP1.2 was formed. In GMSLP1.2, the CSIRO data set was restricted to the region south of 25°N for all longitudes, except where CSIRO was the only data set available (Table 2). Note that the Southern Hemisphere analysis is still entirely based on CSIRO before 1951.

#### **4. GMSLP2**

Although GMSLP1.2 proved to be useful in extratropical regions for model validation (Davies et al., 1995), we still required a fully global data set with improved reliability, especially over extratropical regions. To create this, we first formed a globally complete background field, GMSLP2.0, based on the same inputs as GMSLP1.2 but with adjustments, as described below, to reduce biases. We next blended the COADS gridded MSL pressures, marine observations extracted from the UKMOMDB, land observations derived from the UKMO CLIMAT archive and station time series provided by R.J.Allan and M.J.Salinger (Section 4.2). We then combined the result with GMSLP2.0, by performing a Laplacian interpolation (Reynolds, 1988). The result, GMSLP2.1, is the first *fully* global version of GMSLP, the creation of which is summarised by the flowchart in Figure 4.

##### **4.1 GMSLP2.0**

The coverage provided by the observed data used in the creation of GMSLP2.1 never reached global proportions and, prior to 1950, was quite sparse: for example, in the case of the marine observations, most MSL pressure values were restricted to a few narrow shipping lanes. Therefore we created a globally complete background field and used it to in-fill any areas of missing data for GMSLP2.1. Rather than simply using a monthly normal, a separate background field was created for each month of the data set from 1871 to 1994, so that major aspects of interannual variability were retained, as illustrated in Figure 5. The background field data set, GMSLP2.0, was essentially the same as GMSLP1.2 from 25°N to 90°N, except in 1871-2. Further south, and globally in 1871-2, it was based on the input data sets detailed in Table 1, adjusted to remove regional biases with the aid of a 5° latitude by longitude global monthly climatology based partly on recent model analyses (Section 4.1.1).

###### **4.1.1 Global Monthly Climatology for 1984-89**

Ideally the global climatology would have been calculated from a single data set. However, the only global data set available at the time, derived from UKMO operational analyses, was unreliable in northern polar regions and in parts of Asia (Section 3). So we used a climatology of GMSLP1.2 for 90°N-25°N and the UKMO operational analysis climatology for 20°N-90°S. The join between the two data sets was set at 25°N/20°N to avoid using that part of GMSLP1.2 that included CSIRO (i.e. 20°N-60°S) and therefore avoiding a possible source of error in the climatology due to the relative unreliability of the CSIRO data set, as discussed in Section 3.2.3. The climatologies were calculated over the period from 1984 to 1989, this being a common period when the two data sets were most reliable. As Table 2 shows, GMSLP1.2 was potentially at its most reliable for 1957-1989 due to the inclusion of a maximum number of available input data sets, including CSIRO, while 1984 was the first complete year of data in the UKMO operational analyses.

###### **4.1.2 Creation of GMSLP2.0**

The main problem with GMSLP1.2, besides restricted coverage, was its inability to capture maxima and minima of MSL pressure, most notably in the Southern Hemisphere subtropical and subpolar regions. To avoid these biases in GMSLP2.0, all of the individual input data sets contributing to GMSLP1.2 for the region 20°N-90°S were adjusted by converting each of them to monthly anomalies relative to their own 1984-89 averages (except for Jones, and Jones and Wigley where the anomalies were calculated with respect to their whole periods i.e. 1951-85 and 1957-85

respectively) and then adding the anomalies to the 1984-89 global climatology. These adjusted input data sets were then blended together (with the same combinations as detailed in Table 2) using the 'median' method described in Section 3.1. This method was also used to adjust the whole of GMSLP1.2 in 1871-1872, when only CSIRO was available. Along with GMSLP1.2 north of 20°N for 1873 onwards, these fields constituted a globally incomplete provisional version of GMSLP2.0, with no data at all south of 15°N after July 1993, when the SIO input data set ended (Table 2). To extend GMSLP2.0 to global coverage, a Laplacian interpolation was performed with respect to the 1984-89 global climatology. The data sets were first bilinearly interpolated onto a 1° latitude by longitude resolution and smoothed 1:2:4:6:4:2:1 east-west then north-south. Then the Laplacians of the 1984-89 global climatology were calculated for the 1° areas containing missing data. The missing areas were filled by solving Poisson's equation forced by the Laplacians and with boundary conditions set by the values in the non-missing 1° areas (Reynolds,1988). Although we were able to make GMSLP2.0 globally complete using these techniques, there were several areas consisting almost wholly of climatology, including the region south of 15°N from August 1993 to December 1994.

#### 4.1.3 Analysis of GMSLP2.0

Relative to previous versions of the data set, GMSLP2.0 had increased coverage and much improved data quality, especially in the Southern Hemisphere.

Figures 6 and 7 are examples of the root-mean-square (RMS) and mean decadal differences, respectively, between GMSLP1.2 and GMSLP2.0. The fields are based on up to 120 monthly values at each grid-point, and are for two decades: 1901-1910, when GMSLP1.2 was less reliable, being based on only three input data sets (CSIRO,UKMO and NCAR); and 1951-60 when GMSLP1.2 incorporated almost the maximum number of available input data sets. The RMS differences in each decade are less than 2hPa for much of the Northern Hemisphere and tropics, where GMSLP2.0 is generally lower than GMSLP 1.2 (Figure 7) and are less than 1hPa north of 20°N, where GMSLP2.0 is simply a smoothed version of GMSLP1.2. However, south of 40°S the RMS differences become considerable reaching maxima of 18hPa and 6hPa in 1901-10 and 1951-60 respectively, which, as Figure 7 indicates, is due to the much lower values of MSL pressure found in GMSLP2.0. This is further highlighted in Figure 8 which shows annual time series of MSL pressure at Grytviken (54.17°S, 36.30°W) for 1905-1984 extracted from GMSLP1.2, GMSLP2.0 and observations. The most striking feature is the large discontinuity in GMSLP1.2 (approximately 5hPa), which occurs around 1950 and which is due to a change from one input data set to another in January 1951, i.e. 1905-1950 consists of CSIRO, while 1951-1985 is from Jones. However in GMSLP2.0 this discontinuity has been removed by using the enhanced versions of the input data sets, which eliminated the bias in GMSLP1.2 prior to 1951. The Southern Hemisphere subtropical anticyclones are also stronger in GMSLP2.0 (Figure 7), with values of MSL pressure up to 3hPa higher than in GMSLP1.2.

Figure 9 shows the decadal correlation between GMSLP1.2 and GMSLP2.0, based on up to 120 monthly values at each grid-point, for 1901-10 and 1951-60. For both decades, correlations are in the range 0.9-1.0 over most of the globe reflecting the relative consistency between GMSLP2.0 and GMSLP1.2. The lower correlations (0.8-0.4) south of 40°S, are a result of the seasonally varying improvements in GMSLP2.0 previously highlighted by the RMS differences. The very low correlations in east Africa (-0.2 in 1951-60) occur over a region of very high orography (i.e. altitudes in excess of 2000m) and so neither data set can be wholly relied upon to provide accurate values of MSL pressure. Figure 10 shows the mean annual cycles for 1988-1992 from GMSLP1.2, GMSLP2.0 and the National Center for Environmental Prediction (NCEP) reanalysis (Kalnay et al.,1996) for the grid-box centred on (10°N,35°E), together with a corresponding time series for

Addis Ababa (8.59°N,38.48°E). It is clear that GMSLP2.0 and the NCEP reanalysis are more similar in form to the station time series (with correlations of 0.80 and 0.40 respectively) than GMSLP1.2 (with a correlation of 0.21). Therefore we can conclude that the low correlations in Figure 9 highlight a problem with GMSLP1.2 which has been rectified in GMSLP2.0. However, Figure 10 also shows that for the period 1988-1992, GMSLP2.0 is a constant 3hPa lower than the station and 2-3hPa lower than the NCEP reanalyses. However, when the station data are included in GMSLP2.1, we can expect to see this problem rectified.

The area of high RMS differences over South America in Figure 6 (4hPa in 1901-10), also occurs over a mountainous region. However, as the correlations in Figure 9 are high for this area, we conclude that this is an offset introduced by the UKMO analyses used to create the 1984-89 global monthly climatology.

Figure 11 shows the January and July mean GMSLP2.0 anomalies relative to 1961-90 for two periods, 1871-1900 and 1901-1930. Despite the aforementioned improvements, Figure 11 demonstrates that GMSLP2.0 is affected by persistent biases, in some regions throughout this 60 year period. For example, in January there are areas with positive anomalies in excess of +5hPa in the north Pacific and negative values of -3hPa in the south Pacific, together with further positive anomalies in the southern Atlantic and Indian Oceans. There is also a strong dipole of anomalies to the north-east of India, especially in the earlier period. In July, the anomalies over the north Pacific and Asia are less distinct, although there remains a serious negative bias over the southern oceans of 3hPa or more. A major aim in constructing GMSLP2.1 (Section 4.2) was to use observed data to remove these biases.

In summary, GMSLP2.0 was of a higher quality and more homogenous than GMSLP1.2, despite large portions of the data set being derived from the 1984-89 global climatology (for example the region 65°S-90°S). However, substantial biases remained, and its main purpose remained to act as a background field, which when combined with observed data was used to create GMSLP2.1.

## **4.2 GMSLP2.1**

Although GMSLP2.0 consisted of a globally complete individual MSL pressure field for every month for 1871-1994, it was heavily dependent on the component gridded analyses. To develop and further improve the GMSLP data set, we introduced observed data directly. These data were a blend of marine observations from the UKMOMDB and COADS, and land station time series from R.J.Allan (CSIRO), M.J.Salinger (NIWA), and the UKMO CLIMAT archive. The observations were blended with GMSLP2.0 to create GMSLP2.1.

Several versions of GMSLP2.1 data set were created (Table 3). GMSLP2.1c was the first published version (Allan et al., 1996), but it was found to suffer from bias over the tropical oceans (Section 4.2.2.1), owing to over-correcting marine data for standard gravity (as described in Appendix A, Section 1.1.1). A revised correction scheme was devised and applied to the marine data (Appendix A, Section 1.1.2), ultimately resulting in GMSLP2.1f, which is the most recent version of the data set.

### **4.2.1 Creation of GMSLP2.1**

#### **4.2.1.1 GMSLP2.1a to c**

The 1° gridded data set of marine observations (Appendix A.1) was combined with the quality controlled, blended land station time series (as described in Appendix A.2), to produce a data set of monthly 5° observed data for 1871-1994. This was done by first ascribing all station time series

to a 1° area and then converting all land and marine 1° area values to differences relative to a 1° resolution GMSLP2.0. These values were then spatially averaged to create 5° grid-point differences, checking individual monthly 5° fields for extreme values, which were removed where necessary. These quality controlled differences were then added to a 5° resolution GMSLP2.0. The percentage decadal coverage resulting from this quality controlled data set can be seen in Figure 12. This clearly shows that the majority of the data in the first decade (1871-1880) were concentrated in North America, Europe and along the main shipping routes in the Atlantic and Indian Oceans, with coverage in the Pacific Ocean restricted to a few island stations. However during subsequent decades, the density of coverage increased and by 1901-1910, marine data had begun to extend into the Pacific. Since then both the spatial extent and density of coverage generally increased progressively, until the 1950s, since when it has been consistently high, with the main data-sparse areas restricted to the high latitudes and continental interiors. From examination of the data coverage, it is clear that the areas of bias in GMSLP2.0 (as described in Section 4.1.3), i.e. the Southern Hemisphere mid-latitudes, north Pacific and south-east Asia, appear to coincide with data-sparse regions in the observed data and therefore any simple combination of these data with GMSLP2.0 would result in the introduction of similar bias into GMSLP2.1. So for GMSLP2.1b onwards, monthly climatological values for 1961-90, derived from GMSLP2.0, were added to the relevant fields of observed data in three areas, the Southern Hemisphere south of and including 40°S prior to 1957, and the north Pacific (60°N-20°N, 130°E-130°W) and south-east Asia (50°N-30°N, 70°E-100°E; 30°N-10°N, 90°E-105°E) prior to 1951 (Figure 13). However to prevent the climatology overwhelming real data, its inclusion was restricted to those grid-points within the relevant areas, that were missing data and that were more than 10° latitude equivalent distant (660Km) from any neighbouring grid-points with real data. This data set of combined real data and climatology was then blended with GMSLP2.0 using a Laplacian interpolation (Reynolds, 1988) to infill any remaining areas of missing data. Finally the monthly anomalies of the resulting 5° resolution data set were checked for major bullseyes, with a light smoothing applied where necessary (i.e. 1:2:1 east-west then north-south). The resulting published version (Allan et al., 1996) is GMSLP2.1c (Table 3).

#### 4.2.1.2 GMSLP2.1d to f

Despite the precautions described above, GMSLP2.1c suffered from several local biases, mainly affecting the Pacific region, but also in areas of high altitude, such as the Rockies, owing to problems reducing the observations to sea-level. In addition, spurious trends in the Tropics were found to result from over-correction of marine data for gravity (Section 4.2.2.1 and Appendix A).

In the central Pacific, there was a region with persistently low pressures from 1935-1942 (Figure 14(a)). These values, representing a bias of up to 1hPa from the long-term mean, originated from the background field (GMSLP2.0). As this is a data-sparse area, it was not possible to objectively correct the data and so for GMSLP2.1d onwards climatology was inserted instead (Figure 13).

Over Fiji (Figure 14(b)), an annual average time series showed a jump of 2hPa in 1875, followed by a slight negative trend. The jump was caused by the difference between GMSLP2.0 and the observations, when the observations were introduced in 1875. The trend was caused by the blending of one long term station time series Suva (18.09°S, 178.27°E), which until 1926 was based on relatively high morning-only observations, with several shorter time series after 1940, which were derived from daily means of two or more observations. The trend was removed for GMSLP2.1d onwards by compensating the Suva time series prior to 1926 for the semi-diurnal cycle and reblending it with the shorter time series.

The progression from GMSLP2.1d to f by application of improved gravity corrections is detailed

in Appendix A.

The final data set, GMSLP2.1f, is a great improvement on GMSLP2.0 owing to the inclusion of real, observed data. However, the use of climatology in certain data-sparse areas until the 1950s represents a limitation, to be addressed in future versions of GMSLP.

#### 4.2.2 Analysis of GMSLP2.1f

##### 4.2.2.1 Investigation of trends

Figure 15 shows the trends in annual averages of GMSLP2.1c and GMSLP2.1f for the period 1901-1950 and illustrates the improvements in GMSLP2.1f due to the application of the revised marine gravity correction scheme. Figure 15 also shows the corresponding trends in GMSLP2.0. The trend was calculated at each grid-point from a linear regression of 600 monthly values. As linear regression has been used, apparent trends may arise either from true linear trends in the data or from discontinuities.

In GMSLP2.1c there are extensive areas of positive trends over the oceans and especially in the Tropics, where the Atlantic has a trend in excess of 0.4hPa/decade. There are no corresponding positive trends in GMSLP2.0. These trends in GMSLP2.1c are clearly artificially induced by the gravity corrections and are largely absent from GMSLP2.1f. The large negative trends in both GMSLP2.1 data sets over high northern latitudes are due to persistent anomalously high values of MSL pressure during the period 1901-1930. These may have resulted from biased manual historical analyses (Rodewald, 1950), as data were sparse. GMSLP2.1c and GMSLP2.1f also have scattered bulls-eye trends, especially over north Africa, California and South America. These have been caused by trends in station data and/or GMSLP2.0, or discontinuities incurred by changing between the observations and GMSLP2.0 when the two sources disagree. The latter is the main problem over north Africa.

The main improvements over GMSLP2.0 include the removal of misleading negative trends in high southern latitudes and over south-east Asia. In GMSLP2.1f, positive trends over the subtropical southern oceans are also reduced. In GMSLP2.0 these were a result of relatively weak subtropical high pressures during the early part of this period.

Decadal means and standard deviations of anomalies with respect to 1961-1990, based on 120 monthly values per grid-point, were also examined. Figure 16(a) shows time series of hemispheric MSL pressure anomalies for 1871-1990. Gridded values were area-weighted using the cosine of latitude. The Northern Hemisphere time series is fairly constant, although there is a tendency towards lower mean values in the 1920s and 1930s. The Southern Hemisphere has a slight decrease between 1871 and 1935, followed by a steady increase. The standard deviations of monthly grid-point anomalies (Figure 16(b)) are relatively constant for the Northern Hemisphere until 1925, when there is a slight increase of 0.5hPa, probably due to an improvement in data coverage. The Southern Hemisphere also shows an increase in standard deviation after 1945. Again this represents improved data coverage, with earlier years influenced by climatology.

##### 4.2.2.2 Comparison of GMSLP2.1f and GMSLP2.0 using correlations and RMS differences

Figure 17 shows 124-year time series of the field correlation and RMS differences between GMSLP2.1f and GMSLP2.0, calculated for two latitude zones, 70°N-30°N and 30°N-30°S and the combined zone 70°N-30°S. The statistics are calculated annually from the monthly 5° gridded observations input to GMSLP2.1f rather than GMSLP2.1f itself.

The correlations show increasing trends while the RMS differences show decreasing trends. This is mainly because GMSLP2.0 provided a better background field in recent decades, when a broader selection of input analyses, based on more observations, was available: as a result, the input of observations during the creation of GMSLP2.1f made less difference than for earlier periods. So a lower correlation and a higher RMS difference implies a greater *improvement* of GMSLP2.1f over GMSLP2.0.

The correlation for the overall 70°N-30°S zone is very low in 1871 when GMSLP2.0 is very suspect (less than 0.2), but improves to over 0.8 by 1950, after which the level steadies. However the correlations for the two sub-zones are markedly different. The northern zone has higher correlations, because the analyses input to GMSLP2.0 were based on a denser observational data base over the continents and major shipping lanes (Figure 12), so that the improvement made in creating GMSLP2.1f was not as great as further south, though still substantial before 1950 and especially before 1890. The period of low correlations for 1885-1920 in 30°N-30°S, is due mainly to low correlations over the Indian Ocean, where the observations made GMSLP2.1f substantially better than GMSLP2.0. The particularly low value in 1960 represents improvements due to the incorporation of observations over the Indian and Atlantic Oceans, while the sudden drop in 1994 is caused by low correlations over the Himalayas, probably due to poor reduction of the observations to sea-level.

Unlike the correlations, the RMS differences for 70°N-30°N and 30°N-30°S are very similar, with generally high values (of about 1hPa) until 1915, gradually decreasing to 0.25 by 1965. The initially large differences are due mainly to the removal of positive bias in going from GMSLP2.0 to GMSLP2.1f. The bias in GMSLP2.0 reduced to zero by 1925. Subsequent decreases in RMS differences are mainly due to the improved background field, as stated above. The peaks in 70°N-30°N in 1917 and 1922 can be traced to Russia, where the observations make GMSLP2.1f higher than GMSLP2.0, while the discontinuities in 1939 and 1945 are due to the Second World War, when the observations effected a greater improvement in GMSLP2.1f over GMSLP2.0, especially over the north-east Atlantic and north-west Pacific.

#### 4.2.2.3 El Niño Southern Oscillation and North Atlantic Oscillation

Figures 18 and 19 show the monthly observed (station-based) indices for the El Niño Southern Oscillation (ENSO) and the North Atlantic Oscillation (NAO) respectively, together with indices calculated from GMSLP2.1f. Indices are standardised pressure differences between stations or grid-points (e.g. Ropelewski and Jones (1987) for the Southern Oscillation Index (SOI)). There is a high correlation in both cases, in excess of 0.9, although the GMSLP2.1f SOI is generally less extreme than the observations, possibly due to the effects of smoothing and interpolation.

#### 4.2.2.4 Anomaly percentiles

Figure 20 shows the percentage likelihood that half-year average MSL pressure anomalies observed in (a) January-June 1917 and (b) July-December 1982 exceeded values in the distribution of half-yearly anomalies for 1961-1990. Percentiles were estimated by fitting the half-yearly anomalies to gamma distributions (Horton, 1997). The percentiles give some indication of the spatial coherence of the MSL pressure patterns associated with ENSO and NAO.

The percentiles for January-June 1917 indicate a large area of anomalies exceeding the 98th percentile over the central and eastern Pacific Ocean, together with anomalies falling into the 2nd percentile over much of the west Pacific and Indian Oceans, which is suggestive of a La Niña episode. This is confirmed by the SOI which has a maximum value in January-June 1917 of +3.3 standardised units. There is also a suggestion of a reversed NAO, with an minimum index value

of -1.2 during the first six months of 1917, as pressures over the Azores and Iceland are below the 50th percentile and above the 98th percentile respectively. The high values in the far north in 1917 are a result of bias (Rodewald, 1950).

For July-December 1982, the percentiles show a reversal of the 1917 pattern over the Pacific Ocean, with more extreme values over western areas. This pattern has an associated observed SOI value of -2.9 and is indicative of an El Niño episode. The other area of interest is the subtropical North Atlantic, where there is an area of extreme positive anomalies. This together with a less extreme negative anomaly over Iceland, resulted in a strongly positive NAO of +0.7.

#### 4.2.2.5 Further analysis of GMSLP2.1

Figure 21 shows decadal-averaged annual cycles for three grid-points: (45°S,0°E), in the South Atlantic; (45°N,0°E), in western Europe; and (25°N,5°W), in north-west Africa. It is clear that the mid-latitude South Atlantic (Figures 21(a,b)) is greatly influenced by the insertion of climatology prior to 1951, as the shape of the annual cycle has been maintained throughout the period of the data set. However, north-west Africa has higher pressure by up to +2hPa in April-September during 1871-1910, relative to subsequent decades (Figures 21(e,f)). This may indicate that GMSLP2.1f is biased in this area in the earlier decades. The changes shown for the data-rich European grid-point may be real (Figures 21(c,d)) as they are spatially consistent with the surrounding region.

Figure 22 shows the global distribution of the decadal means and standard deviations of monthly anomalies (w.r.t. 1961-1990) for 1921-1930 and 1981-1990. The anomalies (Figures 22(a,c)) are generally weak, but 1921-1930 shows relatively large positive anomalies over northern Canada and north-eastern Russia, which are probably due to bias (Rodewald, 1950). The standard deviations since 1951 look realistic, with an increase in variance towards the poles in both hemispheres, and where the Northern Hemisphere is the most variable, as illustrated by 1981-1990 (Figure 22(d)). However the earlier decades are affected by a lack of observations and the use of climatology in the Southern Hemisphere to remove bias. As Figure 22(b) shows, 1921-1930 has some indication of greater variance in the mid-latitude region than in the tropics, especially over the data-rich Northern Hemisphere, although the values are generally smaller than in the later decade.

Figure 23 shows values of the T-statistic (a measure of the significance of the decadal mean differences) and the F-statistic (a measure of the significance of the changes of the decadal variance of the monthly data, normalised w.r.t 1961-1990) relative to 1981-1990, for the decades 1891-1900, 1921-1930 and 1971-1980. The statistics are both based on 120 monthly values at each grid-point. These figures show that a high percentage of the globe is covered by values of  $ABS(T) > 1.96$ , significant at the 5% level, especially for the earlier decades (Figures 23(a,c)). However, some of these significant values represent real phenomena, for example Figure 23(e) shows an area over Australia, where the T-statistic is significantly low in 1971-1980 (a period of La Nina) relative to 1981-1990 (a period of El Niño).

The maps of the F-statistic for the earlier decades (Figures 23(b,d)), show a higher percentage of values significant at the 5% level ( $< 0.69$  or  $> 1.43$  for 118 degrees of freedom) over the tropical oceans, when compared with 1971-1980. The high values are due mainly to bias introduced from the background field, where the data coverage is sparse. The areas of low values in decades prior to 1951 reflect regions where climatology is present.

A further problem remains in the Pacific around latitude 30°N, where an empirical orthogonal function (EOF) analysis revealed a marked annual oscillation in the data, caused by problems with

the seasonality of the background field during 1871-1900 (not shown).

## 5. Conclusions

GMSLP2.1f is the most recent version of the Global Mean Sea-Level Pressure data set. GMSLP2.1f is more reliable than GMSLP1.2, as it is strongly influenced by quality-controlled observed data. GMSLP2.1f, or preceding versions, has already been used in various analyses, especially studies of ENSO (Allan et al., 1996) and for model validation (Mullan et al., 1997). However there remain several weaknesses, namely the necessity of using climatology in data-sparse regions, especially in the Southern Hemisphere, together with a lack of reliable observations in the earlier decades. Some initial problems with the quality-control of several key land station time series led to the introduction of noise into early versions of the data set: adjustments have been applied (Section 4.2.1) but further improvements need to be made (Section 4.2.2.2). The problem of noisy data is relatively insignificant on a global scale, but for some regional studies it has been found that band-pass filtered data are of more use.

A completely new GMSLP3 is planned. This will use a background field based on EOF reconstruction techniques, developed by Rayner et al.(1996) for the creation of the GISST data set. By using such techniques, we hope to remove the need for a background field reliant on other data sets and therefore eliminate much of the bias that has affected the creation of GMSLP2.1.

## Acknowledgements

Many thanks to Rob Allan(CSIRO) for his advice and for all his hard work on the collection and preparation of land station time series for GMSLP. Thanks also to Jim Salinger(NIWA) for providing vital Pacific Ocean data and to Brett Mullan(NIWA) for his analysis of GMSLP2.1.

## References

- Admiralty Hydrographic Department 1938. *Admiralty Weather Manual*, HMSO, London, p8-9.
- Allan, R.J., Lindesay, J.A., Parker, D.E. 1996. *El Niño Southern Oscillation and climatic variability*, CSIRO, Australia, 408pp.
- Asnani, G.C. 1993. *Tropical Meteorology, Volume 1*, Pune, India, p363-392.
- Bottomley, M., Folland, C.K., Hsiung, J., Newell, R.E. and Parker, D.E. 1990. *Global Ocean Surface Temperature Atlas (GOSTA)*. Joint Meteorological Office and Massachusetts Institute of Technology Project. Project supported by US Dept. of Energy, US National Science Foundation and US Office of Naval Research. Publication funded by UK Depts. of the Environment and Energy. HMSO, London. 20 + iv pp. and 313 Plates.
- Buchan, A. 1868. *Handy Book of Meteorology*. William Blackwood and Sons, Edinburgh and London. 371 + xii pp. and 6 Plates.
- Davies, J.R., Rowell, D.P. and Folland, C.K. 1995. 'Forcing the Hadley Centre model with GISST: European Variability', from *Workshop on simulations of the Climate of the Twentieth Century using GISST*, Climate Research Technical Note CRTN56, edited by C.K.Folland and D.P.Rowell, April 1995.

- Horton, B. 1997. 'Percentile analysis of gridded global temperature anomalies', Climate Research Technical Note CRTN (in press).
- Jackson, M. 1986. 'Operational superfiles in Met O 13', *Met O 13 technical note 25*, 55pp.
- Jones, P.D. 1991. 'Southern Hemisphere sea-level pressure data: an analysis and reconstructions back to 1951 and 1911', *Int.J.Climatol.*, **11**, 585-607.
- Jones, P.D. and Wigley, T.M.L. 1988. 'Antarctic gridded sea level pressure data: an analysis and reconstruction back to 1957', *J.Climate.*, **1**, 1199-1220.
- Kalnay, E., Kanamitsu, M., Kistler, R., Collins, W., Deaven, D., Gandin, L., Iredell, M., Saha, S., White, G., Woollen, J., Zhu, Y., Chelliah, M., Ebisuzaki, W., Higgins, W., Janowiak, J., Mo, K.C., Ropelewski, C., Wang, J., Leetmaa, A., Reynolds, R., Jenne, R., Joseph, D. 1996. 'The NCEP/NCAR 40-year reanalysis project', *Bull.Amer.Meteor.Soc.* **77**, 437-471.
- Lamb, H.H. and Johnson, A.I. 1966. 'Secular variations of the atmospheric circulation since 1750', *Geophys. Mem.*, **14**, No.110.
- Mullan, A.B., Folland, C.K., Basnett, T., Renshaw, A. 1997. 'Simulation of climate variability for 1871-1994 forced by observed sea surface temperatures', from *Research activities in atmospheric and oceanic modelling*, CAS/JSC report No.25, edited by A.Staniforth. WMO.
- Parker, D.E. 1984. 'The statistical effects of incomplete sampling of coherent data series', *J.Climatol.* **4**, 445-449.
- Parker, D.E., Jones, P.D., Folland, C.K. and Bevan, A. 1994. 'Interdecadal changes of surface temperature since the late nineteenth century', *J.Geophys.Res.* **99**, 14373-14399.
- Potter, K.W. 1981. 'Illustration of a new test for detecting a shift in mean precipitation series', *Mon.Wea.Rev.* **109**, 2040-2045.
- Rayner, N.A., Horton, E.B., Parker, D.E., Folland, C.K. and Hackett, R.B. 'Version 2.2 of the Global sea-Ice and Sea Surface Temperature data set, 1903-1994'. Climate Research Technical Note CRTN74, September 1996.
- Reynolds, R.W. 1988. 'A real-time global sea surface temperature analysis', *J.Climate.* **1**, 75-86.
- Rodewald, M. 1950. 'On the question of atmospheric pressure conditions in the Arctic', Hamburg, Met.Amt Nordwestdtshl., *Ann.Met.*, **3**, No.9/10, pp.284-290.
- Ropelewski, C.F. and Jones, P.D. 1987. 'An extension of the Tahiti-Darwin Southern Oscillation Index', *Mon.Wea.Rev.* **115**, 2161-2165.
- Trenberth, K.E. and Paolino, D.A. 1980. 'The Northern Hemisphere sea-level pressure data set: trends, errors and discontinuities', *Mon.Weath.Rev.*, **108**, 855-872.
- Woodruff, S.D., Slutz, R.J., Jenne, R.L. and Steurer, P.M. 1987. 'A Comprehensive Ocean-Atmosphere Data Set', *Bull.Amer.Meteor.Soc.* **68**, 1239-1250.

## Appendix A: Quality Control of Observed Data

### A.1 Creation of a Gridded Data Set of Observed Marine MSL Pressure

We created a fully quality controlled monthly, 1° latitude by longitude gridded, observed marine MSL pressure data set for 1871-1993. At this stage it was not possible to extend the marine data set beyond 1993 due to the unavailability of observed ships' data from the UKMOMDB after this date. A primary concern when processing all the observed data, was to try and maximise spatial coverage, so a quality control system was designed that accepted a higher proportion of 1° latitude by longitude boxes in the low variance Tropics, such that despite a particular 1° area sample being small, it was accepted if all the observations in the sample were consistent. We were also able to include data derived from the COADS data set. However, as we only had access to the gridded 2° latitude by longitude data rather than the individual raw observations, we only included a gridded COADS value if it compared favourably with neighbouring quality controlled UKMOMDB values. This resulted in a slight extension of the initial gridded UKMOMDB data, with any extensive areas of missing data remaining untouched.

#### A.1.1 Correction for Standard Gravity

Many marine pressure data prior to 1940, although obtained with mercury barometers, were not reduced to standard gravity, which is that at latitude 45°. Table 4 summarises the gravity corrections to be applied (at 1000hPa) to mercury barometers over a range of latitudes, with 0hPa required at 45°, a maximum of +2.6hPa at the poles and a minimum of -2.6hPa at the equator. Although the true correction required is in fact proportional to the magnitude of the raw observation, it will rarely differ by >5% from that required at 1000hPa. Figure A1 shows the seasonal differences between a corrected land station MSL pressure time series for Singapore (1.22°N, 103.55°E) and uncorrected and corrected time series extracted from the UKMOMDB and interpolated onto the station location. It is clear that the uncorrected UKMOMDB time series is about 2hPa higher than the station, prior to 1940, a difference that agrees favourably with the expected correction of -2.6hPa at this latitude (Table A1).

##### A.1.1.1 Linear Gravity Correction Scheme

As neither the individual UKMOMDB observations nor the COADS data gave any indication of the application of gravity corrections, we conducted a survey of ships' logs to establish the proportion of uncorrected MSL pressure observations per decade for the period 1871-1940. As only UK ships' logs were available, it was necessary to assume that UK ships were representative of all ships in the UKMOMDB and COADS data sets. The survey indicated that, for UK ships, mercury barometers were the official barometers used throughout the period 1871-1940, although occasionally a ship's aneroid barometer was used instead. Of the mercury barometer observations, none was corrected until 1924/5, after which the majority were corrected. The Admiralty Weather Manual for 1938 (Admiralty Hydrographic Department, 1938) has specific instructions for the application of gravity corrections, confirming that the majority of UK mercury barometer observations would have been corrected by then.

On the basis of this survey, a correction scheme was devised and applied to the individual UKMOMDB observations, whereby the required gravity corrections (Table A1) were scaled by the proportion of UK ships' logs reporting uncorrected data in the relevant decade, i.e. for an observation during 1871-1920, 100% corrections were applied; for 1921-1930, 50 % corrections were applied and 0% thereafter. However, although this scheme resulted in a slight improvement, especially before 1921, biases remained. For example relative to Singapore (Figure A1) there were peaks in the seasonal time series, in excess of +1.5hPa, for the period 1931-2. To avoid this problem, a 'linear' correction scheme was devised, with a 100% correction for 1871-1920; a

correction, decreasing linearly by 6.25% per year, for 1921-1935 (i.e. 93.75% in 1921 to 6.25% in 1935); and 0% for 1936 onwards. As Figure A1 shows, this reduced the peaks occurring around 1931 in the comparison with Singapore. The 'linear' correction scheme was applied to all individual observations from the UKMOMDB and to all gridded values in the COADS data set prior to 1936 in GMSLP2.1a to d.

#### **A.1.1.2 Revised Gravity Correction Scheme**

Subsequent analysis showed that the 'linear' gravity correction scheme introduced a negative bias over the Tropics prior to 1930 (see Section 4.2.2.1): the marine observations had been over-corrected. Investigation of the data sources revealed that the COADS values had already been corrected for gravity, while the only uncorrected data in the UKMOMDB archive were those derived from Dutch sources for 1871-1938. Therefore a new correction scheme was devised, whereby the UKMOMDB Dutch observations for this period were fully corrected for gravity, all other observations being assumed corrected at source. With the application of this new scheme, it was found that most of the bias in the Tropics ascribed to problems with gravity corrections, had been removed (see Section 4.2.4). The version of the data set created using the revised UKMOMDB marine observations is called GMSLP2.1e; inclusion of COADS yielded GMSLP2.1f (Table 3)

#### **A.1.2 Correction for the Effect of the Semi-Diurnal Oscillation**

MSL pressure samples may be biased by the semi-diurnal oscillation, especially in tropical regions. The oscillation has a maximum amplitude of 1.16hPa at the equator, decreasing to 0hPa at the poles (Asnani, 1993). However, Figure A2 shows that the UKMOMDB observations lying within latitudes 30°N-30°S, are evenly distributed at 4-hour local time intervals before 1931-40 and 6-hour GMT intervals thereafter (see Bottomley et al., 1990). So it is unlikely that monthly averages will be affected by the semi-diurnal oscillation, and no corrections were applied.

#### **A.1.3 Gridding Data from the UKMOMDB**

Figure A3 is a flowchart describing the creation and quality control of the gridded 1° latitude by longitude UKMOMDB MSL pressure data set.

For a target month, all relevant observations were read from the UKMOMDB, with those observations falling over land rejected immediately. The remaining observations were then corrected for standard gravity where necessary (as described in Appendix A.1.1.2) and the relevant GMSLP2.0 background values subtracted. If these differences were  $\pm 10$ hPa or more, then the observation was rejected. Then for each 1° area all relevant observed differences that passed the initial quality control and that lay within a 7° concentric area (centred on the target 1° box) were extracted, with those 1° areas found to have observations in fewer than 5 pentads in the target month rejected and set to missing. A pentad in this case, may have between 4-6 days, but there are always 6 pentads per month and 72 pentads per year (Table A2). For each 1° area with a suitable temporal coverage, several statistics were calculated from the daily mean observed differences within the target month; namely, the standard deviation and standard error, together with the sample error, using the method described by Parker (1984), and lag autocorrelations derived from UKMO operational analyses. Then if the sample error was found to be less than or equal to 20% of the standard deviation or the standard error was less than 1hPa, the 1° area in question was accepted. This method of testing the magnitude of the daily mean standard error was included in a successful attempt to maximise the number of valid 1° areas in the tropics, where the climatological variance is relatively low. If a 1° area was accepted, then the median of the daily mean differences was calculated and added to the relevant GMSLP2.0 background value and assigned to the relevant 1° area in the output field, otherwise the 1° area was set to missing. This sequence of testing was then repeated for all 1° areas in a target month and for all months for 1871-1993, resulting in a gridded

1° observed marine MSL pressure data set of UKMOMDB data.

#### **A.1.4 Blending the Gridded UKMOMDB and COADS Data Sets**

The COADS data set in the form of 2° latitude by longitude monthly fields for 1854-1993, was used to supplement the gridded UKMOMDB data in order to increase coverage. As we did not have the individual observations used to create COADS, we were unable to apply the same quality control as used on the UKMOMDB data. Therefore to maintain some consistency between the two data sets, we used the quality controlled gridded UKMOMDB data set as the primary source, with the COADS data only included where they could be quality controlled relative to the UKMOMDB data. The method used to combine the two data sets is described by the flowchart in Figure A4.

For each target month for 1871-1993, the latitude by longitude values for the 1° gridded UKMOMDB and 2° gridded COADS data, were converted to differences relative to the GMSLP2.0 background field. Initial indications were that the COADS values had not been corrected for gravity and so for GMSLP2.1 versions a-d a correction was applied to all values prior to 1936. However, subsequent investigations showed that the COADS values had been corrected at source and so they were left unaltered in GMSLP2.1f (GMSLP2.1e contained no COADS data (Table 3)). Then for each 2° COADS area, a check was made for coinciding 1° UKMOMDB areas containing data. If a match was found the COADS value was rejected and the coinciding UKMOMDB values were added to the relevant GMSLP2.0 background values and inserted into the combined data set.

Otherwise, the mean was calculated for all non-missing 1° UKMOMDB areas lying within a 10° radius of the centre of the 2° target area. If there were no data to calculate the mean, then the 2° COADS value in question was again rejected. If a mean was available then the 2° COADS value was accepted only if the difference between it and the mean 1° UKMOMDB value was less than 1hPa. Where the COADS value was accepted, it was added to the relevant GMSLP2.0 monthly value and placed into all four coinciding 1° areas in the composite data set. The overall effect of the merging process was to severely restrict the inclusion of the COADS data, but it also resulted in significantly increased coverage, especially in the Atlantic Ocean in the nineteenth and early twentieth centuries and in the Pacific Ocean in more recent years (Figure A5).

#### **A.2 Quality Control of Land Station Data**

We created a data set of quality controlled, monthly, MSL pressure over land. These data were derived primarily from a CSIRO-DAR archive of adjusted, monthly, land station time series (gathered from various sources, including World Weather Records, Monthly Climatic Data for the World and Reseau Mondial) which had been combined with a number of time series for New Zealand stations and South Pacific islands provided by NIWA. This combined archive was supplemented by time series for stations north of latitude 60°N derived from the UKMO CLIMAT archive. CLIMAT data, where available, were also used to update CSIRO-DAR/NIWA station time series into the 1990s.

All the station data in the CSIRO-DAR/NIWA archive had undergone a preliminary quality control, performed by R.J.Allan (CSIRO). This consisted of an initial check to remove jumps and trends from individual time series, with reference to all available station histories, followed by a comparison of nearest neighbours to identify and correct outliers, and the application of a version of the 'Potter' method (Potter, 1981) to objectively check for further discontinuities in individual time series relative to their neighbours (Allan et al., 1996).

Despite these extensive checks, many of the time series from the CSIRO-DAR/NIWA archive were excluded during the next stage of quality control, detailed in Figure A6. Each series in the CSIRO-

DAR/NIWA archive, together with a corresponding CLIMAT time series, was plotted as annually averaged differences relative to the background field, GMSLP2.0. Any station showing jumps, biases or extremes not shown by its neighbours (usually lying within the same WMO country group) was excluded for further investigation and possible inclusion in future versions of GMSLP. However, occasionally, when such jumps and biases occurred in groups of stations, we were able to identify problems in the background field. For example these checks identified a major discontinuity in GMSLP2.0 that occurred in 1899 over much of Europe and Asia (Figure A7), when the NCAR gridded data set was first included (Table 2). If there was any doubt about a station, then time series of station actual values and co-located background actual values were plotted to check the veracity of the station data. On occasion, when a station had individual extreme annual deviations from the background field, the relevant monthly deviations were checked and unlikely values deleted. Also, several stations had data excluded, where they were deemed to be suspect during the earliest parts of their records. In order to increase coverage, especially in data-sparse areas, several long-period CSIRO-DAR/NIWA stations that had been initially discarded, were re-examined and adjusted, and included in GMSLP2.1.

Many of the CSIRO-DAR/NIWA station time series ended during the 1980s and so where possible, they were updated to the end of 1994, using CLIMAT data for the corresponding station, if the CLIMAT time series was found to be consistent with the earlier records. For regions north of latitude 60°N, we included a number of long-period CLIMAT station time series, subject to the same quality controls, as in general this region was not included in the original CSIRO-DAR/NIWA archive.

As a result of this quality control, nearly 700 land station MSL pressure time series were accepted for inclusion in GMSLP2.1, with around 100 CSIRO-DAR/NIWA stations excluded for future investigation.

Table 1: Gridded data sources contributing to GMSLP2.

Data source	Area covered	Period	Resolution
UKMO Historical	15°N-90°N	1873-1995	Nodes of grid are at multiples of 5°lat.x 10°long.
UKMO Operational	Globe	1985-1995	Nodes of grid are at multiples of 2.25°lat.x 3.75°long.
NCAR	15°N-90°N	1899-1995	Nodes of grid are at multiples of 5°lat.x 5°long.
SIO	42.5°S-72.5°N	1951-1993	Nodes of grid are at multiples of 5°lat.x 10°long.
CSIRO	60°S-60°N	1871-1989	Nodes of grid are at multiples of 10°lat.x 10°long.
Jones	15°S-60°S	1951-1985	Nodes of grid are at staggered multiples of 5°lat.x 10°long.
Jones and Wigley	60°S-75°S	1957-1985	Nodes of grid are at staggered multiples of 5°lat.x 10°long.

## TABLE 2 CREATION OF GMSLP1.2

KEY: MO - UK MET OFFICE historical files, Northern Hemisphere (90N-15N) 1873-1994  
 NC - NCAR, Northern Hemisphere (90N-15N) 1899-1994  
 SC - SIO, near-global (72.5N-42.5S) 1951-1993(July)  
 CS - CSIRO(provisional), near-global (60N-60S) 1871-1989  
 JS - Jones, Southern Hemisphere (15S-60S) 1951-1985  
 JA - Jones and Wigley, Antarctic (60S-75S) 1957-1985

1871-1872	60N - 60S	CS
1873-1898	90N - 25N	MO
	20N - 15N	MO,CS
	10N - 60S	CS
1899-1950	90N - 25N	MO,NC (Dec. 1944:MO)
	20N - 15N	MO,NC,CS (Dec. 1944:MO,CS)
	10N - 60S	CS
1951-1985	90N - 75N	MO,NC (1980-1985:NC)
	70N - 25N	MO,NC,SC
	20N - 15N	MO,NC,SC,CS
	10N - 10S	SC,CS
	15S - 40S	SC,CS,JS
	45S - 55S	JS
	60S	JS (1957-1985 :CS,JS,JA)
	65S - 75S	JA (1957-1985)
1986-1989	90N - 75N	NC
	70N - 25N	MO,NC,SC
	20N - 15N	MO,NC,SC,CS
	10N - 40S	SC,CS
	45S - 60S	CS
1990-1994	90N - 75N	NC (1993- :MO,NC)
	70N - 15N	MO,NC,SC (Aug 1993-Dec 1994: MO,NC)
	10N - 40S	SC (1990-1993 (July))

### METHOD:

Where 2 data sets provided values, the mean was taken.

Where 3 or more data sets provided values, the median was taken.

Bulls-eyes over north-eastern Asia were adjusted with the aid of station data.

**Table 3**  
**Versions of GMSLP2.1**

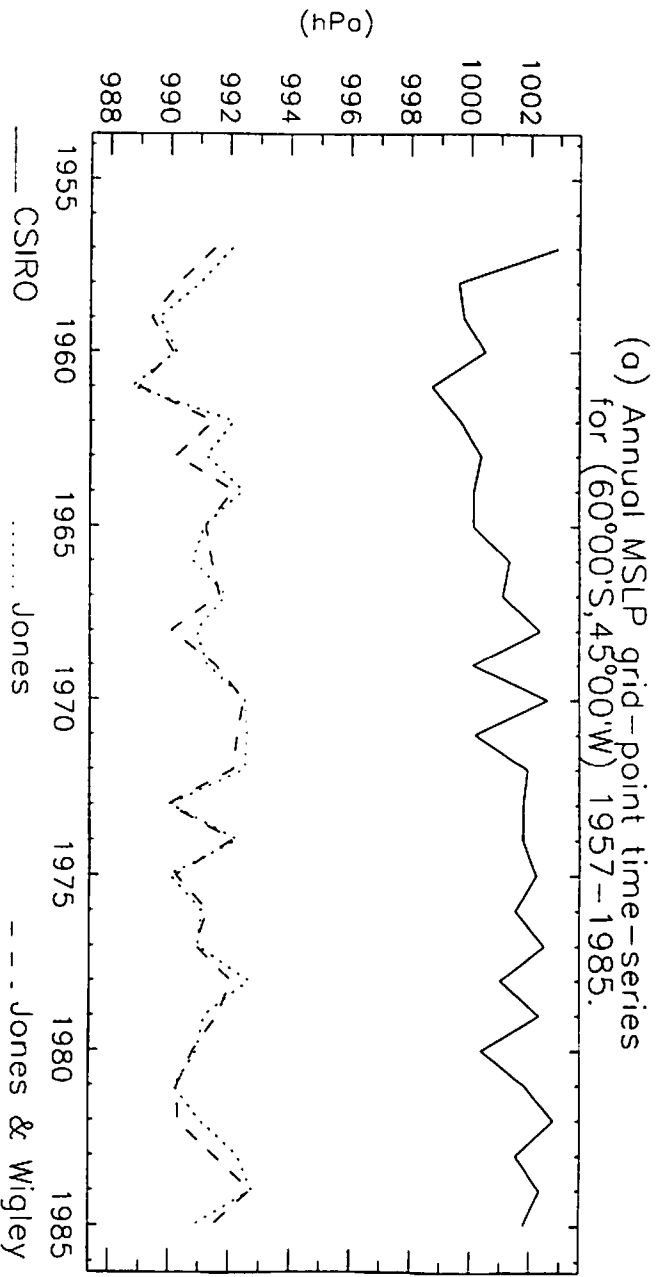
- a** Experimental version. Has linear gravity correction scheme (Appendix A, Section A.1.1.1) applied to UKMOMDB and COADS values, but includes no areas of climatology (as described in Figure 13).
- b** As (a), but includes areas of climatology (Figure 13).
- c** As (b), but includes station time series for Chatham and Campbell islands in the Southern Hemisphere. This version was published in Allan et al. (1996).
- d** As (c), but including a further area of climatology in the central Pacific (Figure 13) and corrections to the Suva, Fiji station time series.
- e** As (d), but using the revised gravity correction scheme (Appendix A, Section A.1.1.2) applied to the UKMOMDB values. COADS values were excluded.
- f** As (e), but including COADS values without over-correction for gravity (Appendix A, Section A.1.1.2).

**TABLE A1:**  
**Variation of Gravity Corrections with Latitude**

Latitude (°N/S)	Correction (hPa) (eg/ wrt 1000hPa)	Latitude (°N/S)	Correction (hPa) (eg/ wrt 1000hPa)
90	+ 2.6	40	- 0.5
80	+ 2.5	30	- 1.3
70	+ 2.1	20	- 2.1
60	+ 1.3	10	- 2.5
50	+ 0.5	0	- 2.6
45	0.0	-	-



**Figure 1:**  
**GMSLP1.1: Evidence of Discontinuity at 60°S.**



GMSLP1.1: mean MSLP values for 1957–1985 (15°S–90°S)

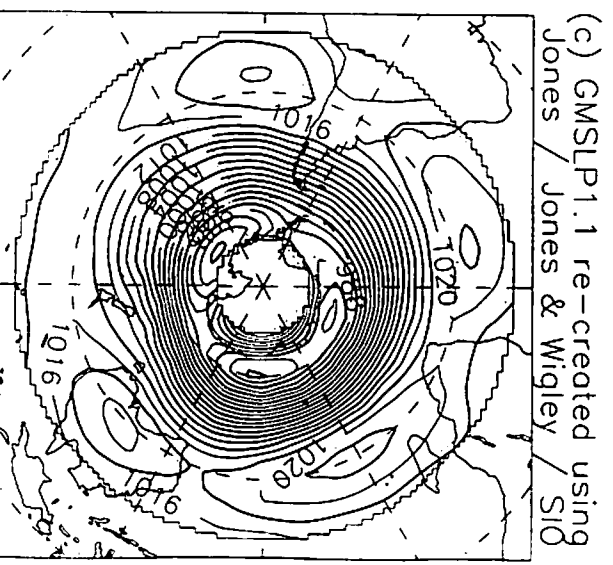
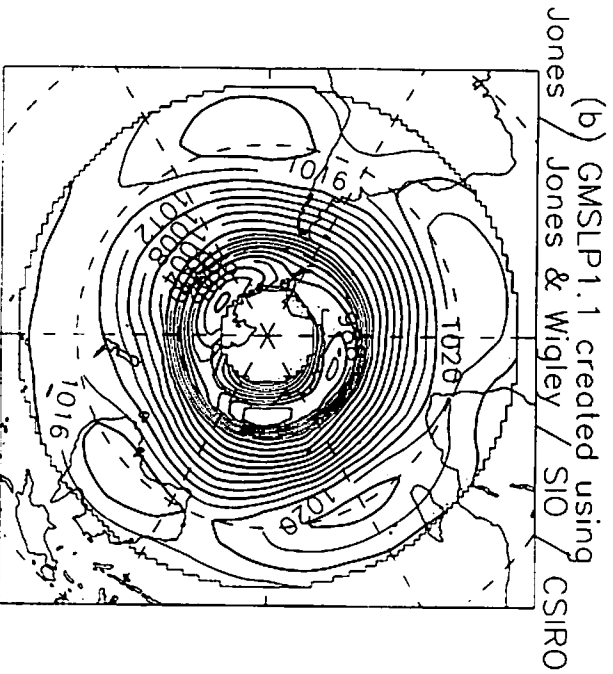
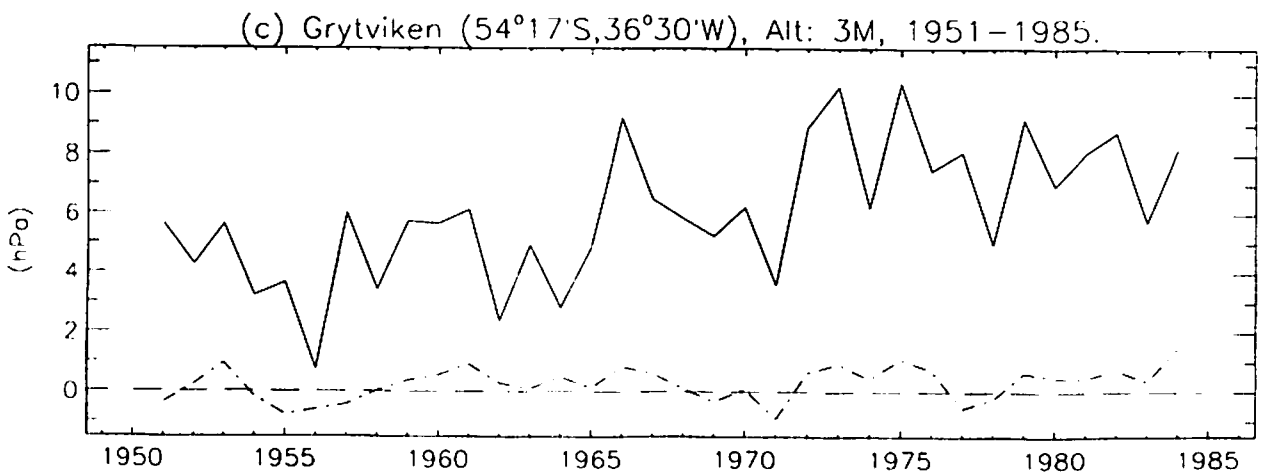
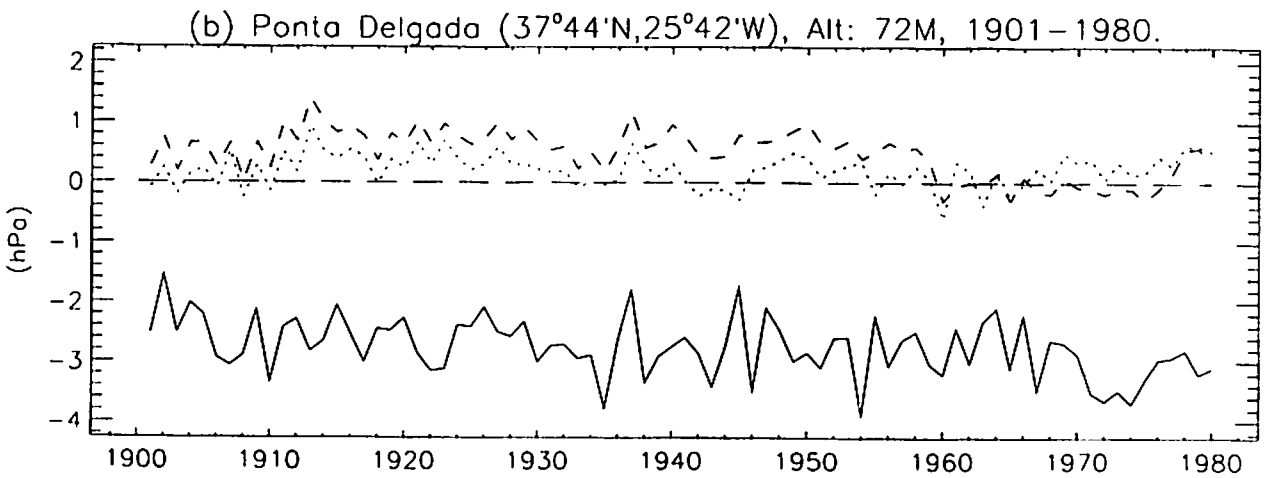
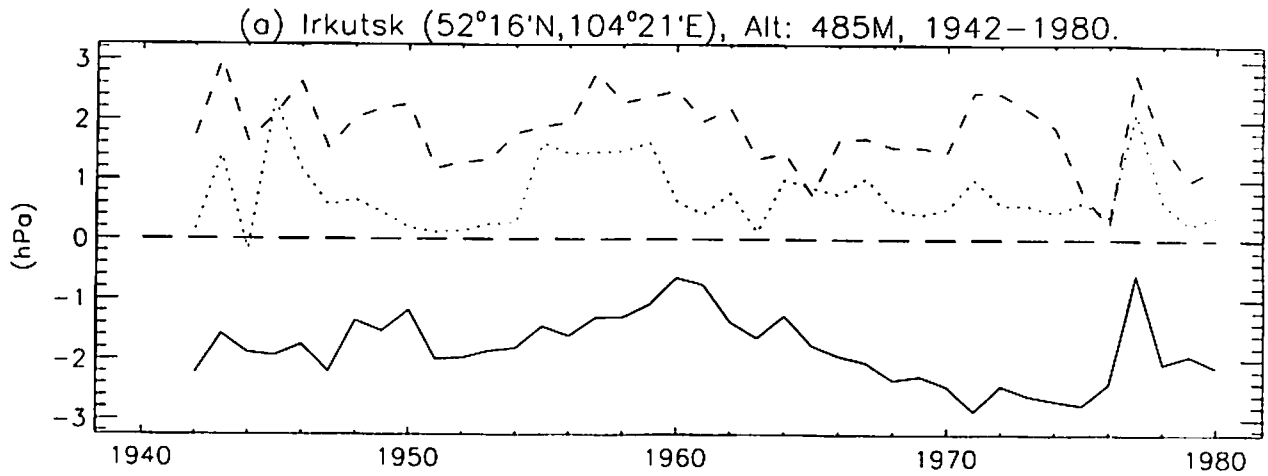


Figure 2: Annual Differences Between MSLP Interpolated from Gridded Data Sets and Observed Values.



— CSIRO      ..... NCAR      - - - UKMO      - . . . Jones

Figure 3:  
Annual MSLP Differences (hPa):  
CSIRO minus SIO meaned over the period 1951-1980

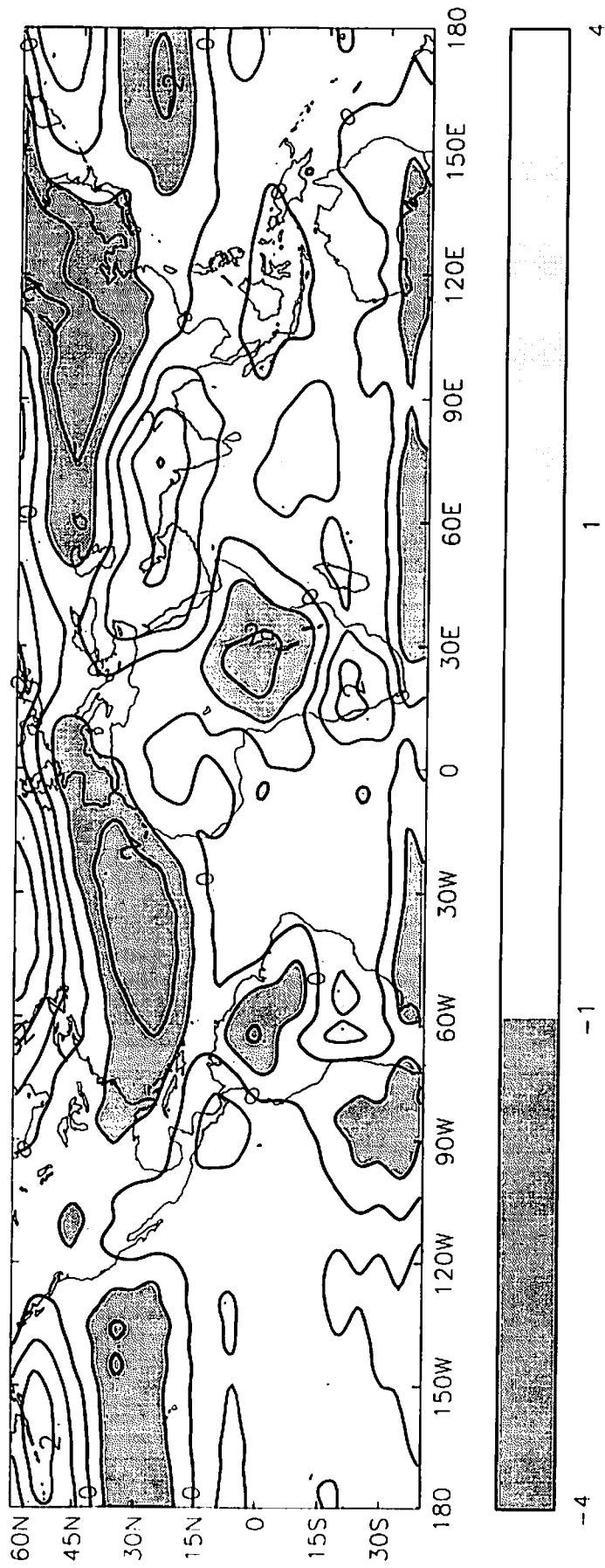


Figure 4: Flowchart to Summarise the Creation of GMSLP2.1f

30 Apr 97

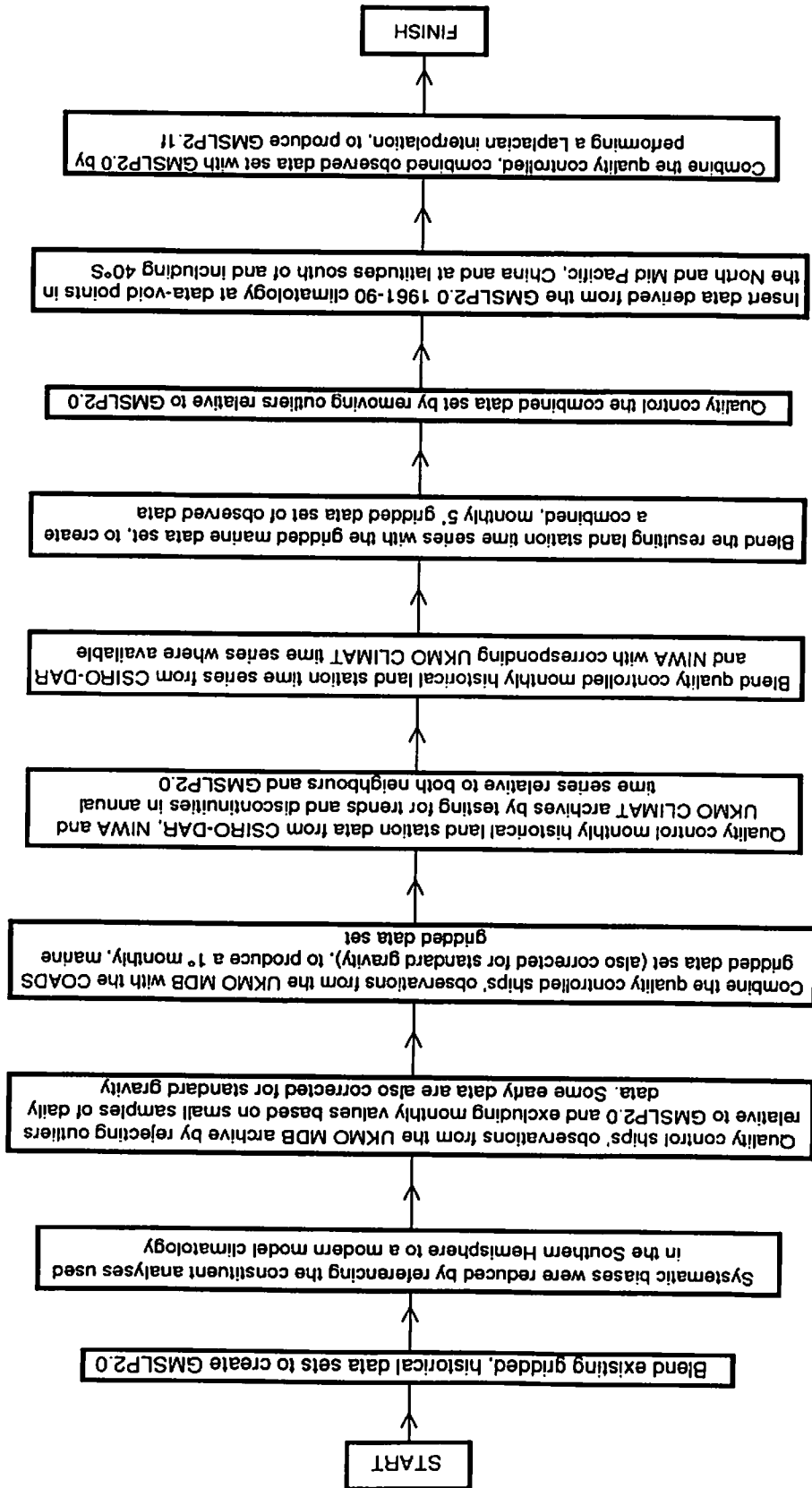




Figure 6  
RMS Differences (hPa): GMSLP2.0 wrt GMSLP1.2  
(contours every 1hPa)  
1901-1910

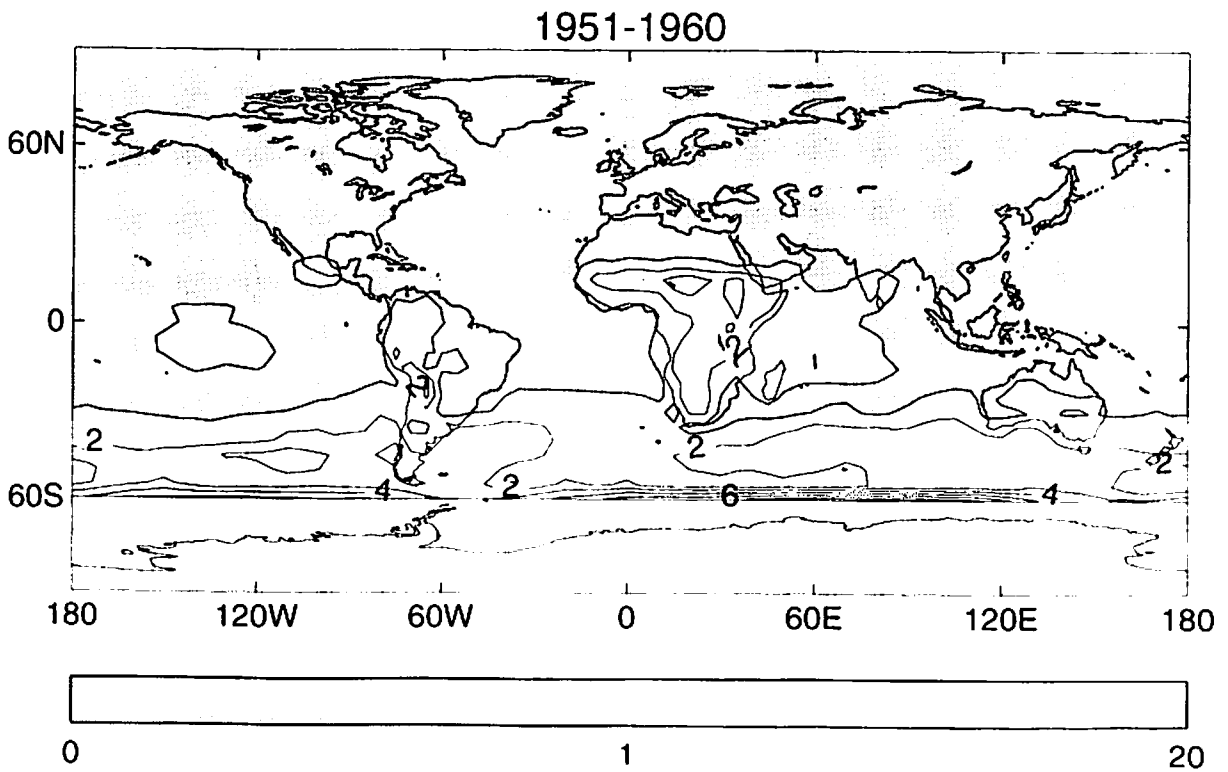
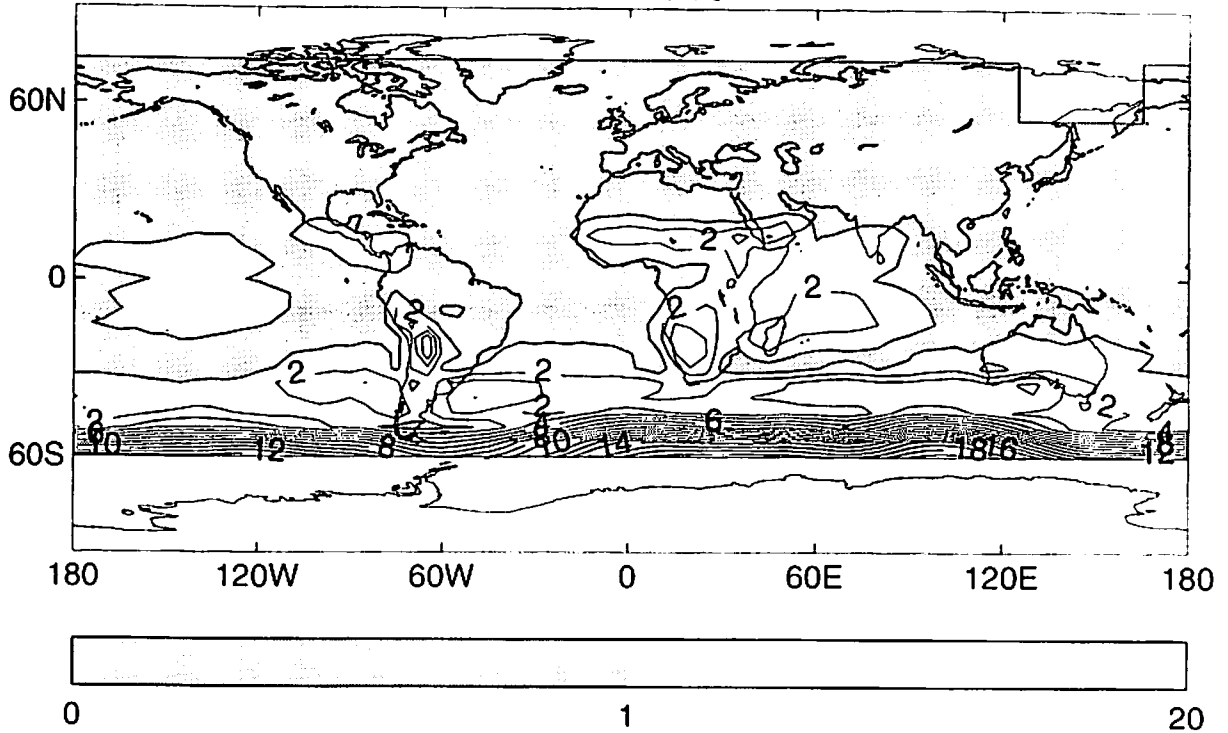
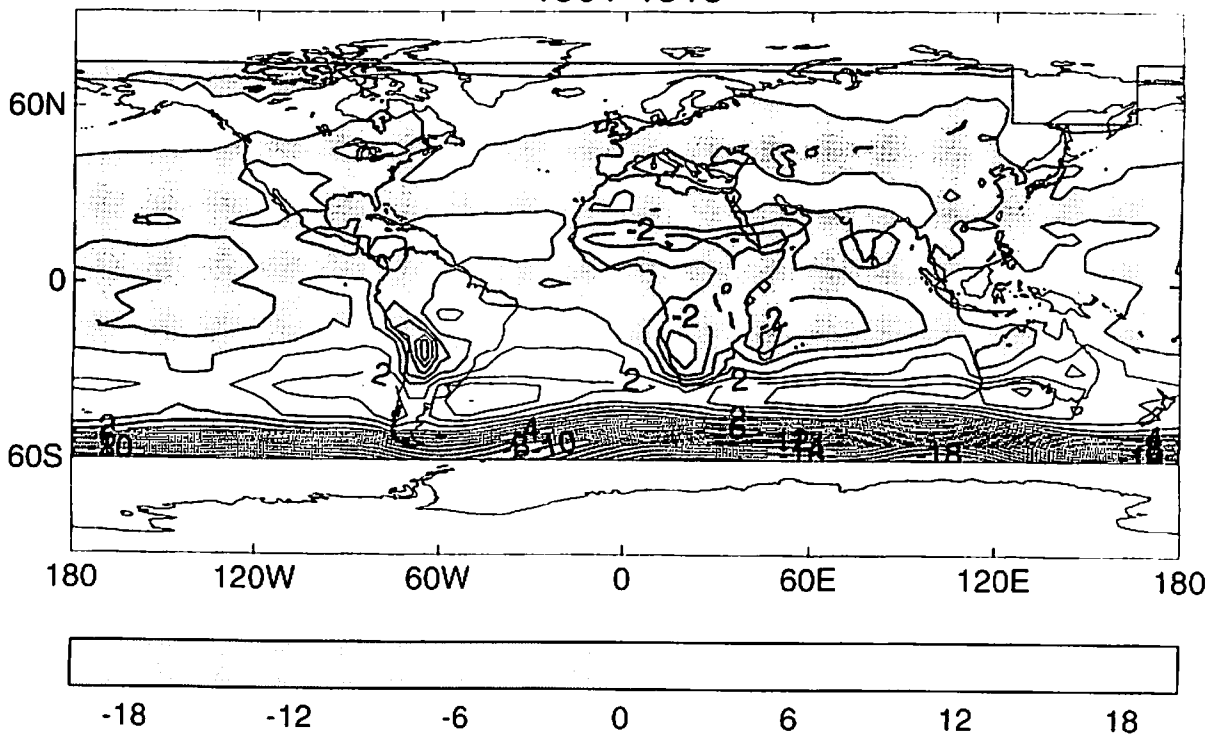


Figure 7  
Decadal Mean MSLP Differences (hPa):  
GMSLP2.0 minus GMSLP1.2 (contours every 1hPa)

1901-1910



1951-1960

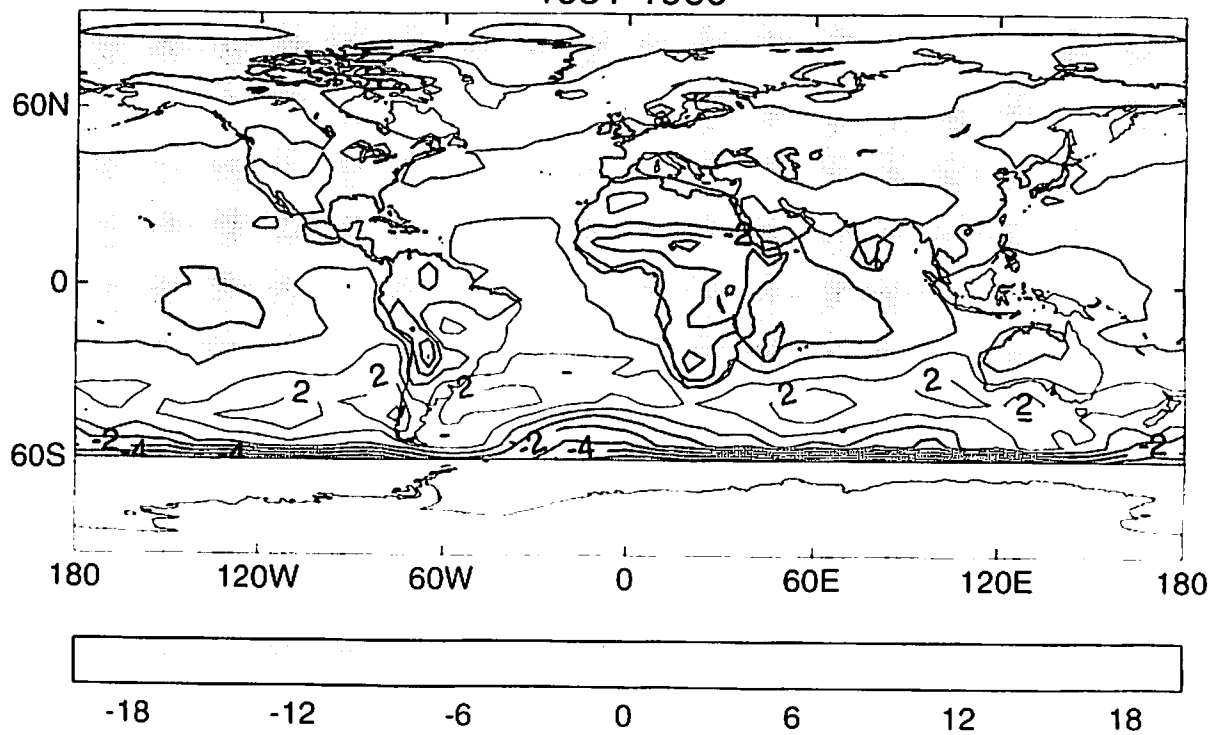


Figure 8:  
Annual MSLP time series for Grytviken (54°17'S, 36°30'W),  
Alt: 3M, 1905-1984.

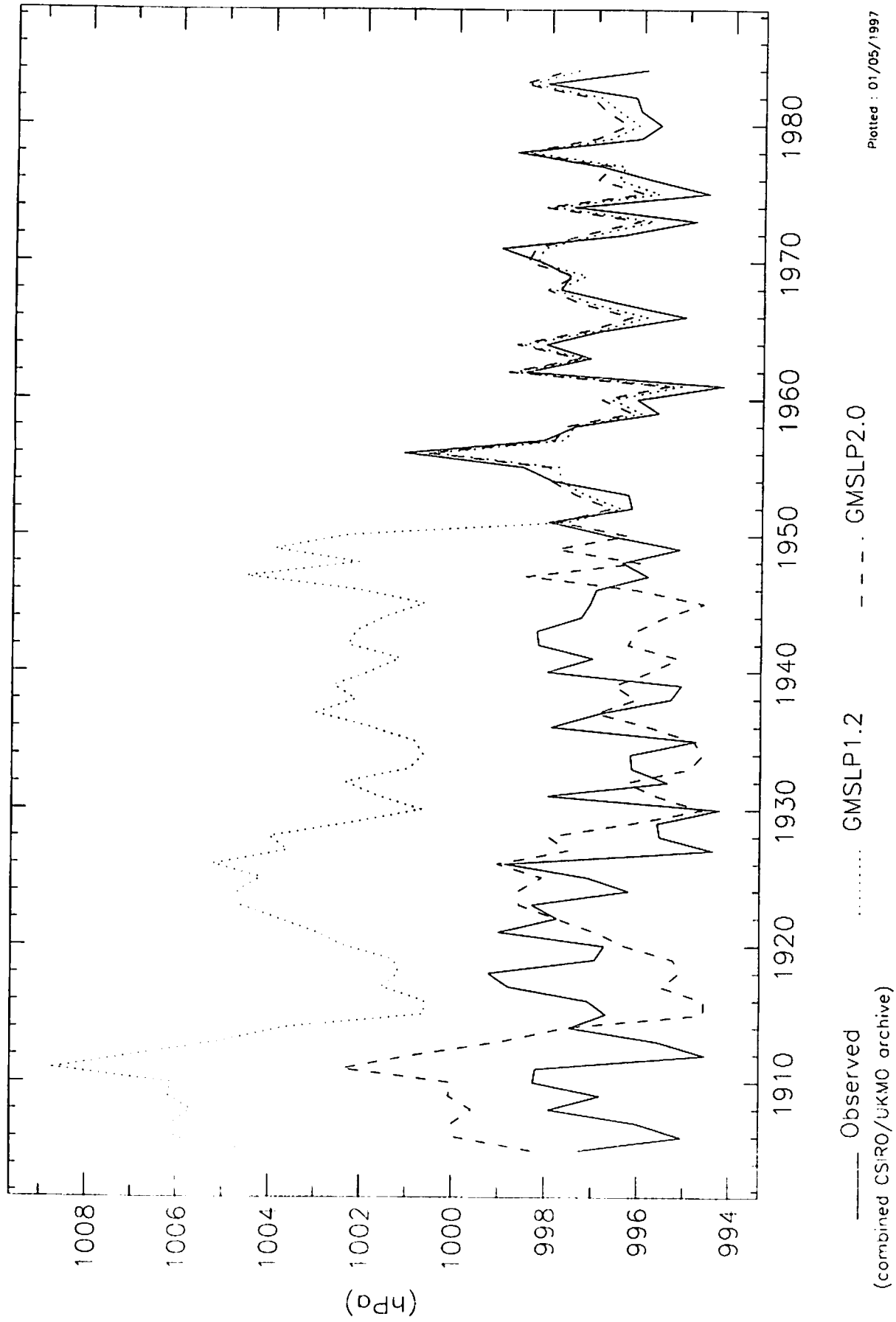
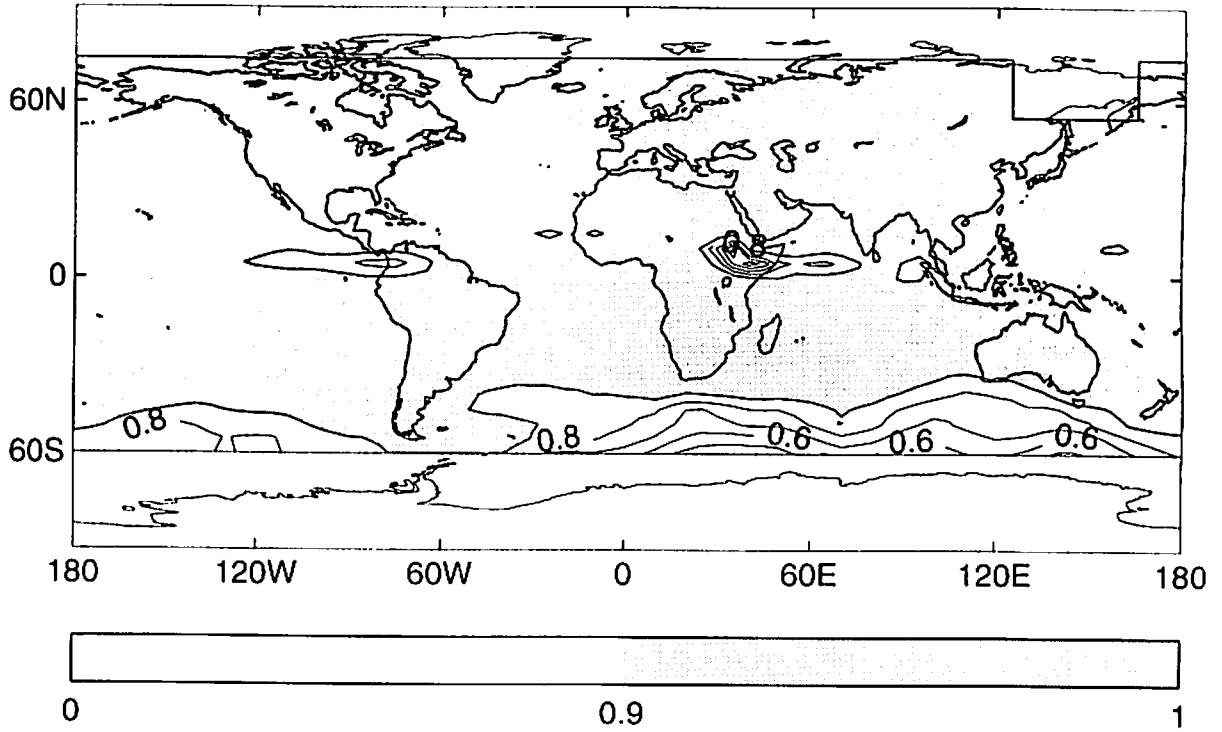


Figure 9  
CORRELATIONS: GMSLP2.0 with GMSLP1.2  
(contours every 0.1)

1901-1910



1951-1960

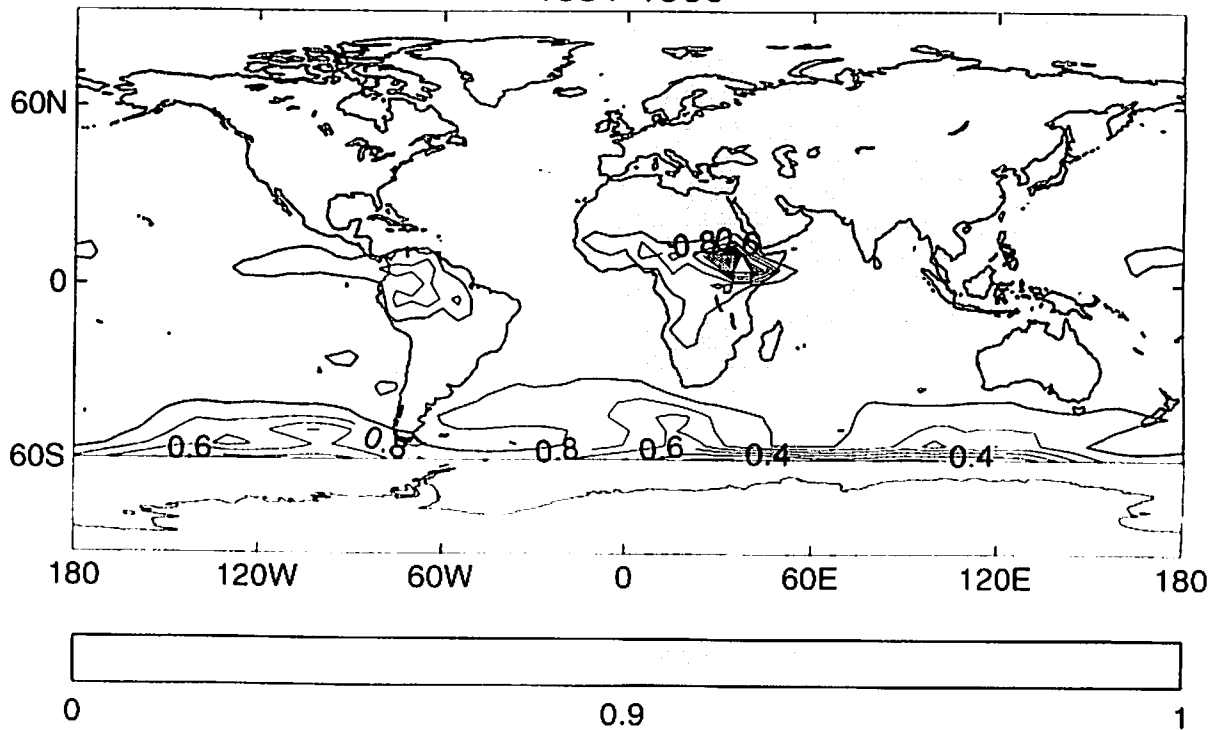


Figure 10: Comparison of Mean Annual MSLP Cycles for 1988-92 at Addis Ababa (8°59'N, 38°48'E) and Grid-Point (10°N, 35°E)

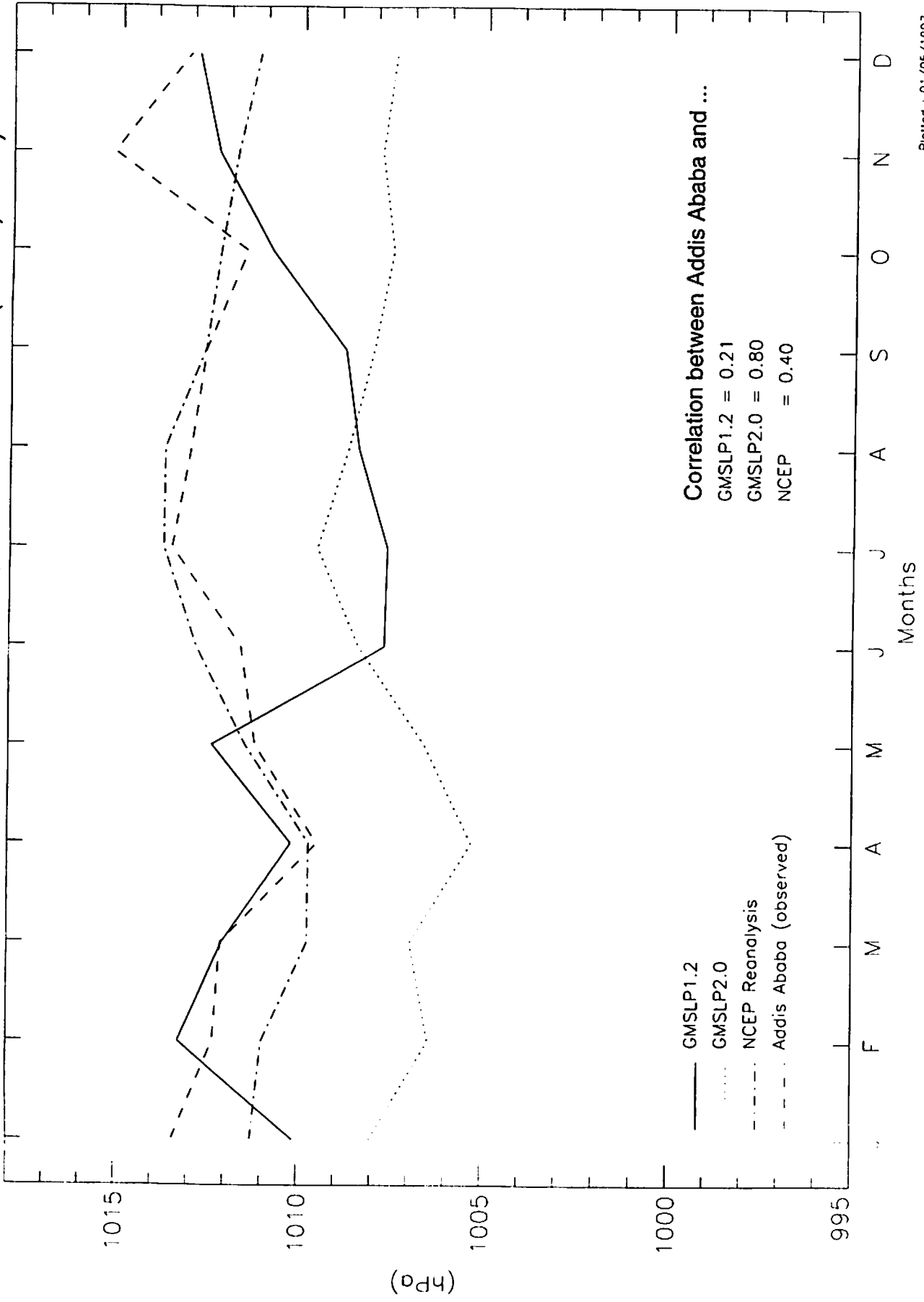
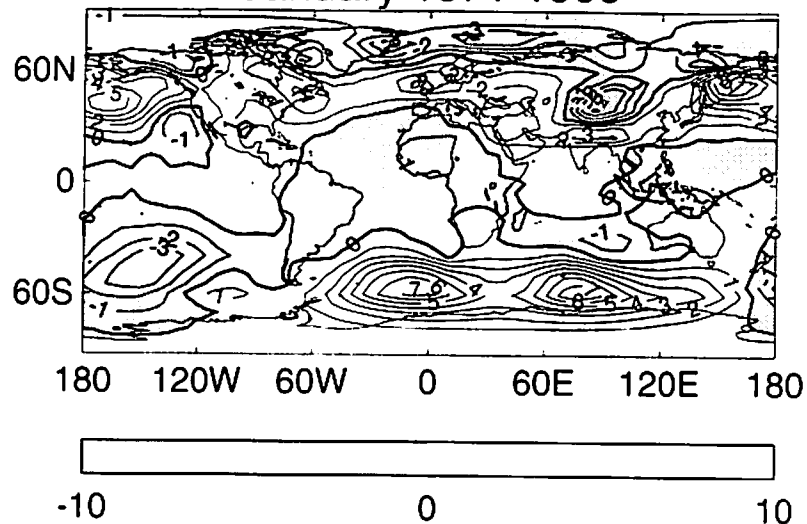
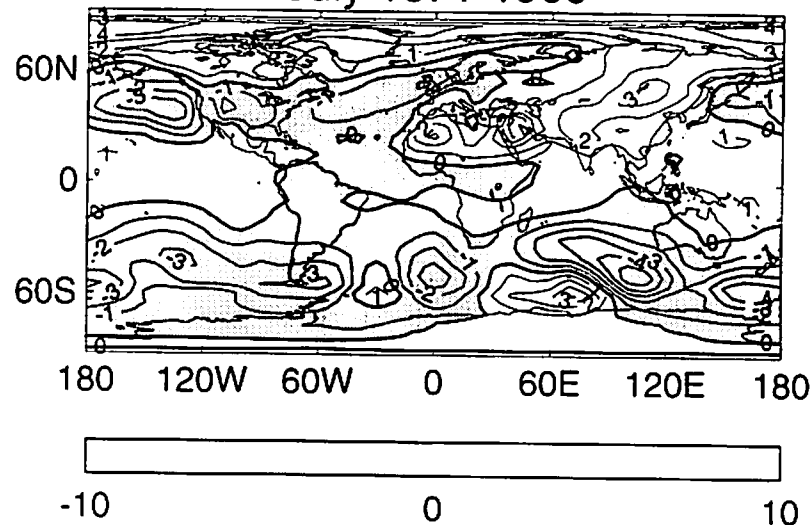


FIGURE 11:  
GMSLP2.0: Anomalies w.r.t. 1961-1990 (contours every 1hPa)

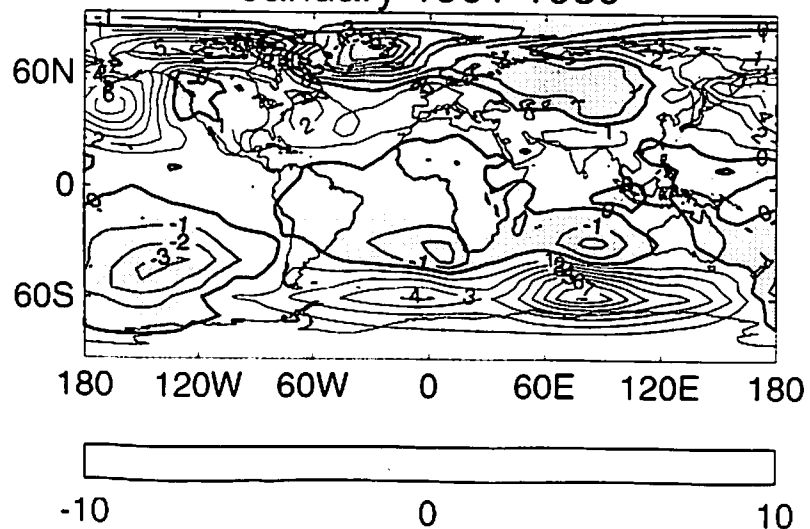
January 1871-1900



July 1871-1900



January 1901-1930



July 1901-1930

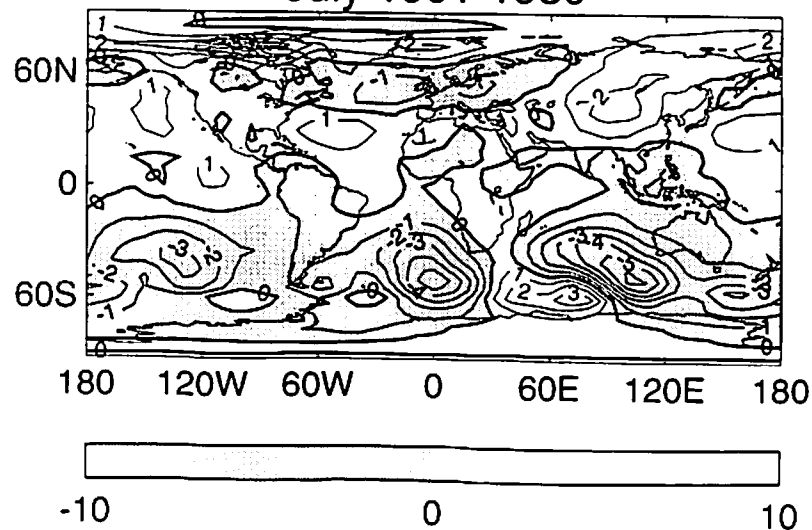


Figure 12 (a)  
GMSLP2.1f: Mean Decadal Data Coverage (%)

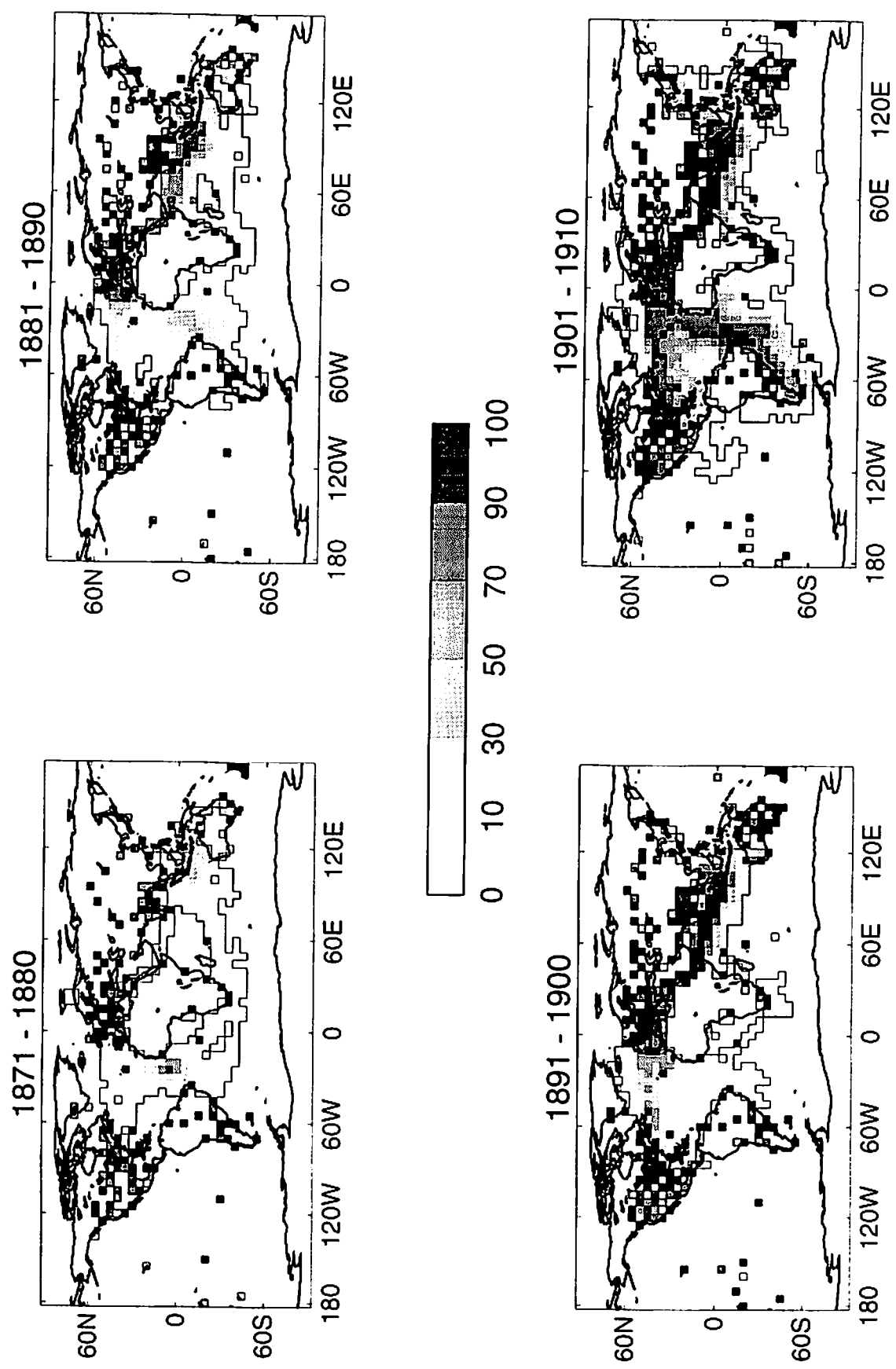


Figure 12 (b)  
GMSLP2.1f: Mean Decadal Data Coverage (%)

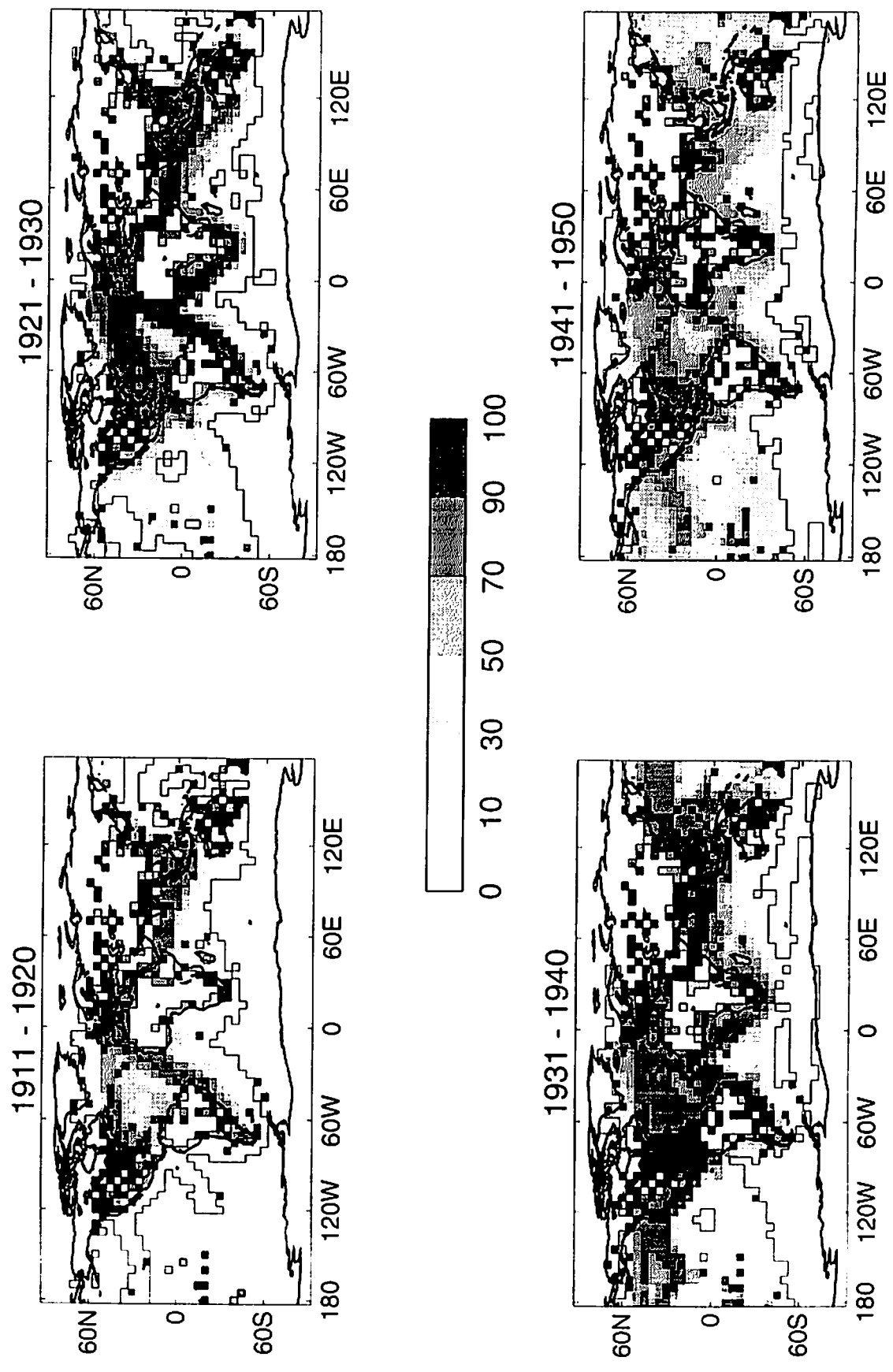


Figure 12 (c)  
GMSLP2.1f: Mean Decadal Data Coverage (%)

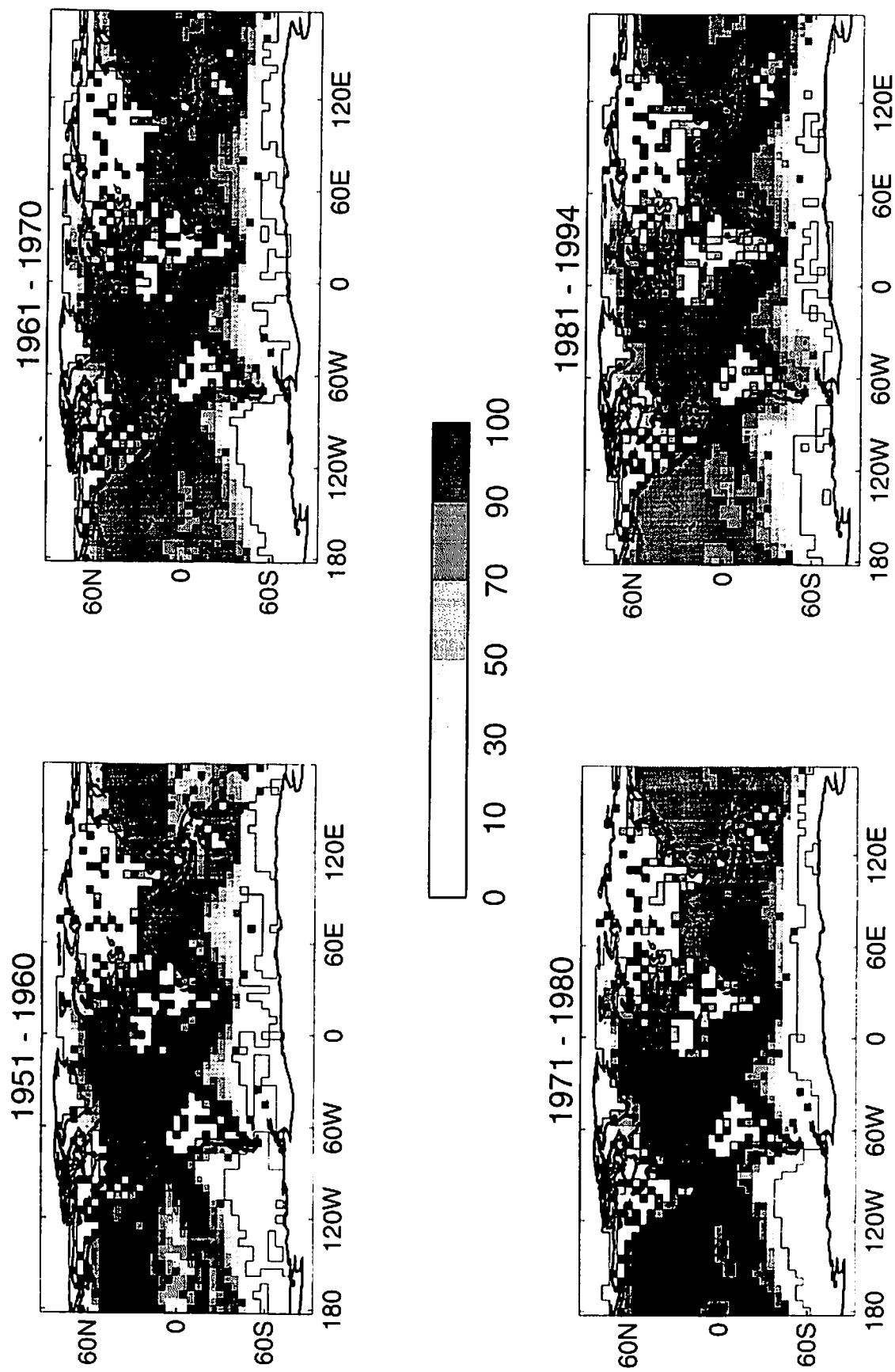
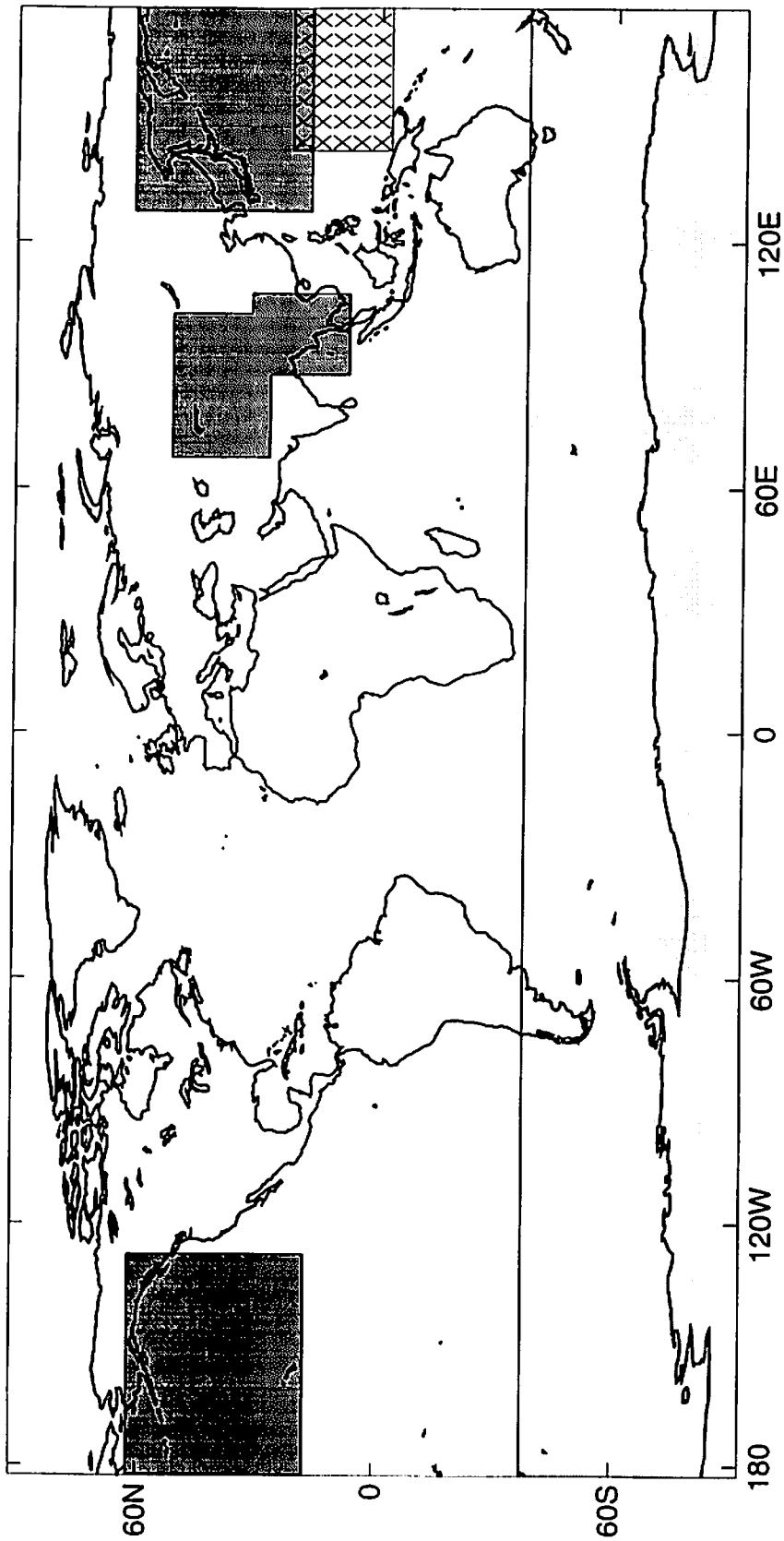


Figure 13:  
Shaded areas indicate location of climatology included in GMSLP2.1  
to remove bias



DARK (LIGHT) SHADING: climatology included for 1871-1950 (1871-1956),  
only if no real data within 10° latitude equivalent distance, (GMSLP2.1 versions b to f).  
HATCHING: climatology included for 1931-1945 at all data-void grid-points,  
(GMSLP2.1 versions d to f).

Figure 14  
GMSLP2.1c: Annual average grid-point anomalies, 1871-1990.  
Low-pass filtered with 20 month cut-off.

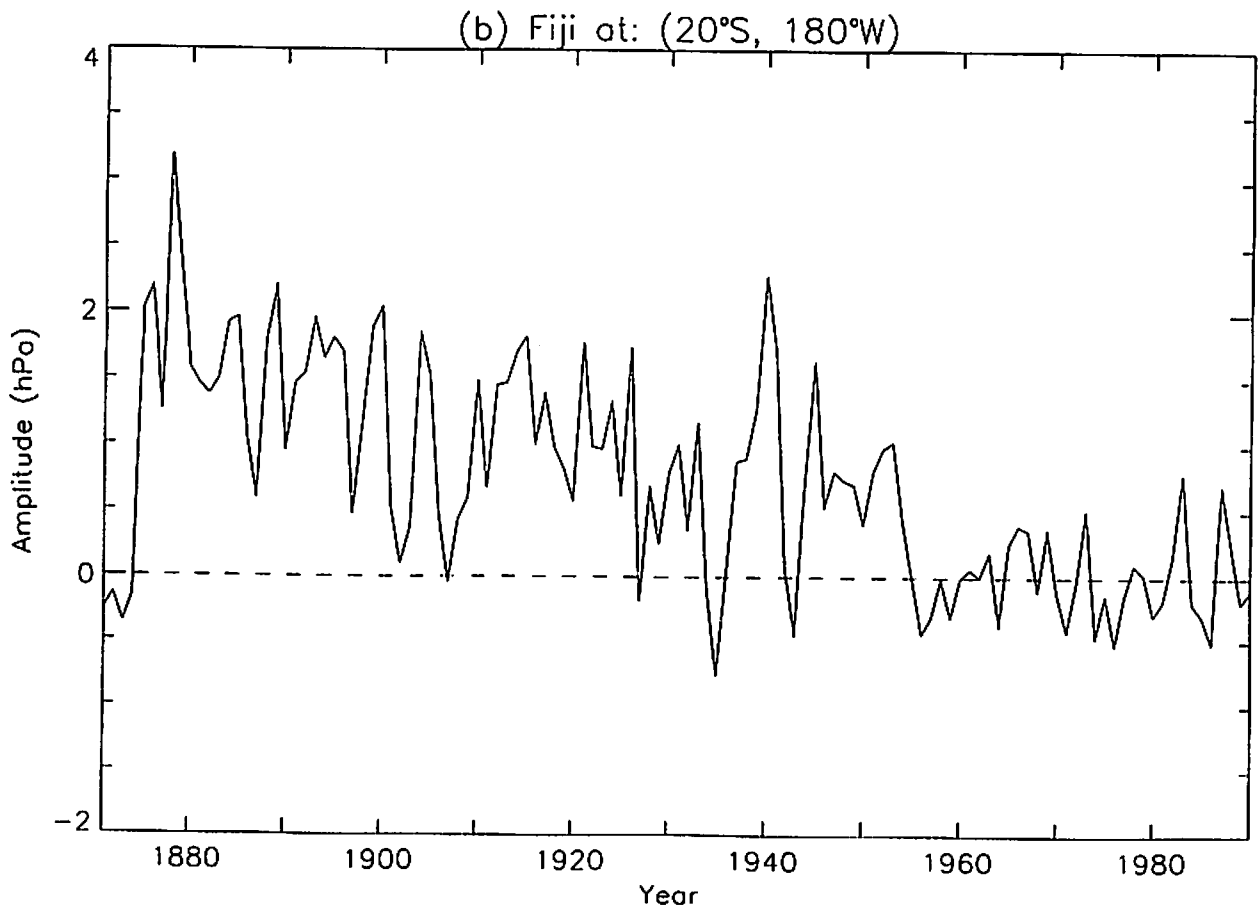
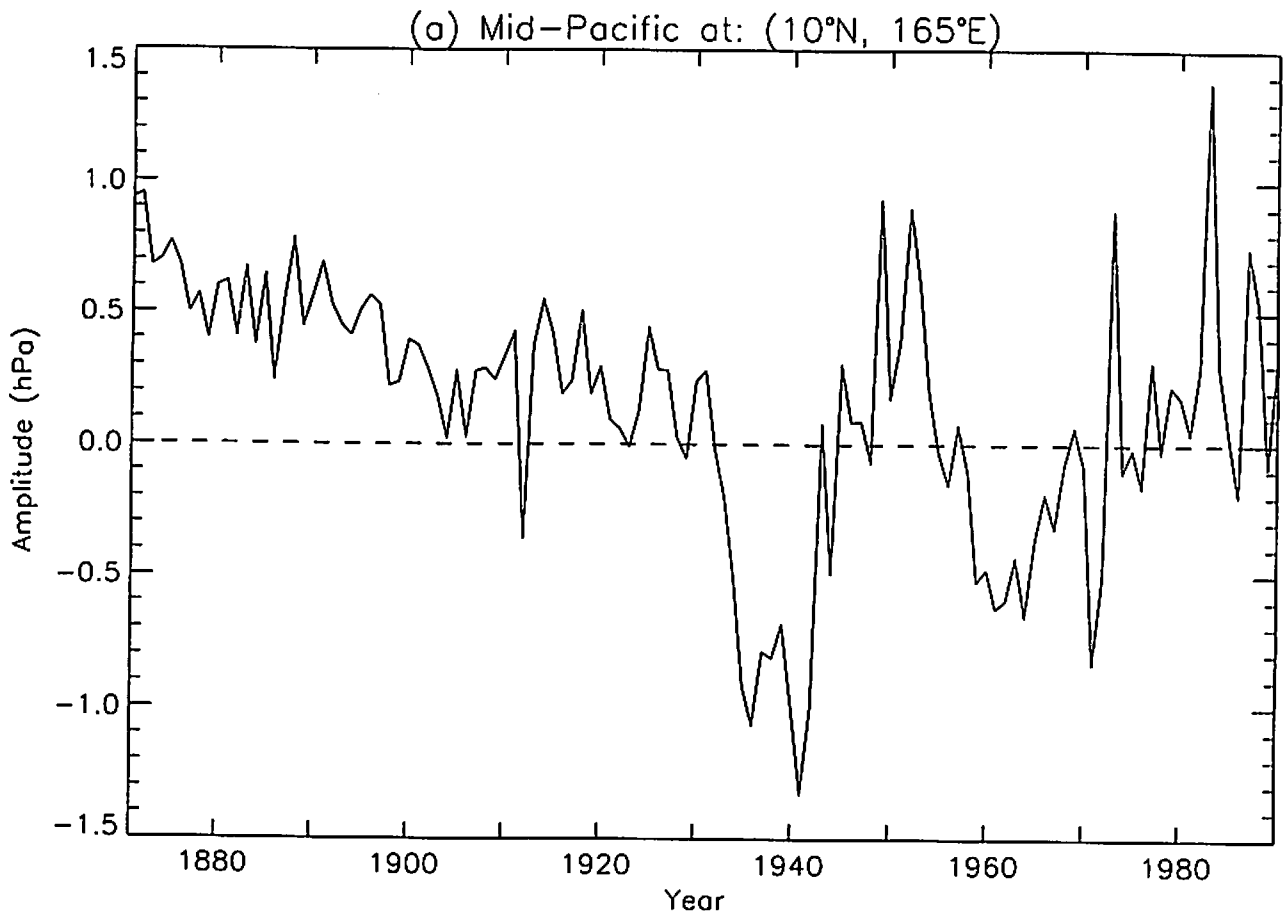


Figure 15  
GMSLP Decadal Trends for 1901-1950 (hPa/decade)  
(contours every 0.2hPa)

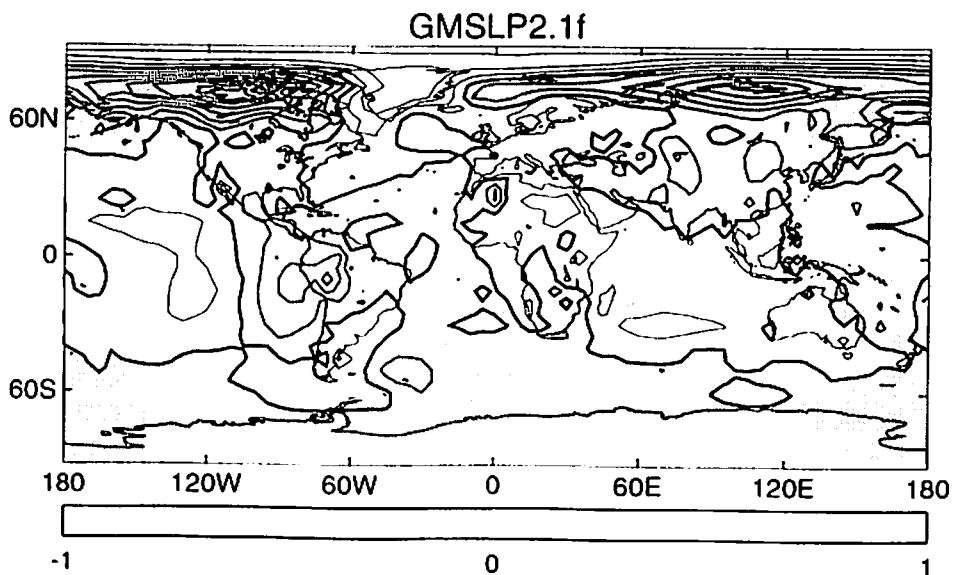
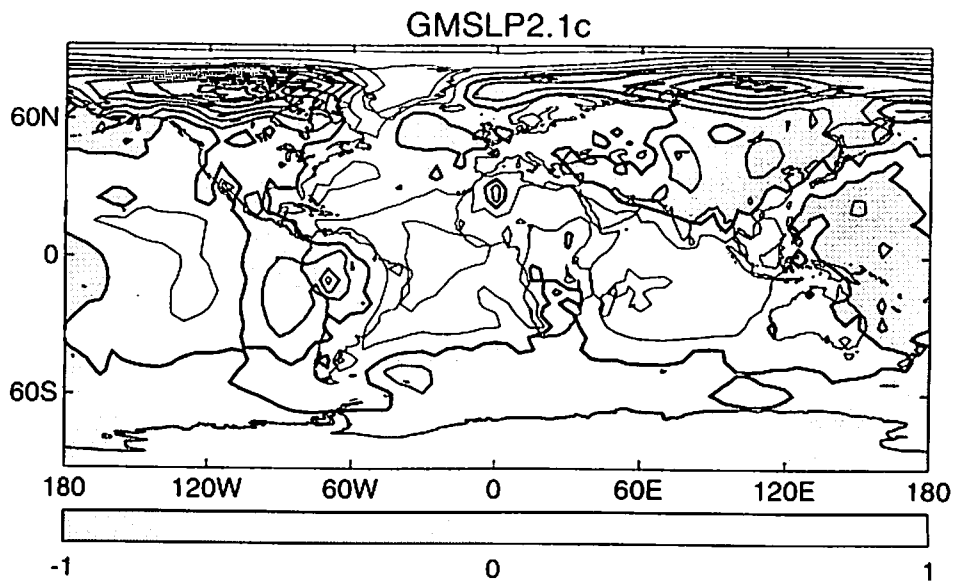
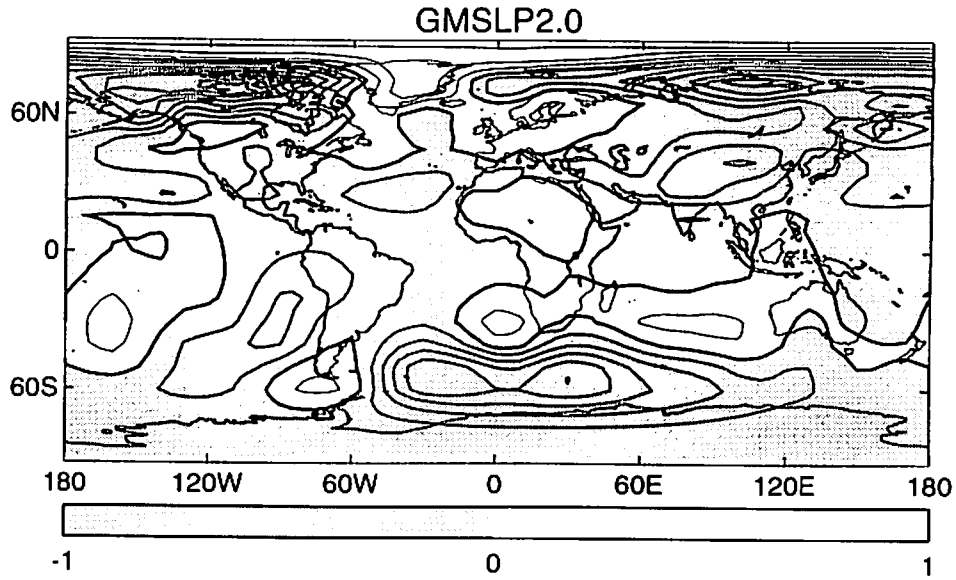
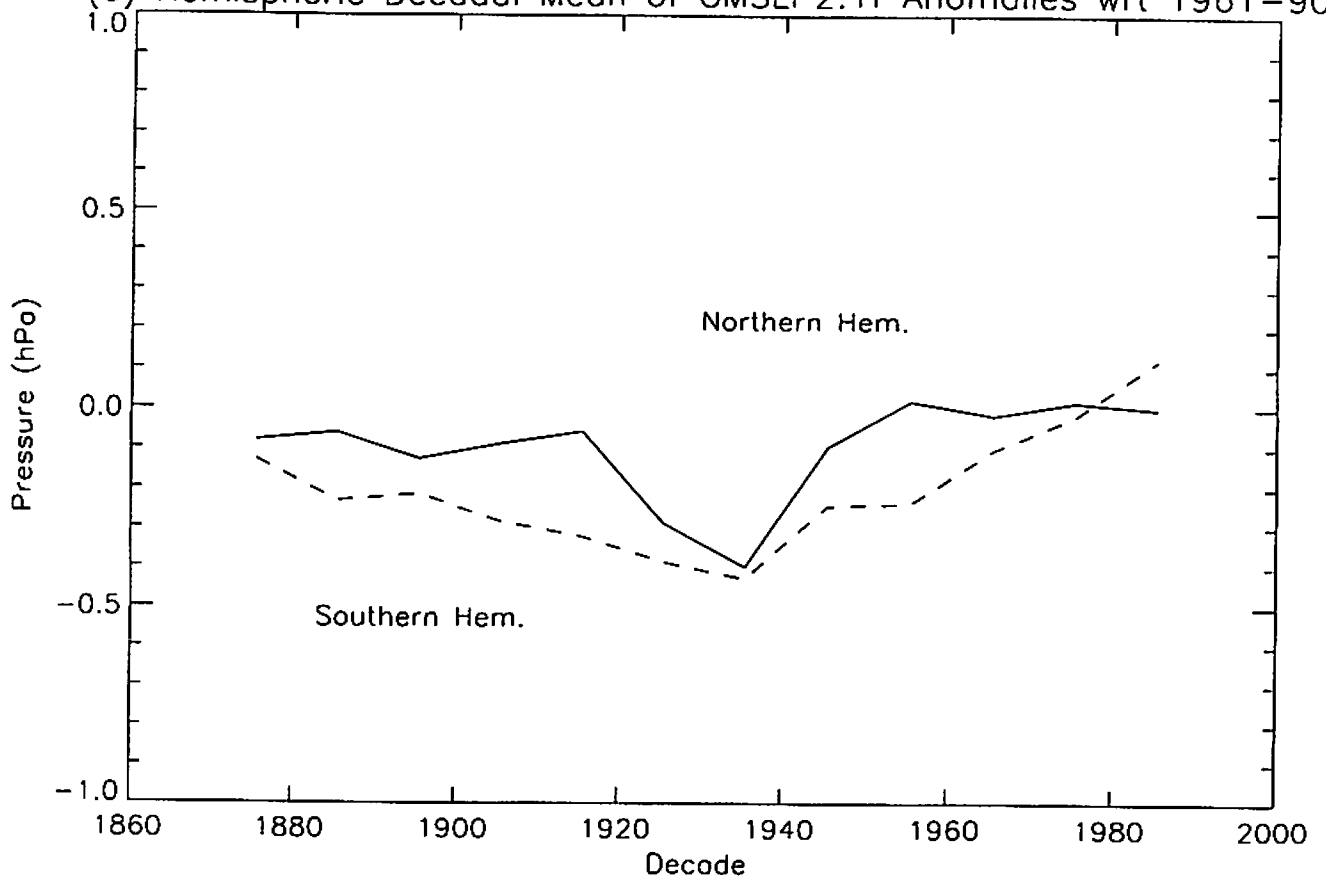


Figure 16

(a) Hemispheric Decadal Mean of GMSLP2.1f Anomalies wrt 1961-90



(b) Hemispheric Decadal S.D. of GMSLP2.1f Anomalies wrt 1961-90

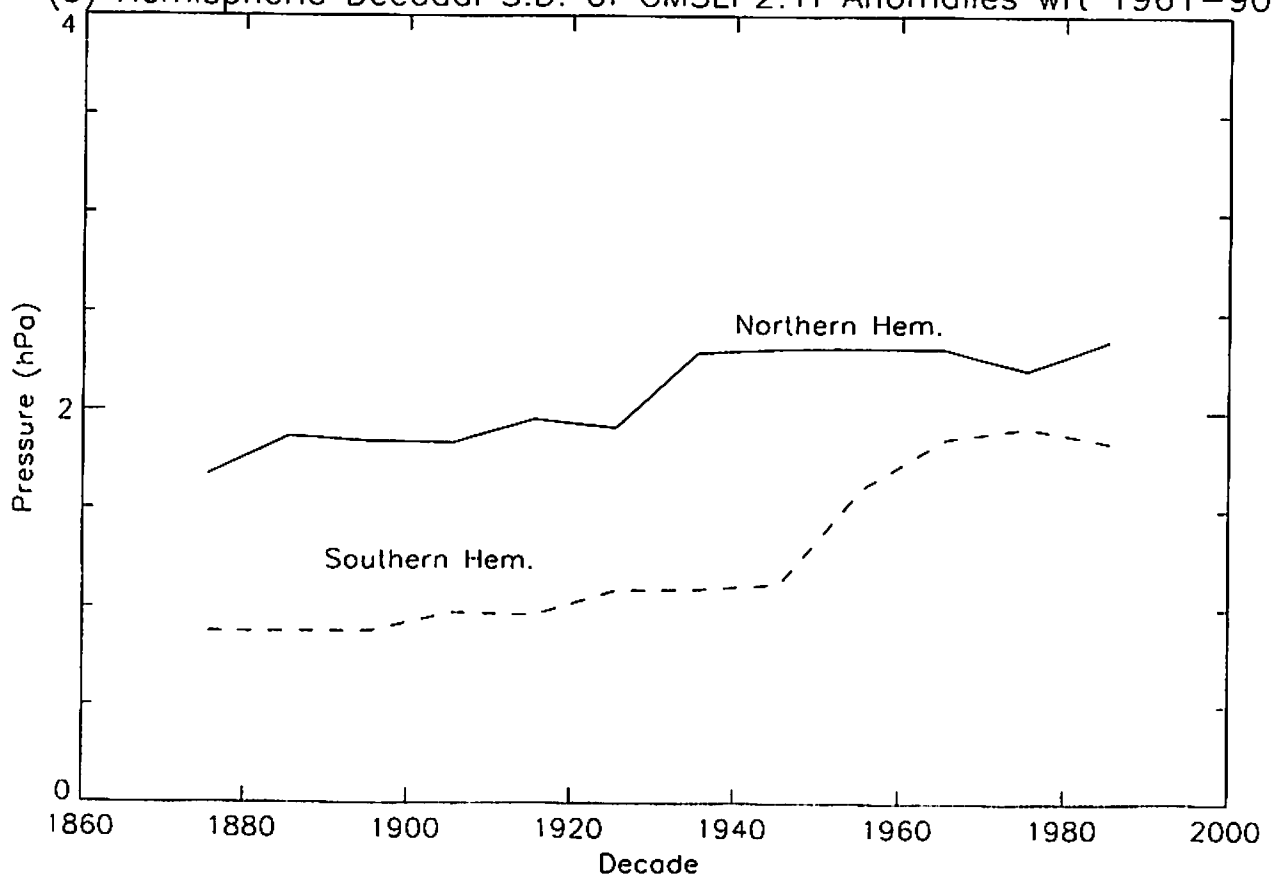


Figure 17  
Comparison of GMSLP2.1f observations and GMSLP2.0, 1871-1994.  
Field correlations and RMS differences of annual data.

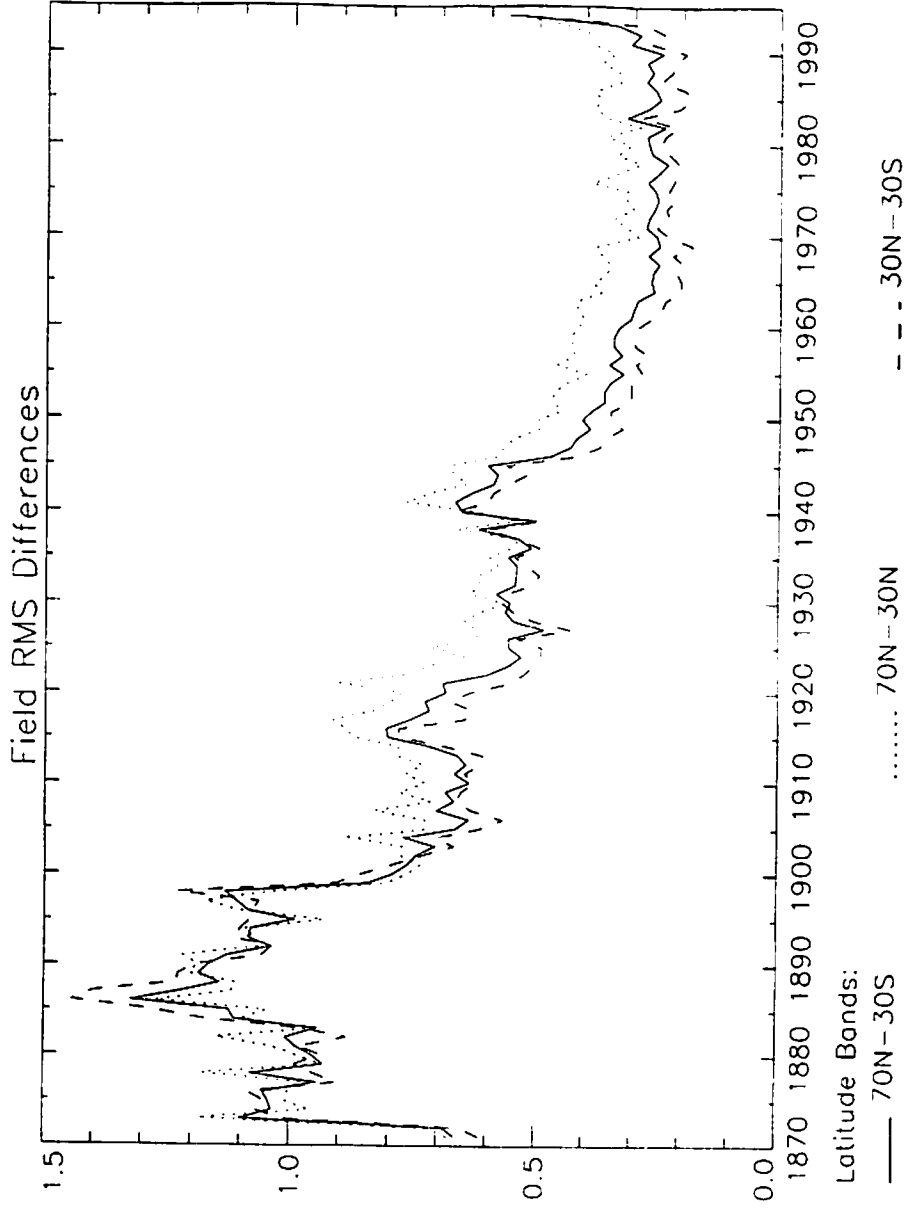
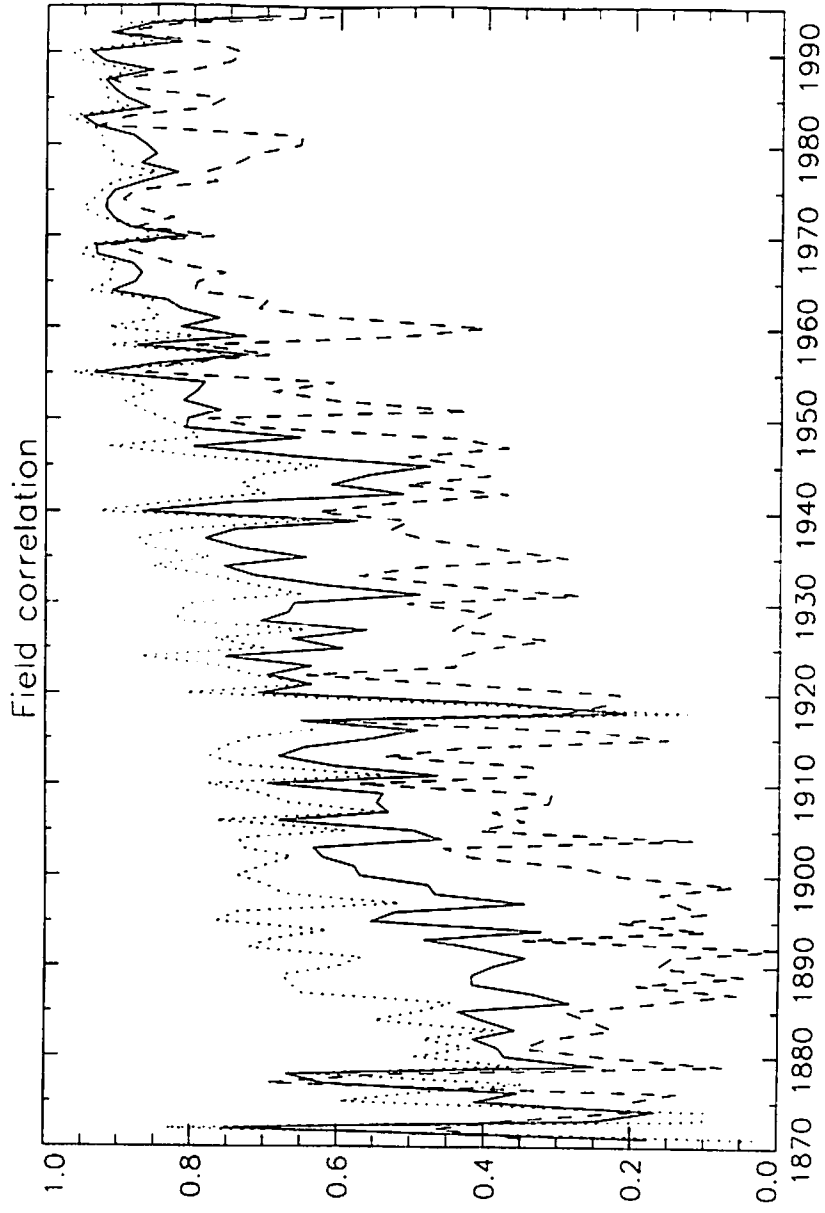


Figure 18  
Normalised and low-pass filtered (9mth cut off) monthly SO Index, 1871-1994:  
GMSLP2.1f (solid line) and Tahiti - Darwin (dashed line)

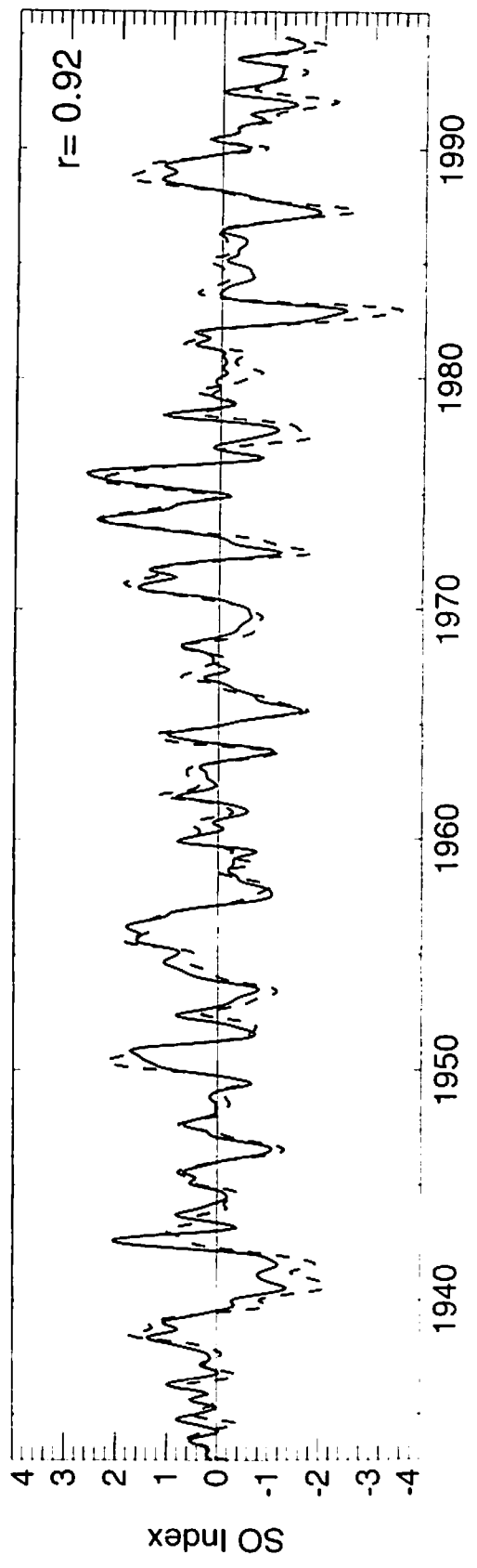
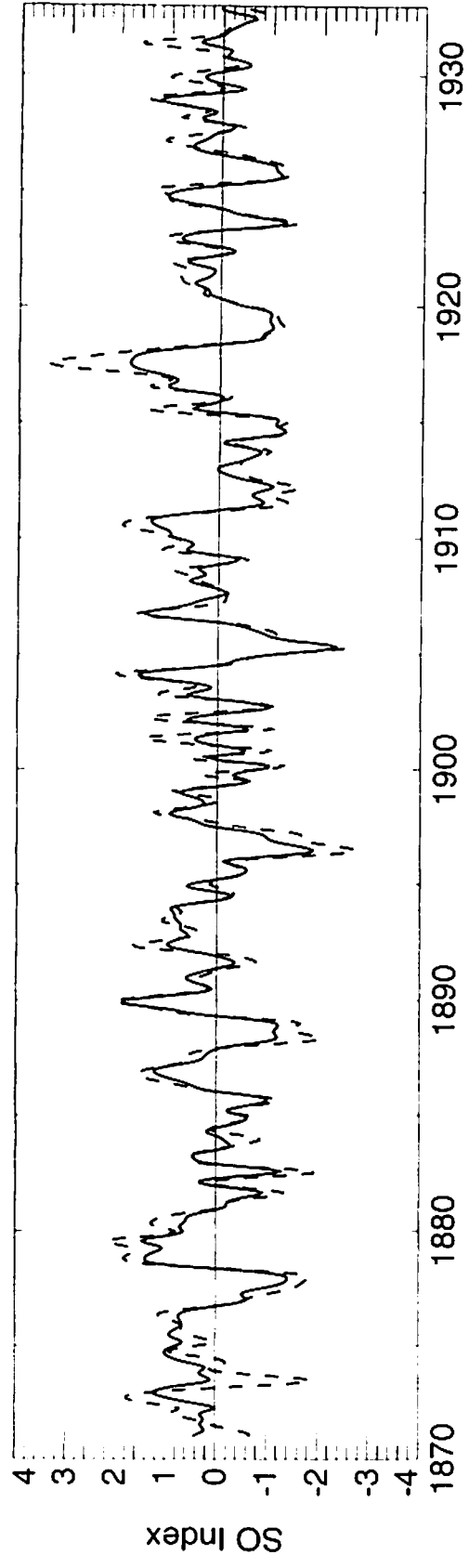


Figure 19  
Normalised and low-pass filtered (9mth cut-off) monthly NAO index, 1871-1994:  
GMSLP2.1f (solid line) and Ponta Delgada - Stykkisholmur (dashed line)

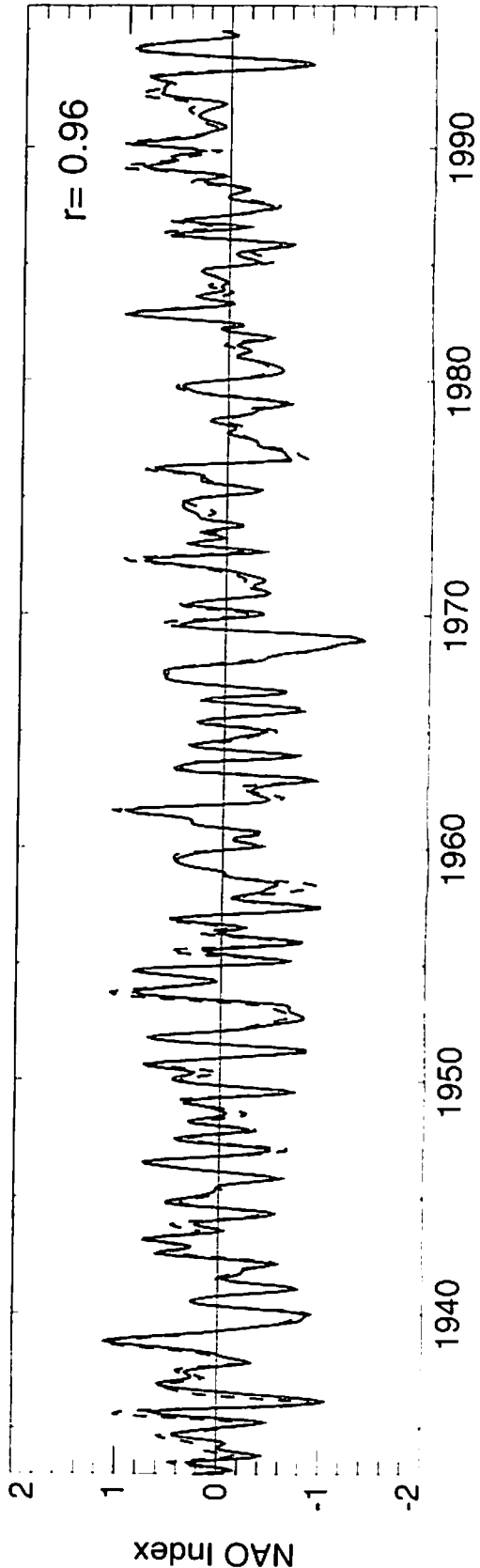
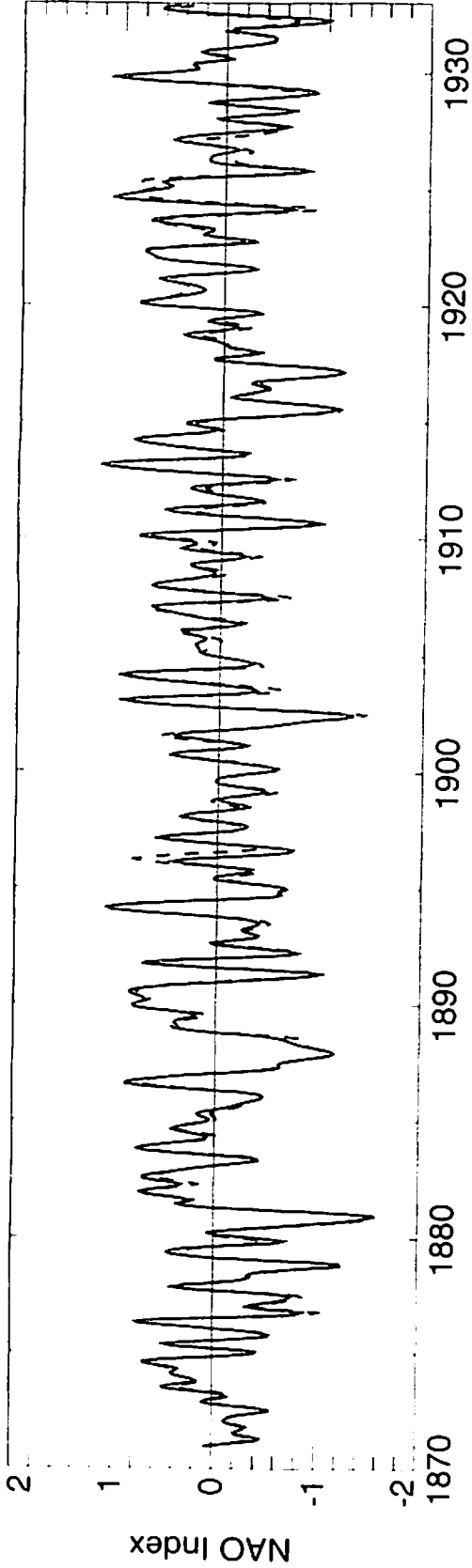


Figure 20:  
GMSLP2.1f Anomaly Percentiles (w.r.t. 1961-90)  
(anomalies fitted to gamma distributions)

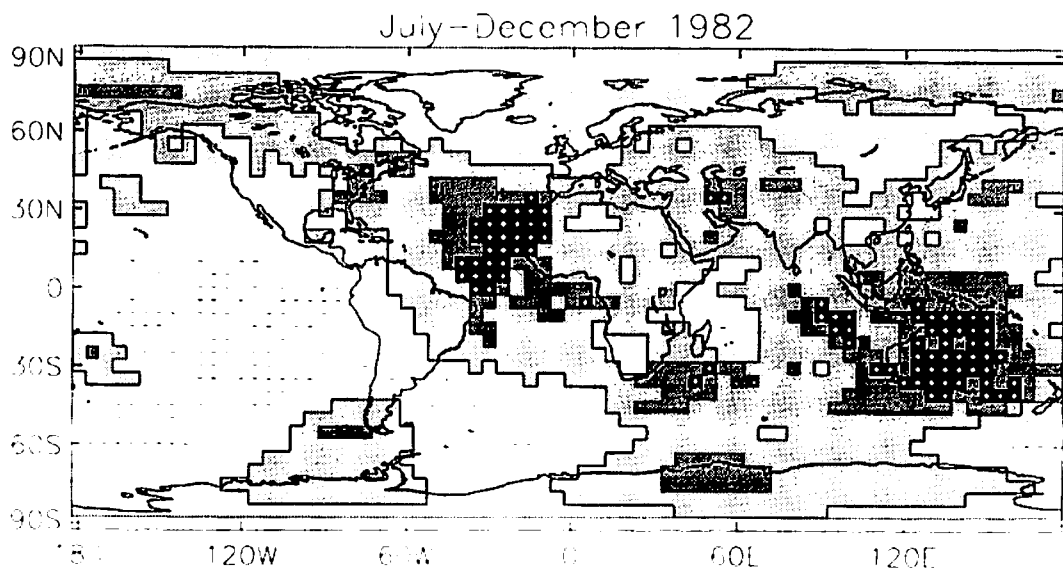
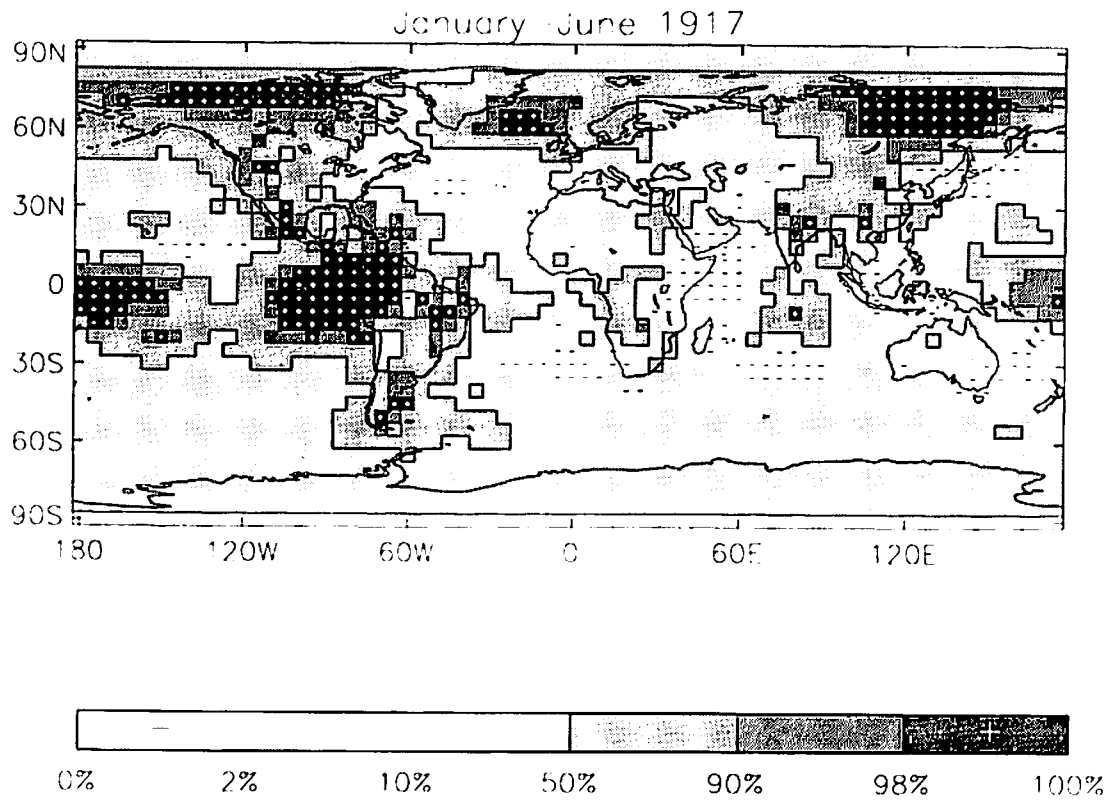


Figure 21: GMSLP2.1f Annual Cycles for decades beginning in the years indicated.

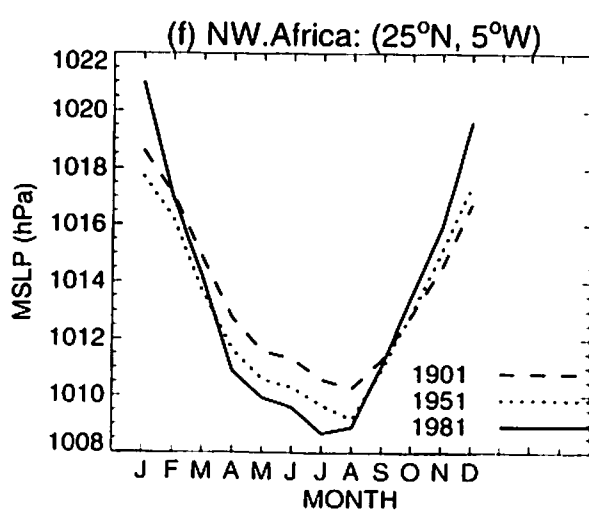
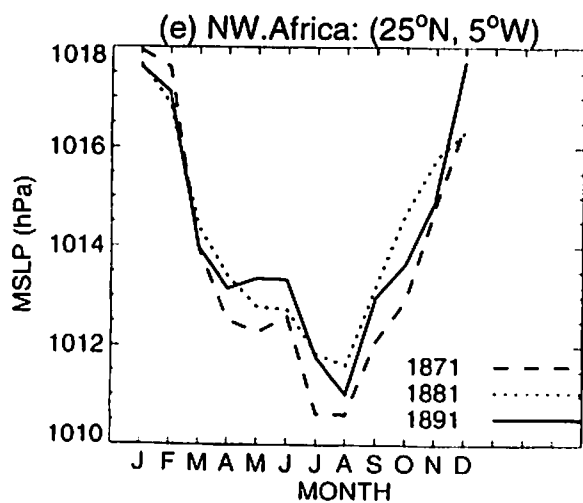
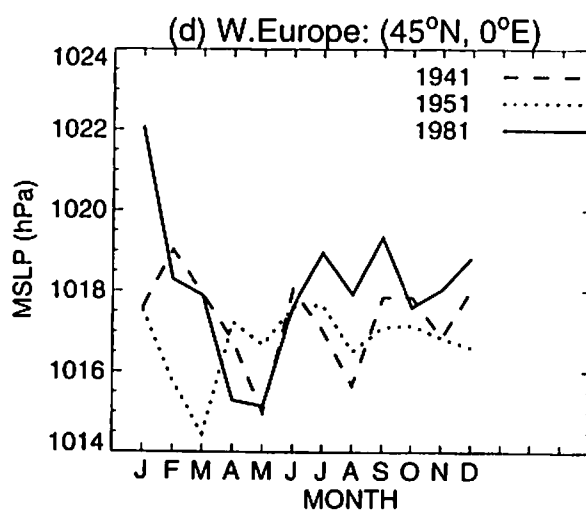
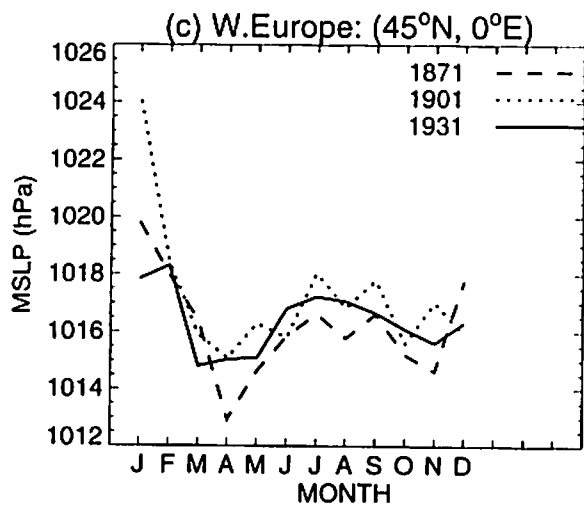
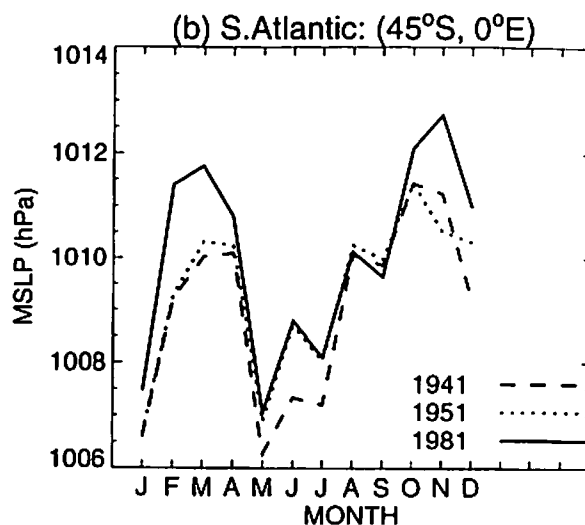
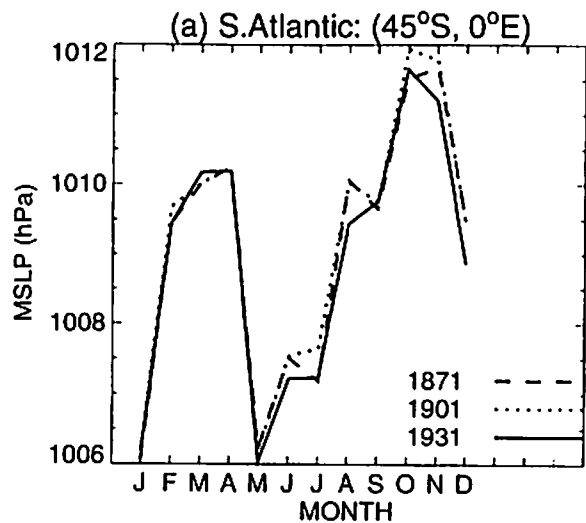
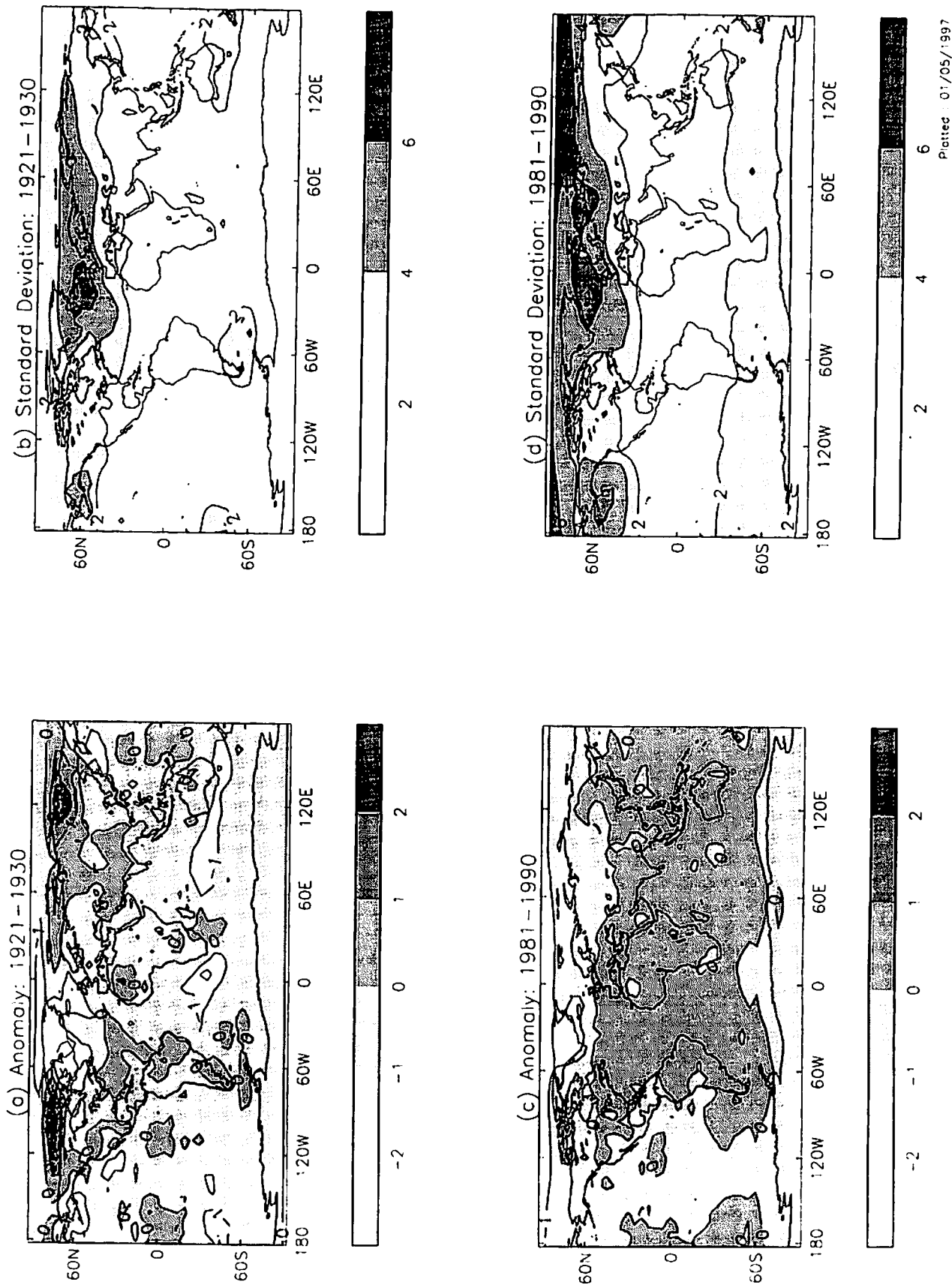
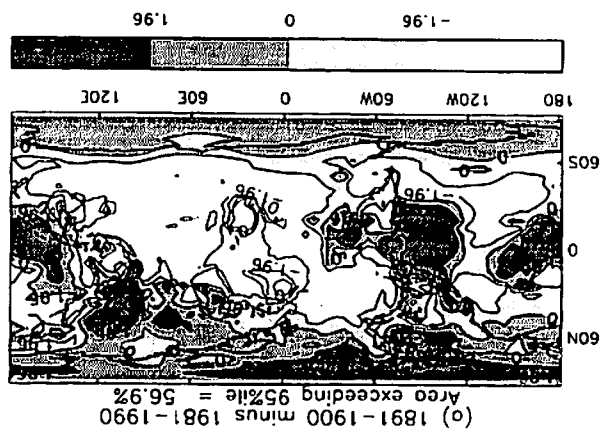
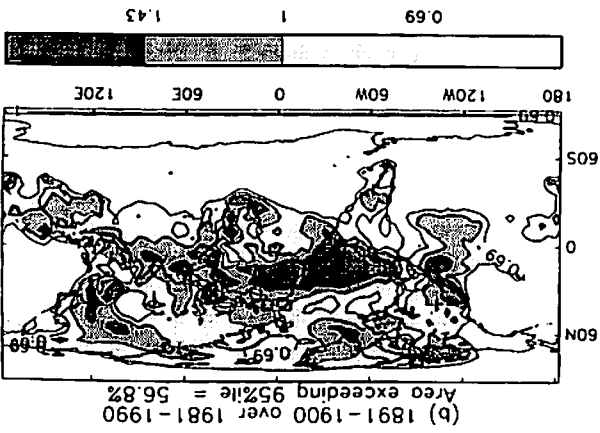
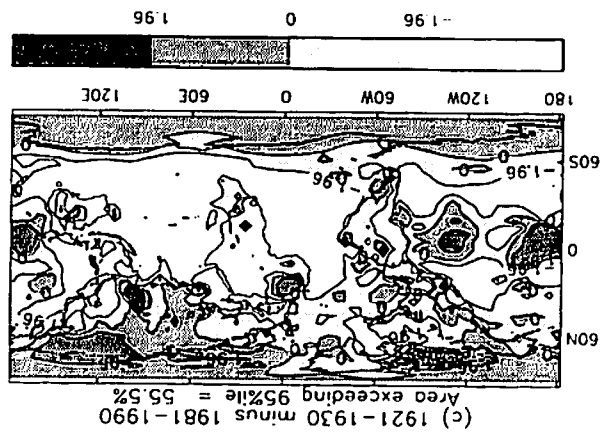
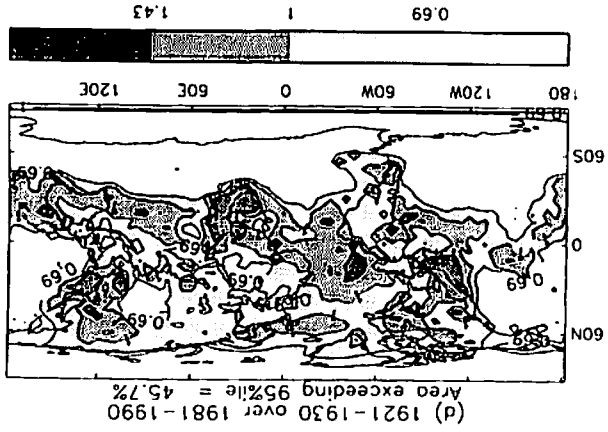
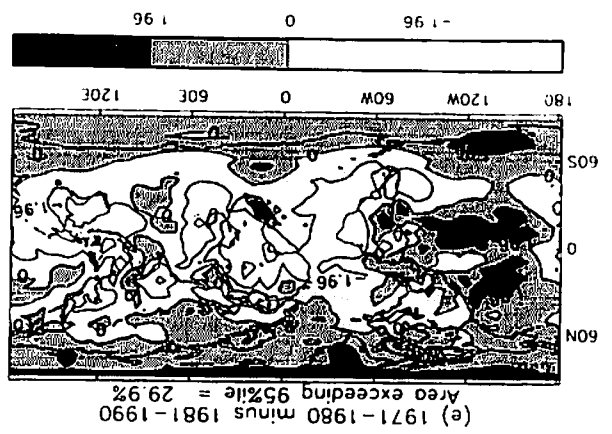
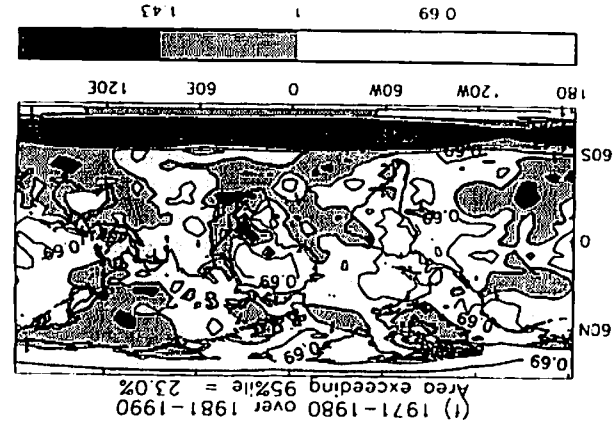


Figure 22:  
Decadal GMSLP2.1f Anomalies and Standard Deviations wrt 1961-90





F-STATISTIC:  
Ratio of decadal variances (GMSLP2.1f)

T-STATISTIC:  
Difference of decadal means (GMSLP2.1f)

Figure 23

Seasonal differences between MSLP interpolated from gridded data sets, and Singapore ( $1^{\circ}22'N, 104^{\circ}55'E$ ), Alt: 32M, 1911-1982, illustrating the effects on marine MSLP of correcting for standard gravity.

Figure A1

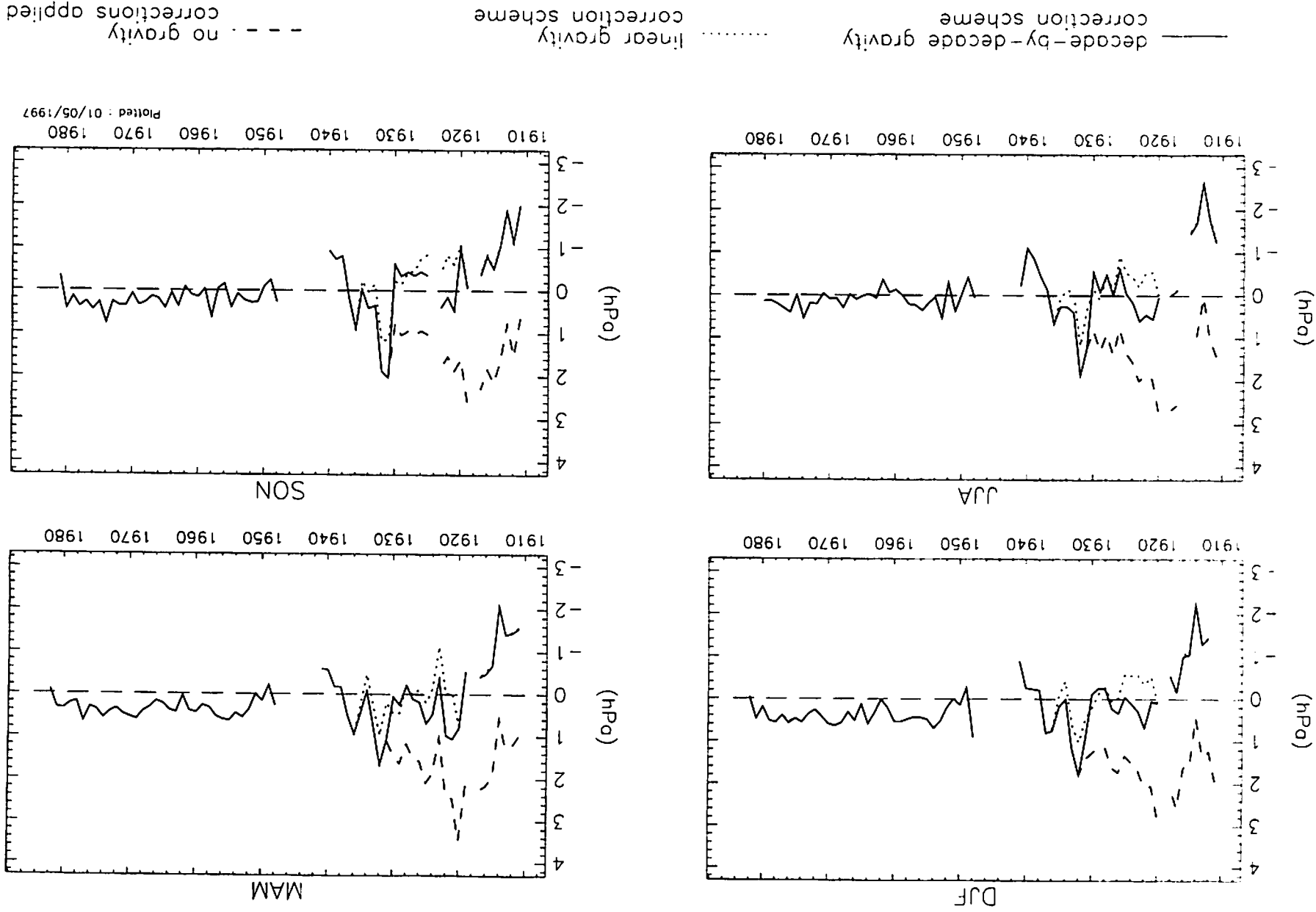


Figure A2: Hourly distribution of marine MSLP observations per decade, for latitudes 30°N-30°S.

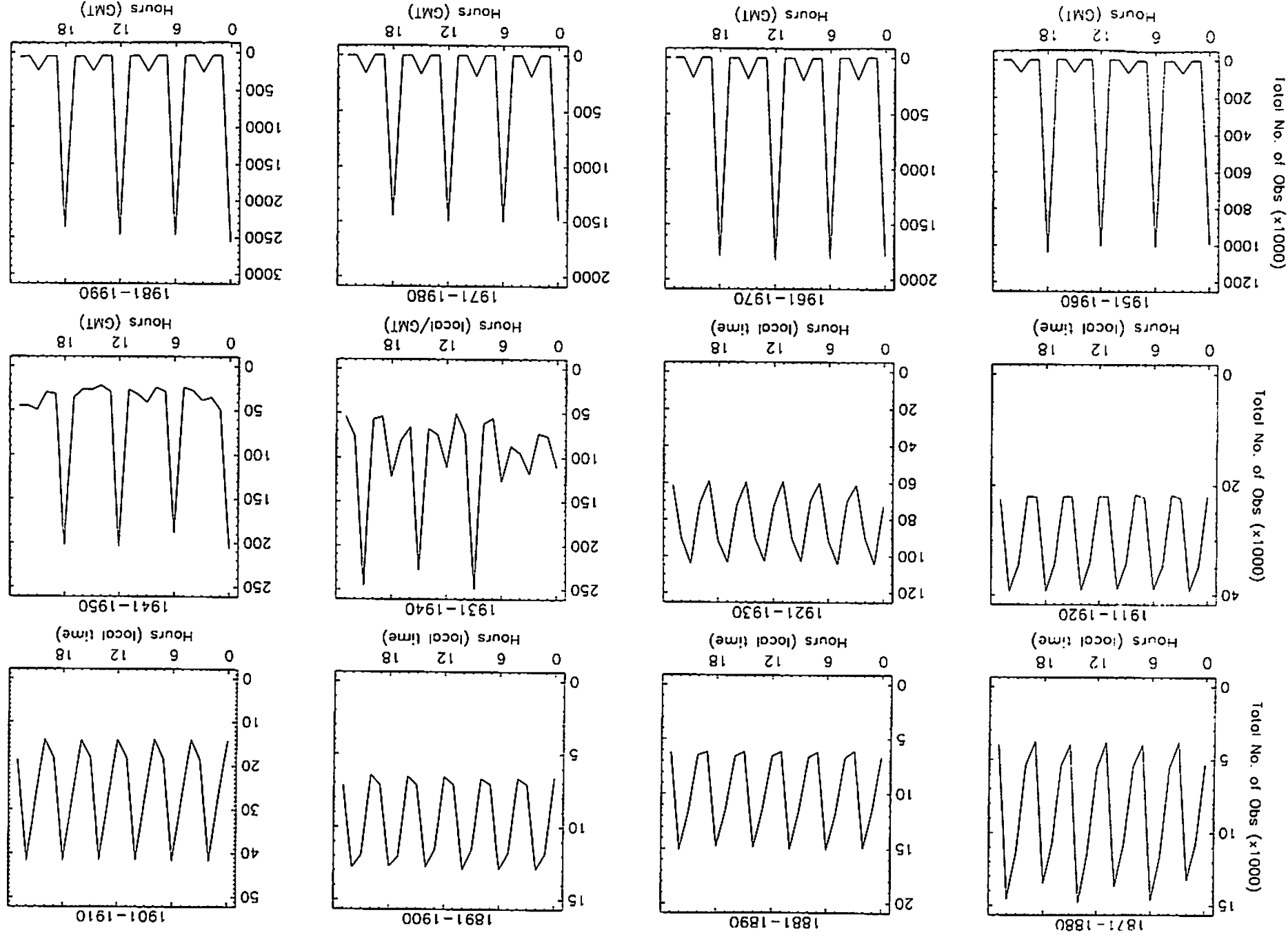
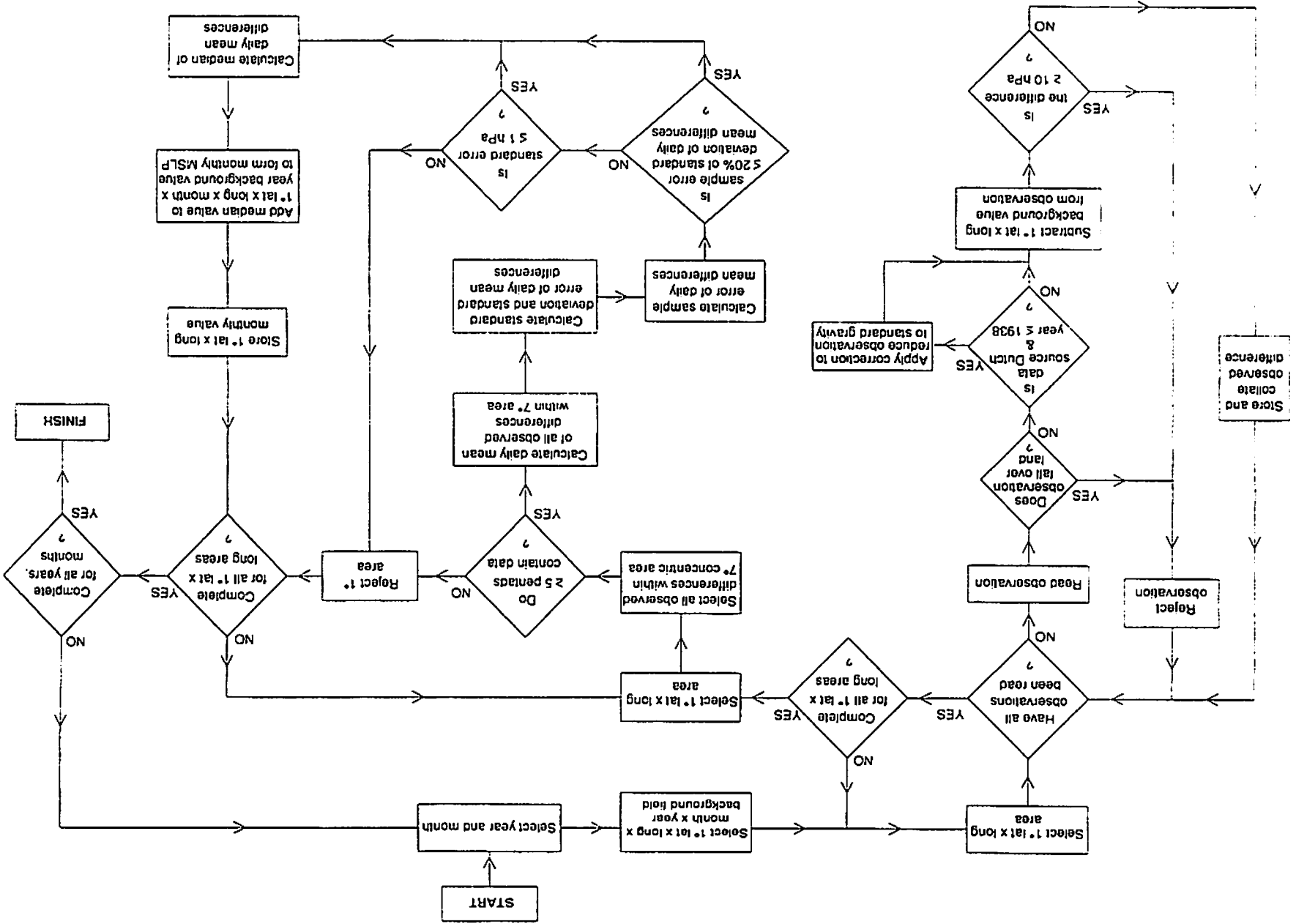


Figure A3: Flow chart to describe the quality control and gridding of 1° UKMO MDB MSLP used in GMSLP2.1f

28 Apr 97



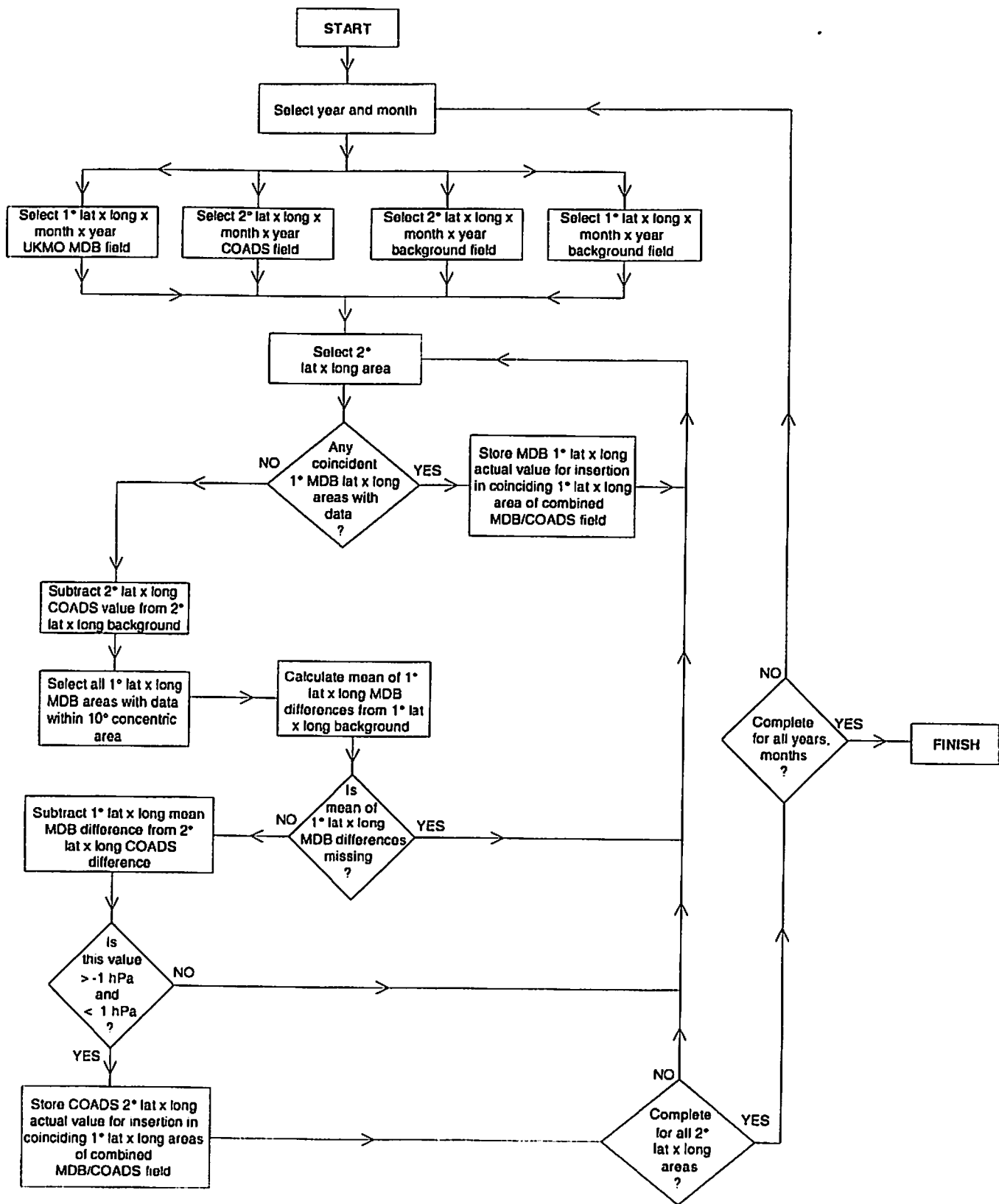
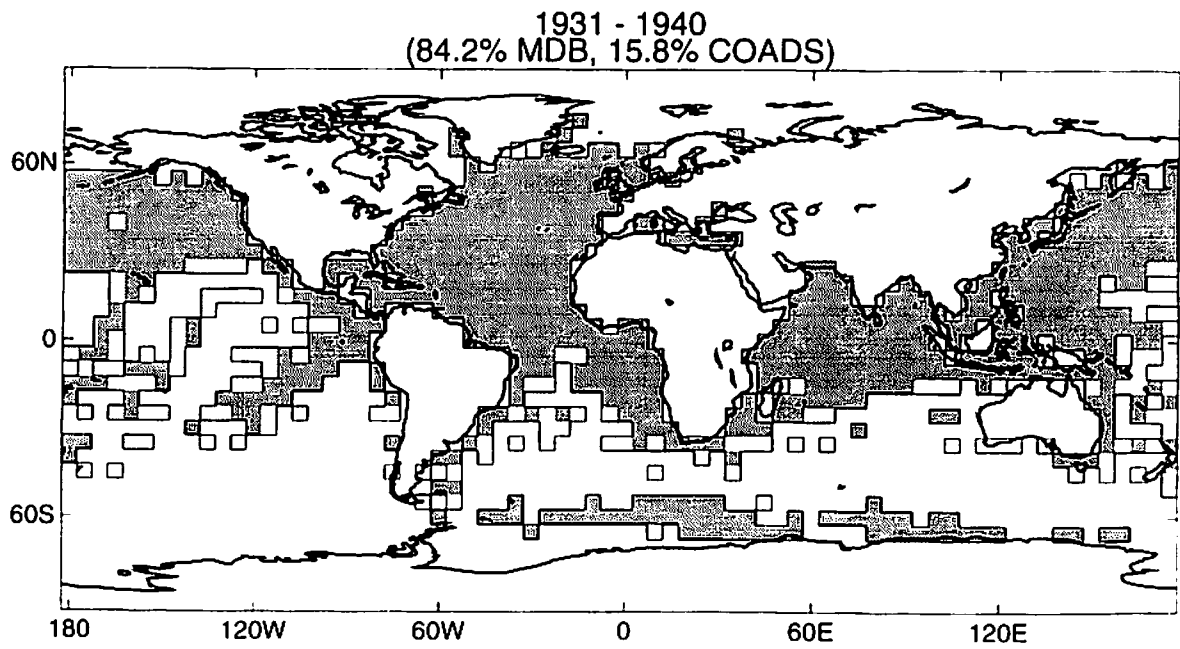
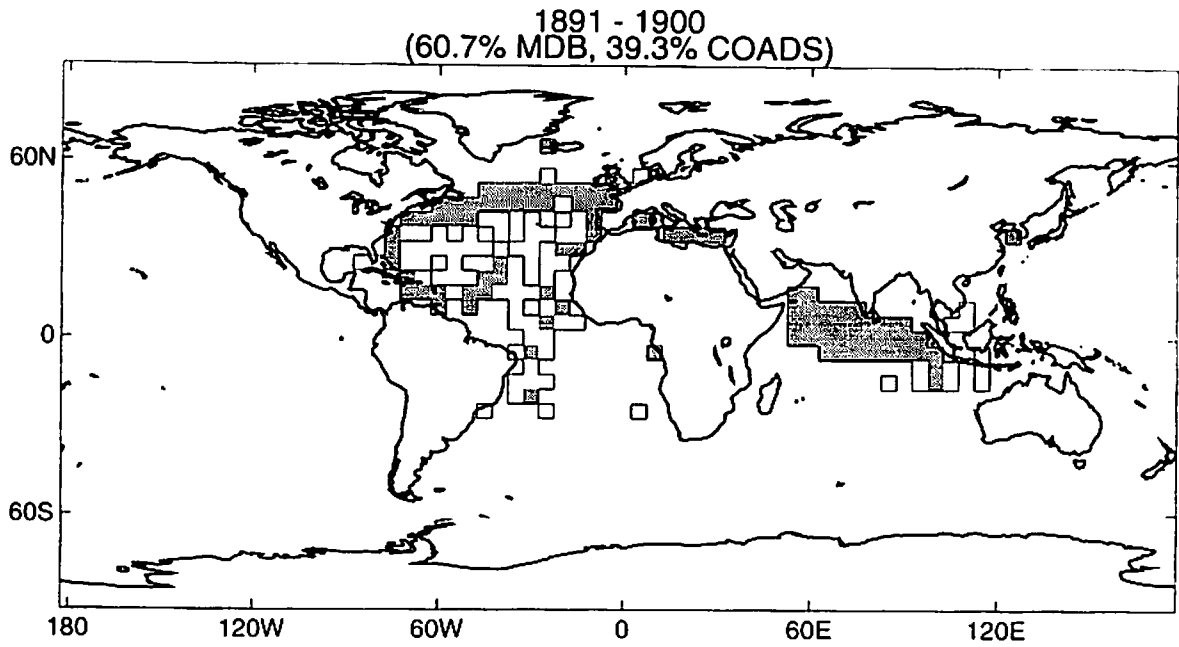


Figure A4: Flow chart to describe the merge of 2° gridded COADS MSLP data with 1° gridded UKMO MDB MSLP data, used in GMSLP2.1f.

# Figure A5

Total Decadal Coverage of Observed Marine MSLP Data in GMSLP2.1f  
(UKMOMDB: dark shading and COADS: light shading)



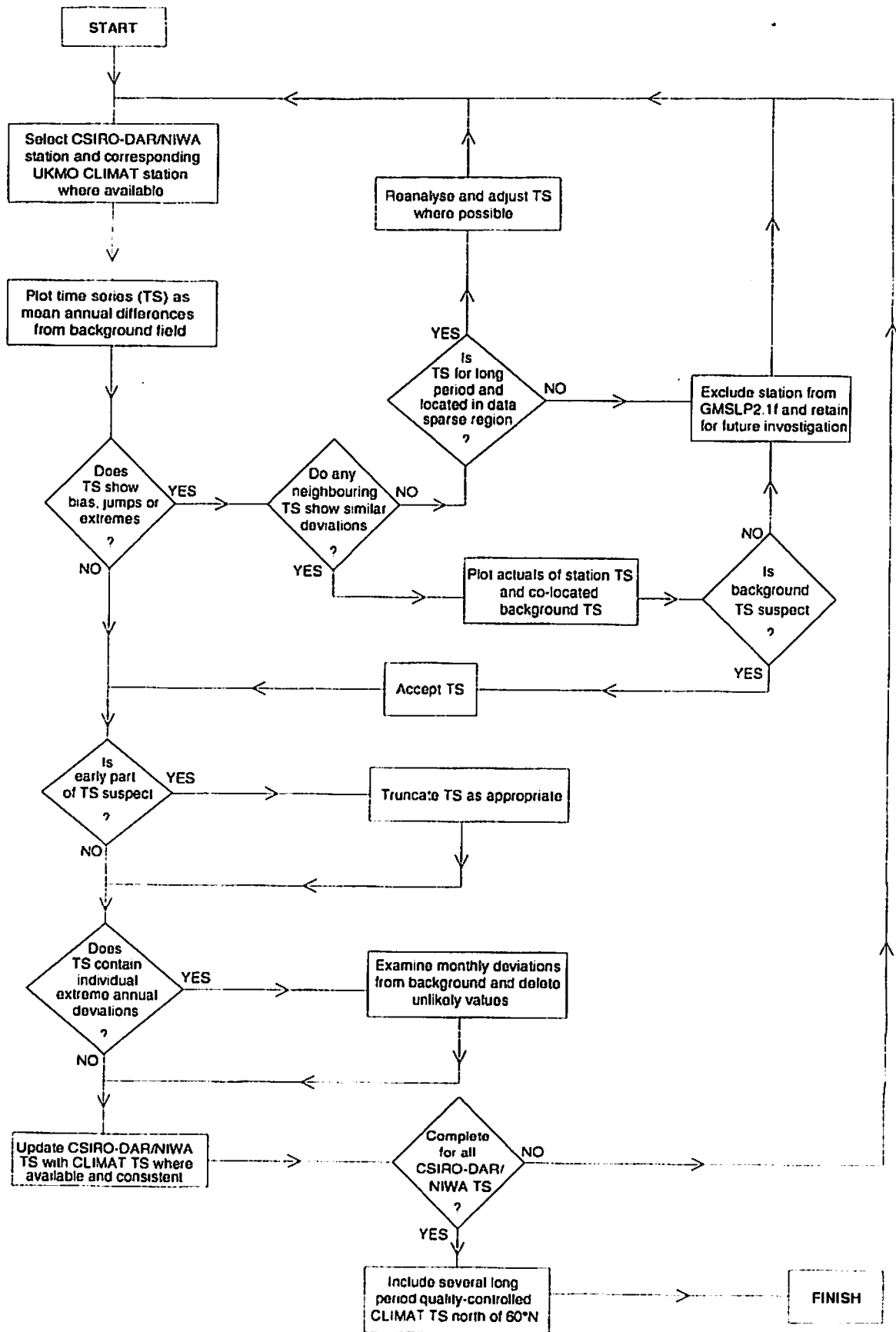
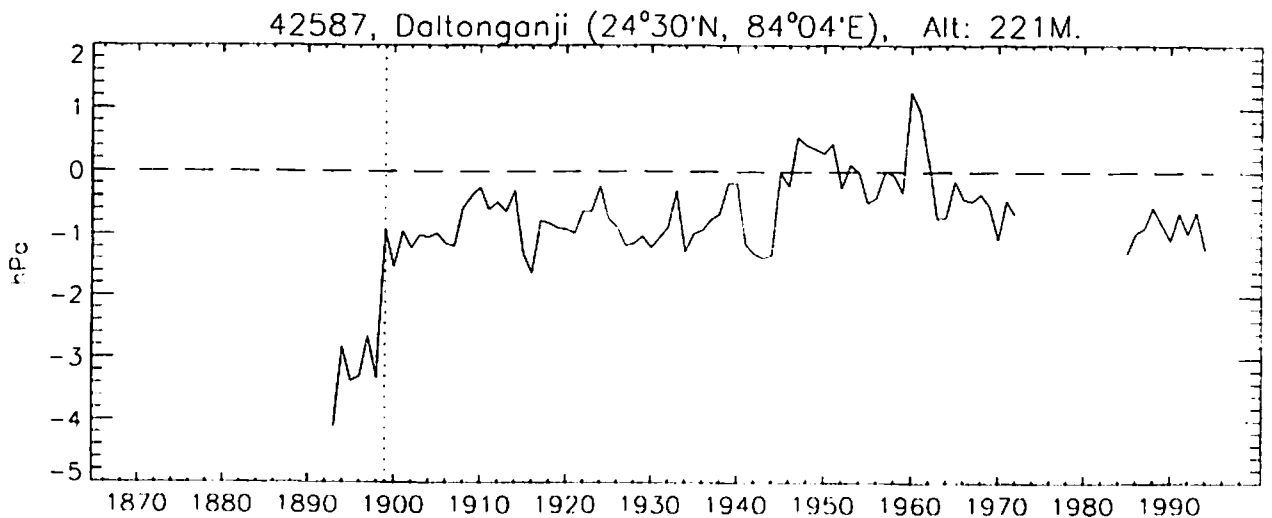
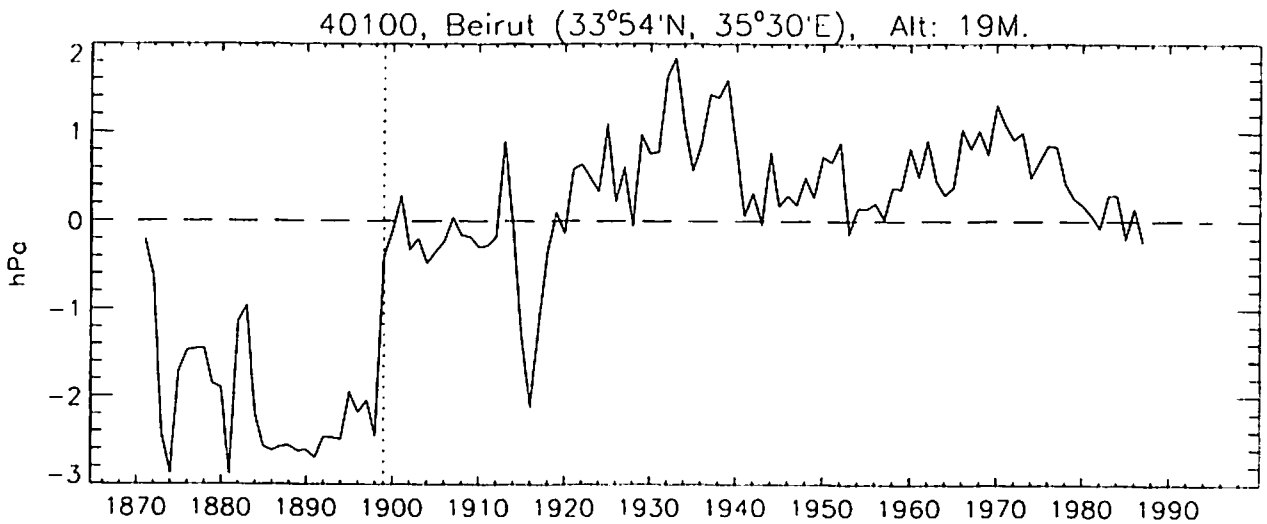
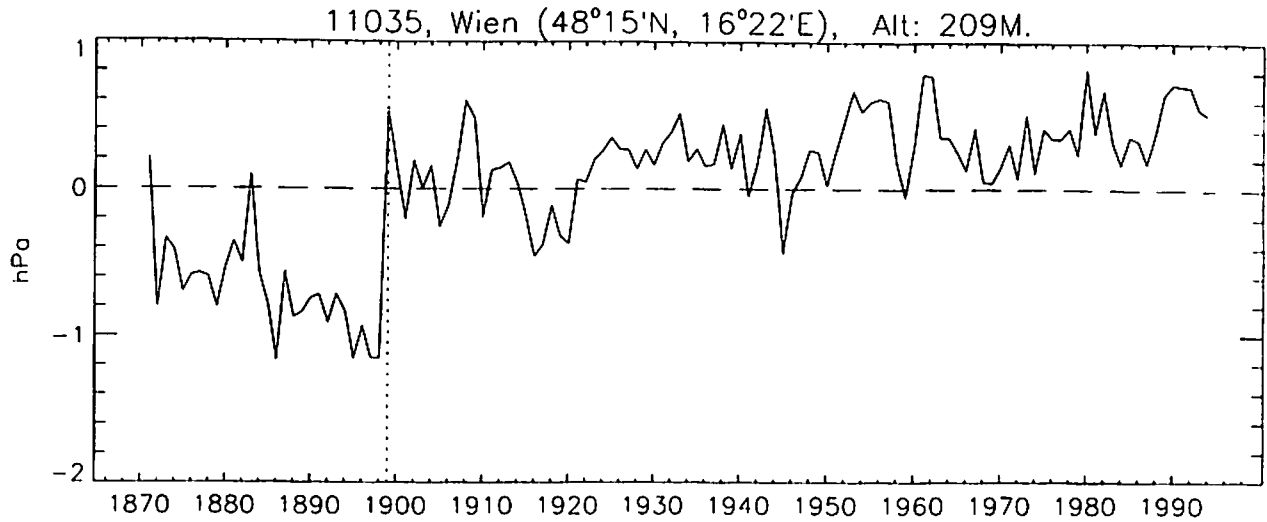


Figure A6: Flow chart to describe the quality control of land station MSLP time series

28 Apr 97

Figure A7  
Annually Averaged Differences Relative to GMSLP2.0, illustrating  
a discontinuity occurring in the background field in 1899.



## CLIMATE RESEARCH TECHNICAL NOTES

- CRTN 1      Oct 1990    Estimates of the sensitivity of climate to vegetation changes using the Penman-Monteith equation.  
P R Rowntree
- CRTN 2      Oct 1990    An ocean general circulation model of the Indian Ocean for hindcasting studies.  
D J Carrington
- CRTN 3      Oct 1990    Simulation of the tropical diurnal cycle in a climate model.  
D P Rowell
- CRTN 4      Oct 1990    Low frequency variability of the oceans.  
C K Folland, A Colman, D E Parker and A Bevan
- CRTN 5      Dec 1990    A comparison of 11-level General Circulation Model Simulations with observations in the East Sahel.  
K Maskell
- CRTN 6      Dec 1990    Climate Change Prediction.  
J F B Mitchell and Qing-cun Zeng
- CRTN 7      Jan 1991    Deforestation of Amazonia - modelling the effects of albedo change.  
M F Mylne and P R Rowntree
- CRTN 8      Jan 1991    The role of observations in climate prediction and research.  
D J Carson
- CRTN 9      Mar 1991    The greenhouse effect and its likely consequences for climate change.  
D J Carson
- CRTN 10     Apr 1991    Use of wind stresses from operational N.W.P. models to force an O.G.C.M. of the Indian Ocean.  
D J Carrington
- CRTN 11     Jun 1991    A new daily Central England Temperature series, 1772-1991.  
D E Parker, T P Legg and C K Folland
- CRTN 12     Jul 1991    Causes and predictability of Sahel rainfall variability.  
D P Rowell, C K Folland, K Maskell, J A Owen, M N Ward

## CLIMATE RESEARCH TECHNICAL NOTES

- CRTN 13 Jul 1991 Modelling changes in climate due to enhanced CO<sub>2</sub>, the role of atmospheric dynamics, cloud and moisture.  
C A Senior, J F B Mitchell, H Le Treut and Z-X Li
- CRTN 14 Sep 1991 Sea temperature bucket models used to correct historical SST data in the Meteorological Office.  
C K Folland
- CRTN 15 Aug 1991 Modelling climate change, and some potential effects on agriculture in the U.K.  
P R Rowntree, B A Callander and J Cochrane
- CRTN 16 Aug 1991 The Boreal Forests and Climate  
G Thomas and P R Rowntree
- CRTN 17 Aug 1991 Development of a Stratosphere-Troposphere Data Assimilation System.  
R Swinbank.
- CRTN 18 Sep 1991 A study of asynchronous coupling using a simple climate model.  
M K Davey.
- CRTN 19 Sep 1991 The Oceanic Carbon Cycle.  
N K Taylor
- CRTN 20 Nov 1991 Worldwide ocean-atmosphere surface fields in Sahel wet and dry years using provisionally corrected surface wind data.  
M N Ward
- CRTN 21 Dec 1991 Coupled tropical ocean global atmosphere models at the UKMO.  
M K Davey, C Gordon, S Ineson and S Lawrence
- CRTN 22 Dec 1991 Empirical parameterisation of tropical ocean-atmosphere coupling.  
M Allen, M K Davey, D L T Anderson and P D Killworth
- CRTN 23 Feb 1992 The temporal evolution of Equatorial Currents in the Indian Ocean  
D L T Anderson, D J Carrington, R A Corry and C Gordon
- CRTN 24 Feb 1992 Stratospheric analyses provided by the U.K. Meteorological Office  
M J Bailey, A O'Neill and V D Pope

CLIMATE RESEARCH TECHNICAL NOTES

- CRTN 25 Feb 1992 Modelling interannual variability in the Indian Ocean using momentum fluxes from the UKMO and ECMWF operational weather analyses. D L T Anderson and D J Carrington
- CRTN 26 Mar 1992 A GCM simulation of the impact of Amazonian deforestation on climate using an improved canopy representation  
J Lean and P R Rowntree
- CRTN 27 Mar 1992 The parameterization of rainfall interception in GCMs  
A J Dolman and D Gregory
- CRTN 28 Jun 1992 Development of worldwide marine data eigenvectors since 1985  
A W Colman
- CRTN 29 Jun 1992 A tropical ocean model with reduced physics  
M K Davey
- CRTN 30 Jun 1992 International Temperature Workshop, Boulder, Colorado, USA, 16 January 1992  
Edited by D E Parker
- CRTN 31 Jul 1992 Simulation of clear-sky outgoing longwave radiation over the oceans using operational analyses  
A Slingo and M J Webb
- CRTN 32 Sep 1992 A prediction of the transient response of climate  
J M Murphy
- CRTN 33 Nov 1992 LEPS scores for assessing climate model simulations and long-range forecasts.  
C K Folland
- CRTN 34 Jan 1993 Stratospheric Data Assimilation System Guide  
Editor: R Swinbank
- CRTN 35 Mar 1993 A Stratosphere-Troposphere Data Assimilation System  
R Swinbank and A O'Neill
- CRTN 36 Mar 1993 Validation of hydrological schemes for climate models against catchment data.  
P R Rowntree and J Lean

## CLIMATE RESEARCH TECHNICAL NOTES

- CRTN 37    Apr 1993    Modelling of palaeoclimates: Examples from the recent past  
J F B Mitchell
- CRTN 38    May 1993    A simulation of seasonality in ENSO forecast skill  
M K Davey, D L T Anderson and S Lawrence
- CRTN 39    Jul 1993    ENSO Prediction experiments using a simple ocean-atmosphere model  
D-H Wu, D L T Anderson and M K Davey
- CRTN 40    Sep 1993    Diagnosis of dynamic sea-surface and sea-level changes from the Cox ocean model  
J M Gregory
- CRTN 41    Sep 1993    Seasonal variations of the clear-sky greenhouse effect: the role of changes in atmospheric temperatures and humidities  
M J Webb, A Slingo and G L Stephens
- CRTN 42    Nov 1993    Sea-level changes under increasing atmospheric CO<sub>2</sub> in a transient coupled ocean-atmosphere GCM experiment.  
J M Gregory
- CRTN 43    Dec 1993    Global and regional patterns of climate change: recent predictions for the Arctic  
P R Rowntree
- CRTN 44    Feb 1994    The effect of changing horizontal diffusion in the atmospheric version of the unified climate model  
C D Hall and R A Stratton
- CRTN 45    Mar 1994    Simulation of El-Niño/Southern Oscillation like variability in a global AOGCM and its response to CO<sub>2</sub> increase.  
S F B Tett
- CRTN 46    Apr 1994    Global data required for monitoring climate change.  
D E Parker and C K Folland
- CRTN 47    May 1994    Seasonal uptake of anthropogenic CO<sub>2</sub> in an ocean general circulation model.  
N K Taylor

CLIMATE RESEARCH TECHNICAL NOTES

- CRTN 48 Jun 1994 A tropic-wide oscillation of boreal summer rainfall and patterns of sea-surface temperature.  
M N Ward, K Maskell, C K Folland, D P Rowell and R Washington
- CRTN 49 Jun 1994 Simulation of the tropical Pacific using a simplified ocean model  
M A Balmaseda, D L T Anderson and M K Davey
- CRTN 50 Sep 1994 Simulation of global mean temperature using a box-diffusion climate model  
P R Rowntree
- CRTN 51 Sep 1994 Seasonal dependence of ENSO prediction skill  
M A Balmaseda, M K Davey and D L T Anderson
- CRTN 52 Nov 1994 Simulation of the Indian Monsoon and Tropical Intraseasonal Variability by a General Circulation Model  
P M Inness and D Gregory
- CRTN 53 Mar 1995 A comparison of modelled surface fluxes with climatological estimates.  
C Gordon and D K Wright
- CRTN 54 Mar 1995 The representation of moist convection in atmospheric models.  
D Gregory
- CRTN 55 Mar 1995 A consistent treatment of the evaporation of rain and snow for use in large-scale models  
D Gregory
- CRTN 56 Apr 1995 Workshop on simulations of the Climate of the Twentieth Century using GISST, 28-30 November 1994, Hadley Centre, Bracknell, UK  
Edited by C K Folland and D P Rowell
- CRTN 57 May 1995 Enhanced shortwave cloud radiative forcing due to anthropogenic aerosols.  
S E Swartz and A Slingo
- CRTN 58 May 1995 The simulation of the tropical oceans in models of different horizontal resolution.  
C Gordon, D K Wright and C M Roberts
- CRTN 59 Sep 1995 The water budget of middle latitude continental regions - a modelling and observational study  
P R Rowntree
- CRTN 60 Sep 1995 Intraseasonal variability of the Indian summer monsoon simulated by the Hadley Centre climate model  
K Ashok, D Gregory and P M Inness

CLIMATE RESEARCH TECHNICAL NOTES

- CRTN 61 Sep 1995 Climate simulations with the Unified Model: AMIP runs  
C D Hall, R A Stratton and M L Gallani
- CRTN 62 Nov 1995 Validation of surface parameters over the oceans in climate simulations with the unified model.  
C D Hall
- CRTN 63 Dec 1995 The GISST2.2 sea surface temperature and sea-ice climatology  
D E Parker, M Jackson and E B Horton
- CRTN 64 Dec 1995 Parametrization of momentum transport by convection. II: Tests in single column and general circulation models.  
D Gregory, R Kershaw and P M Inness
- CRTN 65 Jan 1996 Understanding the sensitivity of a GCM simulation of Amazonian deforestation to the specification of vegetation and soil characteristics.  
J Lean and P R Rowntree
- CRTN 66 Jan 1996 On the efficient calculation of infra-red fluxes and cooling rates using the two-stream equations.  
J M Edwards
- CRTN 67 Jan 1996 The second Hadley Centre coupled ocean-atmosphere GCM: Model description, spinup and validation.  
TC Johns, RE Carnell, JF Crossley, JM Gregory, JFB Mitchell, CA Senior, SFB Tett and RA Wood
- CRTN 68 Feb 1996 The sensitivity of climate simulations to the specification of mixed phase clouds  
D Gregory and D Morris
- CRTN 69 Apr 1996 Using an ensemble of Multi-Decadal GCM simulations to assess potential seasonal predictability  
D P Rowell
- CRTN 70 May 1996 North Atlantic and European Seasonal Predictability using an Ensemble of Multi-Decadal AGCM Simulations  
J R Davies, D P Rowell and C K Folland
- CRTN 71 Jun 1996 A description of the Second Hadley Centre Coupled Model (HADCM2)  
T C Johns
- CRTN 72 Jul 1996 Palaeoclimate Modelling Intercomparison: UKMO GCM simulations for 6kBP and 21kBP  
C D Hewitt and J F B Mitchell

CLIMATE RESEARCH TECHNICAL NOTES

- CRTN 73 Aug 1996 ENSO responses and low frequency weather variability in the North Pacific/American sector 1949-93  
A C Renshaw, D P Rowell and C K Folland
- CRTN 74 Sep 1996 Version 2.2 of the Global sea-Ice and Sea Surface Temperature data set, 1903-1994  
N A Rayner, E B Horton, D E Parker, C K Folland and R B Hackett
- CRTN 75 Sep 1996 A new gravity wave drag scheme incorporating anisotropic orography and low level wave breaking : Impact upon the climate of the UK Met Office Unified Model  
D Gregory, G J Shutts and J R Mitchell
- CRTN 76 Nov 1996 Middle atmosphere variability in the UKMO Unified Model  
R Swinbank, W Lahoz, C Douglas, A Heaps, R Brugge, W Norton, A O'Neill, D Podd
- CRTN 77 Dec 1996 A high resolution AMIP run using the Hadley Centre model HadAM2b  
R A Stratton
- CRTN 78 Jan 1997 The climate response to CO<sub>2</sub> of the Hadley Centre coupled AOGCM with and without flux adjustment  
J M Gregory and J F B Mitchell
- CRTN 79 May 1997 Development of the Global Mean Sea Level Pressure Data Set GMSLP2  
T A Basnett and D E Parker